University of Pannonia

Doctoral School of Chemical Engineering and Material Sciences

Submitted for the degree of
Doctor of Philosophy
of the University of Pannonia, Hungary

Author: Zhenghui Lu
Supervisor(s): Dr. habil. Gusztáv Fekete and Dr. András Kovács

DOI:10.18136/PE.2026.996

Dissertation Title: Data-Driven Personalized Lattice Footwear Design and Biomechanical Optimization

Veszprém
2026

Data-Driven Personalized Lattice Footwear Design and Biomechanical Optimization

Thesis for obtaining a PhD degree in the Doctoral School of Chemical Engineering and Material Sciences of the University of Pannonia

in the branch of Bio-, Environmental- and Chemical engineering

Written by
Zhenghui Lu

Supervisor: **Dr. habil. Gusztáv Fekete**
Co-supervisor: **Dr. András Kovács**

I recommend the dissertation for acceptance: yes / no

….…….
supervisor

I recommend the dissertation for acceptance: yes / no.

…….
supervisor

I recommend the dissertation for peer review.

…….
chair of the DDHC

The PhD-candidate has achieved ……. % at the public debate.

The composition of the Final Examination Committee:

chair:……..……

reviewers:..……

members:……

Veszprém,

…….
chair of the committee

Qualification of degree: ….....

Veszprém,

…….
chair of the UDHC

Content

Data-Driven Personalized Lattice Footwear Design and Biomechanical Optimization

Abstract

In recent years, advances in 3D printing, computational mechanics, and machine learning have begun to shift footwear biomechanics from conventional material tuning toward structurally programmable and fully personalized design paradigms. However, existing studies remain largely confined to localized functional optimization, static loading simulations, or structures of limited dimensionality, and thus fall short of providing an integrated structure–function framework applicable to authentic gait conditions. In particular, substantial gaps persist in understanding how programmable lattice architectures can be systematically exploited to enhance cushioning capacity, gait stability, and propulsive efficiency across heterogeneous foot morphologies and pathological conditions under real-world locomotion.

This dissertation addresses the aforementioned challenges through three central research questions.

(1) How can parametrically defined lattice architectures enable programmable modulation of footwear mechanical performance? Existing studies on lattice-based insoles or heel pads typically rely on a single topology or narrowly constrained parameter sets, making it difficult to establish a systematic geometric–mechanical mapping.

(2) How can region-specific lattice midsoles be generated according to the functional demands of different plantar zones, and how can the coupling mechanisms between structural modulation and gait-phase dynamics be elucidated? Conventional footwear predominantly employs homogeneous materials, which fail to precisely accommodate the three primary gait tasks—rearfoot cushioning, midfoot stabilization, and forefoot propulsion.

(3) How can authentic gait dynamics be incorporated into multi-objective optimization of lattice structures to enable genuinely personalized footwear design? Traditional design pipelines lack a closed-loop connection among individual gait patterns, structural parameters, and functional outcomes, resulting in optimization processes that remain largely empirical and trial-and-error in nature.

Building upon these research questions, this dissertation establishes three corresponding research objectives.

(1) To develop a multidimensional parametric lattice modeling framework and to construct a programmable geometric–mechanical mapping via finite element analysis. The parameter space

encompasses unit-cell geometric descriptors, porosity, strut thickness, and orientation, enabling the systematic generation of diverse topologies and the characterization of their mechanical responses.
(2) To propose a region-specific lattice midsole design methodology—covering the rearfoot, arch, lateral midfoot, and forefoot—and to elucidate their functional roles and synergistic interactions across different gait phases.
(3) To construct a dynamic–gait–driven multi-objective optimization framework that integrates rearfoot impact mitigation, arch-collapse control, and forefoot propulsion into a unified optimization scheme, followed by multi-subject physical validation through 3D printing and gait experimentation.
Methodologically, the dissertation integrates three-dimensional foot scanning, medical-image-based reconstruction, individualized foot–footwear coupled finite element modeling, surrogate-based multi-objective Bayesian optimization, and multi-subject gait experimentation to realize a complete closed loop from structural modeling to cross-morphology human-subject verification. Through systematic mechanical characterization of unit-cell architectures, dynamic loading simulations using individualized foot–footwear coupled FE models across healthy and pathological subjects, and surrogate-model–guided exploration of the design space, personalized lattice configurations are progressively generated in accordance with subject-specific gait demands while preserving framework-level generalizability. The final wearable prototypes are fabricated via 3D printing and evaluated in the laboratory through plantar pressure analysis and comprehensive kinematic and kinetic gait assessments.

The findings of this study demonstrate that:

(1) The proposed parametric lattice framework enables continuous, programmable modulation of mechanical behavior, spanning from high energy absorption to high structural support, while maintaining robust predictive accuracy across a multidimensional parameter space.
(2) The region-specific lattice configuration establishes a coherent functional chain across the gait cycle—impact attenuation, stability control, and propulsive output. Rearfoot lattices markedly reduce peak plantar pressures; arch and lateral midfoot structures enhance mid-stance stability; and forefoot lattices increase plantarflexion moments and push-off efficiency.
(3) The gait-driven, dynamically optimized midsole design substantially reduces equivalent soft-tissue stress in the heel region (by approximately 25% on average across subjects), preserves more natural subtalar joint motion patterns, and enhances forefoot propulsive performance under subject-specific constraints.
(4) Wear experiments corroborate the finite element predictions, and subjective evaluations indicate that the 3D-printed prototypes outperform the control footwear in overall comfort, arch support, and rearfoot cushioning.
Collectively, this research establishes the first comprehensive design framework for personalized

footwear grounded in parametrically programmable lattice architectures and tailored to authentic gait dynamics. The integrated methodology—encompassing structural programmability, functional zoning, dynamic optimization, and experimental validation—provides a methodological foundation for transitioning the footwear industry from standardized manufacturing toward data-driven, on-demand production. Moreover, it offers a promising technological pathway for advancing athletic performance, orthopedic rehabilitation, and intelligent wearable systems.

Abbreviations

FE: finite element

GRF: ground reaction force

ROM: range of motion

ML: machine learning

GPR: gaussian process regression

CNN: convolutional neural network

LSTM: long short-term memory

DFIS: dynamic biplane fluoroscopy system

CAD: computer-aided design

IK: inverse kinematics

ID: inverse dynamics

TPU: thermoplastic polyurethane

FDM: fused deposition modeling

STL: stereolithography file

CT: computed tomography

MRI: magnetic resonance imaging

VAS: visual analog scale

AFOs: ankle–foot orthoses

List of Figures

List of Tables

1. Introduction

1.1 Lower-Limb Function and Footwear Biomechanics

1.1.1 Fundamental Foot Anatomy

As the terminal load-bearing structure of the human body, the foot not only fulfills the dual roles of support and locomotion but also serves as a critical hub for force transmission and energy regulation within the lower-limb kinetic chain[1]. Its anatomical organization is exceptionally complex, consisting of 26 bones, 33 joints, and more than 100 ligaments and muscles, which together constitute a mechanical system that harmonizes rigid support with compliant cushioning (Figure 1.1.1). This structurally diverse and hierarchically integrated architecture enables the foot to maintain stable weight-bearing while accommodating the diverse demands of dynamic locomotion.

Figure 1.1.1 Anatomical illustration of foot bones, ligaments, and soft tissues.[2]

As one of the most critical components within the osseous and soft-tissue systems of the foot, the arch complex plays an indispensable biomechanical role[3]. As illustrated in Figure 1.1.2, the medial longitudinal arch, lateral longitudinal arch, and transverse arch collectively form a three-dimensional vaulted structure that not only preserves plantar morphology but also exhibits pronounced elastic behavior during locomotion. Experimental evidence has shown that the arches deform during the stance phase to store elastic strain energy, which is subsequently released through the recoil of the plantar fascia and associated ligaments during toe-off. This “spring effect” substantially enhances the energetic efficiency of walking and running, enabling the foot to function as a mechanical system equipped with an intrinsic elastic energy-storage mechanism. The stability of the arches is highly dependent on soft-tissue constraints—particularly the plantar fascia, the long and short plantar ligaments, and the spring ligament—which collectively maintain arch height and prevent excessive collapse that could compromise mechanical balance. Clinically, diminished arch-support function is closely associated with plantar fasciitis, pes planus, and chronic overuse injuries.

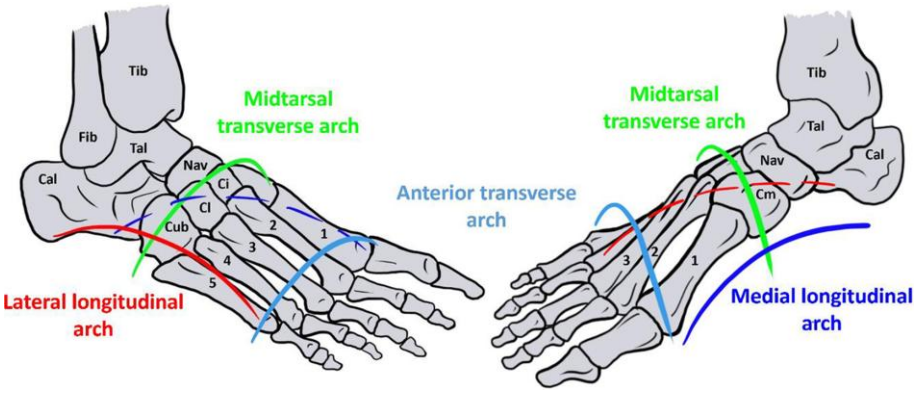

Figure 1.1.2 Schematic illustration of the right foot arches (left: lateral view; right: medial view, adapted from published literature).[4]

During the propulsion phase of gait, the metatarsals play a central role in transmitting concentrated ground reaction forces, with the first and second metatarsals typically bearing the highest loads. Prolonged asymmetry or imbalance in plantar pressure distribution is often implicated in metatarsalgia, stress fractures, and other overuse-related injuries. Beyond supporting longitudinal loading, the metatarsals—together with the transverse arch—contribute critically to mediolateral stability of the forefoot, enabling the toes to flex and extend with agility while ensuring efficient transfer of energy to the ground during push-off. Even subtle alterations in metatarsal head position or load distribution can substantially influence gait stability and the distribution of joint stresses.

The ankle joint, situated between the lower leg and the foot, serves as a pivotal hub within the lower-limb kinetic chain[5]. Comprising the tibia, fibula, and talus, it primarily facilitates dorsiflexion and plantarflexion, while the subtalar joint enables inversion and eversion, thereby enhancing the foot's adaptability to uneven terrain. The stability of the ankle is maintained by a complex ligamentous system, among which the medial deltoid ligament and the lateral talofibular ligament complex are particularly critical, as they constrain abnormal motion and prevent joint malalignment or sprains. During locomotion, the ankle bears the weight transmitted from the trunk and, through coordinated interaction with the arches and metatarsals, dissipates impact forces and modulates the lower-limb kinetic chain. At initial heel contact, the ankle typically adopts a dorsiflexed posture to absorb impact; during toe-off, plantarflexion combined with the elastic recoil generated by Achilles tendon stretching contributes to energy return, thereby propelling the body forward.

1.1.2 Functional Roles of the Foot in Support, Cushioning, and Propulsion

From the perspective of the integrated lower-limb kinetic chain, the foot serves not only as the direct

interface between the body and the ground but also as a crucial nexus within the global energy-transfer network. Its intricate anatomical architecture requires it to simultaneously fulfill multiple roles during gait: providing stable support, delivering effective impact attenuation, and enabling efficient propulsion.

The plantar surface serves as the primary interface through which forces are transmitted between the body and the ground. Its pressure distribution reflects not only localized load-bearing conditions but also the overall coordination of the lower-limb kinetic chain. Under typical gait patterns, plantar pressure is predominantly concentrated in three regions—the heel, the lateral midfoot, and the forefoot—each exhibiting distinct functional roles across the gait cycle.

In the initial contact phase of gait, the heel is the first region to engage the ground, with the calcaneus transmitting impact forces to the lower leg through the ankle joint. At this moment, the arches have not yet undergone substantial deformation; shock attenuation is therefore primarily governed by the bony architecture and the heel fat pad[6]. Prior studies indicate that the posteromedial region of the calcaneus is a focal site of impact stress, and insufficient cushioning in this area can lead to overload of the plantar fascia and ankle structures. As the gait progresses into mid-stance, the arches gradually collapse and begin to store elastic energy under the tension of the ligaments and the plantar fascia. The longitudinal and transverse arches work synergistically to distribute body weight more uniformly across the metatarsal heads and the lateral border of the foot. Clinical anatomical investigations have shown that the medial longitudinal arch is characterized by pronounced elasticity[7], whereas the lateral arch complex provides comparatively greater structural stability. The dynamic modulation of the arch system not only reduces peak ground reaction forces but also attenuates shock transmission to upstream joints such as the knee, hip, and spine. During the toe-off phase, the arches recoil from their flattened configuration, and extension of the metatarsophalangeal joints releases the stored elastic energy, generating forward propulsive power. At this stage, the first and second metatarsals bear the highest loads, serving as key structures for propulsion and energy transfer. Finite element analyses have shown that stress in the central region of the third metatarsal increases markedly during propulsion[8], a finding that corresponds closely with the common clinical sites of stress fractures.

From the perspective of the integrated kinetic chain, dysfunctions in foot mechanics often trigger a cascade of compensatory responses throughout the lower limb. For example, collapse of the arches in individuals with pes planus can induce knee valgus and compensatory rotational adjustments at the hip[9], whereas pes cavus, characterized by insufficient shock absorption, increases susceptibility to stress fractures and ankle injuries. These phenomena underscore that the coordinated interplay of support, cushioning, and propulsion within the foot directly governs the stability and energetic efficiency of the lower-limb kinetic chain. A deeper understanding of foot

function across the gait cycle not only elucidates the biomechanical mechanisms underlying lower-limb injuries but also provides critical insight for footwear design and rehabilitative interventions. Footwear that achieves targeted optimization of support, cushioning, and propulsion holds the potential to enhance gait mechanics and mitigate the risk of lower-limb musculoskeletal disorders.

1.1.3 Plantar Pressure

During the initial contact phase, the heel first engages the ground, with the posteromedial calcaneus bearing most of the impact load. Although the pressure peak in this region is high, its duration is brief, serving primarily to attenuate impact and establish a stable foundation for the subsequent stance phase. As gait transitions into mid-stance, pressure progressively shifts toward the longitudinal and transverse arches. The contact area increases and the pressure per unit area decreases, reflecting the role of the arches in distributing body weight and maintaining balance. Murphy et al.[10] reported that both pressure magnitude and contact area in the midfoot exhibit high consistency across repeated gait trials (ICC > 0.9), indicating that this region demonstrates stable and highly repeatable mechanical behavior. Such findings further substantiate the pivotal function of arch deformation in providing cushioning and facilitating load transfer during stance. In the toe-off phase, pressure becomes increasingly concentrated in the forefoot, particularly beneath the first and second metatarsal heads and the phalanges. This period is characterized by high peak pressures and prolonged loading duration, marking the forefoot as the principal contributor to propulsive force generation.

It is noteworthy that plantar pressure distribution varies not only across different gait phases but also as a function of multiple individual and environmental factors, including foot morphology (e.g., pes planus or pes cavus), movement habits, and footwear design. For instance, individuals with pes planus typically exhibit greater contact area and elevated pressure along the medial midfoot, whereas those with pes cavus often display concentrated loading in the rearfoot and forefoot due to reduced arch engagement[11]. These distinctions hold significant relevance for assessing injury risk and informing footwear design strategies. In various athletic activities, particularly high-impact tasks such as running and jumping, the regional characteristics of plantar loading become even more pronounced. During initial contact, the heel experiences peak impact forces, and its cushioning capacity directly influences shock attenuation throughout the lower limb. The arches, functioning as elastic structures, absorb and release energy during mid-stance, thereby contributing to gait stability. However, persistent abnormal pressure concentration can predispose individuals to conditions such as bone stress injuries, stress fractures, or osteoarthritis. Consequently, the dynamic distribution of plantar pressure is not only integral to daily comfort but also indicative of the biomechanical state of the lower limb, with direct implications for athletic performance and injury

susceptibility[12].

1.1.4 Biomechanical Influence of Footwear on Lower-Limb Function

Footwear functions not only as an essential component of daily living and athletic activity but also as a critical external modulator of lower-limb dynamics and movement performance. The geometric configuration and material properties of a shoe directly shape the pathways of force transmission, thereby altering gait patterns, joint loading, and overall stability.

The design of the midsole represents one of the most common and influential structural elements of modern footwear. Cushioning-oriented athletic shoes typically incorporate highly elastic materials within the midsole to absorb the impact generated at heel strike, thereby reducing the magnitude of shock transmitted to the tibia and knee joint—as illustrated in Figure 1.1.3, which depicts stress distribution in the knee under specific loading conditions. By mitigating these peak forces, such designs help decrease the risk of soft-tissue overload and joint-related injuries.Recent systematic reviews and meta-analyses have further demonstrated that moderate midsole cushioning can enhance running economy (RE), defined as the oxygen consumption per unit body mass at a given running speed[13]. This improvement arises primarily from reduced energy dissipation during the stance phase, allowing for more efficient energy transfer throughout the gait cycle.

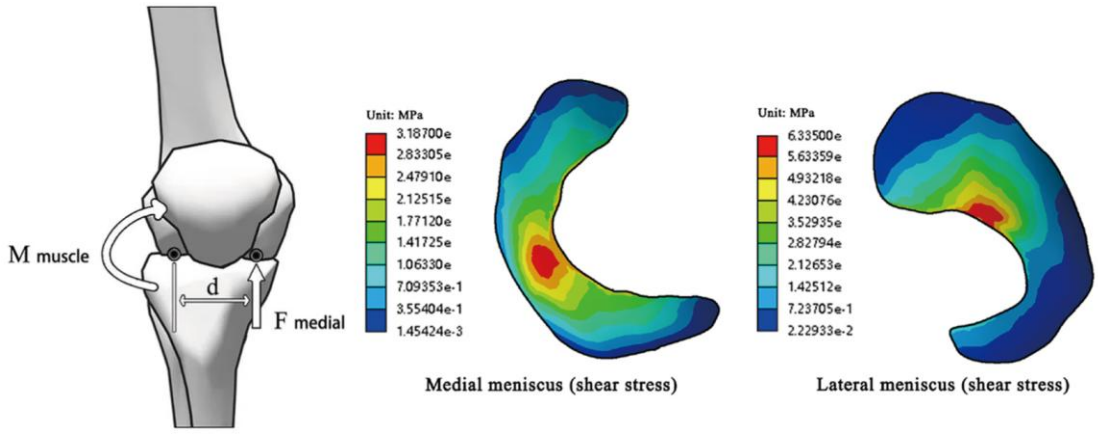

Figure 1.1.3 Meniscal stress distribution under loading.[9, 12]

The relationship between cushioning and running economy is not linear. Studies have shown that a moderate midsole thickness, for example, around 10 mm, can improve RE, whereas excessive cushioning, such as 20 mm, may increase metabolic cost. This effect arises because overly thick soles can diminish the elastic energy–storage contributions of the arches and the Achilles tendon. Sole mass further influences running economy: an additional 100 g of shoe weight has been associated with roughly a 1% increase in VO_2, thereby reducing RE. Consequently, the design of

cushioning materials must balance multiple objectives, impact attenuation, joint protection, weight minimization, and efficient energy transfer, to achieve meaningful improvements in performance and running economy.

Heel height is a critical determinant of gait dynamics and the mechanical environment of the lower limb. Moderate elevation of the heel alters the initial posture of the ankle and shifts the body's center of mass forward, which in turn induces compensatory changes such as reduced step length, decreased walking speed, and prolonged double-support duration[14]. However, excessive heel height increases the mechanical load on the knee extensors and ankle plantarflexors, reduces posterior stability, and elevates the risk of falls. Long-term use of high-heeled footwear has also been associated with a higher incidence of knee osteoarthritis and chronic ankle instability. An appropriate heel-height design must therefore strike a balance among cushioning, stability, and energy efficiency. Overly elevating the heel can disrupt the coordination of the lower-limb kinetic chain and compromise both safety and locomotor performance.

Excessive foot pronation alters the mechanical pattern of the lower-limb kinetic chain, increasing stress on both the knee and the ankle and elevating injury risk. Incorporating firmer materials or reinforced structures along the medial side of the midsole can enhance arch support and medial stability; footwear with such features is commonly referred to as motion-control shoes. Randomized controlled trials have shown that[15], over a six-month follow-up period, recreational runners wearing motion-control footwear exhibited significantly lower overall injury risk than those wearing neutral shoes (HR = 0.55). The effect was most pronounced in individuals with pronated feet, whose injury risk decreased by nearly 66 percent. However, the protective benefits of motion-control footwear are primarily limited to runners with excessive pronation. Among individuals with neutral or supinated foot types, additional motion-control features do not confer notable advantages and may even increase discomfort[16]. Motion-control footwear therefore has a clearly targeted role in enhancing stability and reducing injury risk, and its use should be tailored to the specific morphological characteristics of the foot.

In sports medicine and rehabilitation, the biomechanical influence of footwear is equally significant[17]. As illustrated in Figure 1.1.4, personalized orthotic insoles and arch-support devices are widely used in clinical practice to redistribute plantar pressure and offload high-stress regions. Such interventions effectively alleviate conditions such as metatarsalgia, plantar fasciitis, and diabetic foot complications. For individuals recovering from lower-limb injuries, footwear that provides adequate cushioning and stability can offer essential protection during rehabilitation, reducing the risk of reinjury and facilitating the restoration of normal gait mechanics. Even among healthy athletic populations, evidence indicates that well-designed footwear interventions can reduce the incidence of stress fractures, tendinopathies, and other chronic overuse injuries, thereby

contributing to long-term lower-limb health.

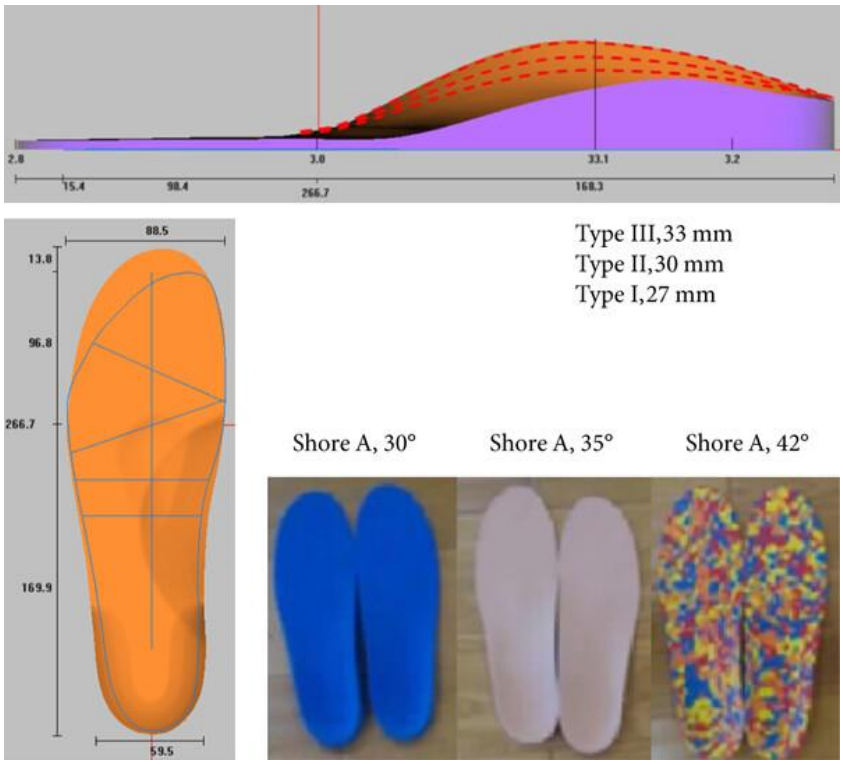

Figure 1.1.4 Meniscal stress distribution under.[18]

Footwear, through its combined effects on cushioning, stability, and structural support, not only improves the mechanical environment of the lower-limb kinetic chain but also plays a pivotal role in injury prevention and rehabilitative care. Well-designed footwear can simultaneously enhance athletic performance, protect joint health, and meet clinical intervention needs, providing reliable external support for the general population, older adults, and individuals with chronic conditions. This multifaceted influence positions footwear research as a central topic at the intersection of sports medicine, biomechanics, and rehabilitation engineering.

1.2 Advantages and Advances of 3D Printing in Footwear Design

1.2.1 Limitations of Traditional Footwear Manufacturing

Conventional footwear manufacturing relies predominantly on mold-based fabrication and standardized lasts. This approach is grounded in the assumption of an “average foot,” whereby a limited range of sizes is expected to accommodate the majority of users. However, analysis of more than 1.2 million three-dimensional foot scans from consumers in North America, Europe, and Asia has revealed substantial variability in foot length, width, instep height, and heel width across regions, sexes, and even among individuals sharing the same nominal shoe size[19]. As illustrated in Figure 1.2.1, these dimensions exhibit striking dispersion. For example, Asian populations generally present wider feet, whereas European populations tend to have higher insteps. Within a single shoe size, the foot-width span of 90 percent of individuals can reach 15–20 mm, far exceeding the coverage provided by traditional width grading systems. Such morphological diversity indicates that size scaling based on a single last cannot adequately address the needs for individualized fit or biomechanical compatibility. Geometric mismatch may lead to localized compression or gapping in regions such as the forefoot, arch, or heel, compromising natural gait mechanics and reducing comfort while altering plantar pressure patterns. For certain populations, including individuals with pes planus or diabetic foot conditions, these mismatches may further exacerbate high-pressure regions beneath the metatarsal heads and increase the risk of soft-tissue injury[20].

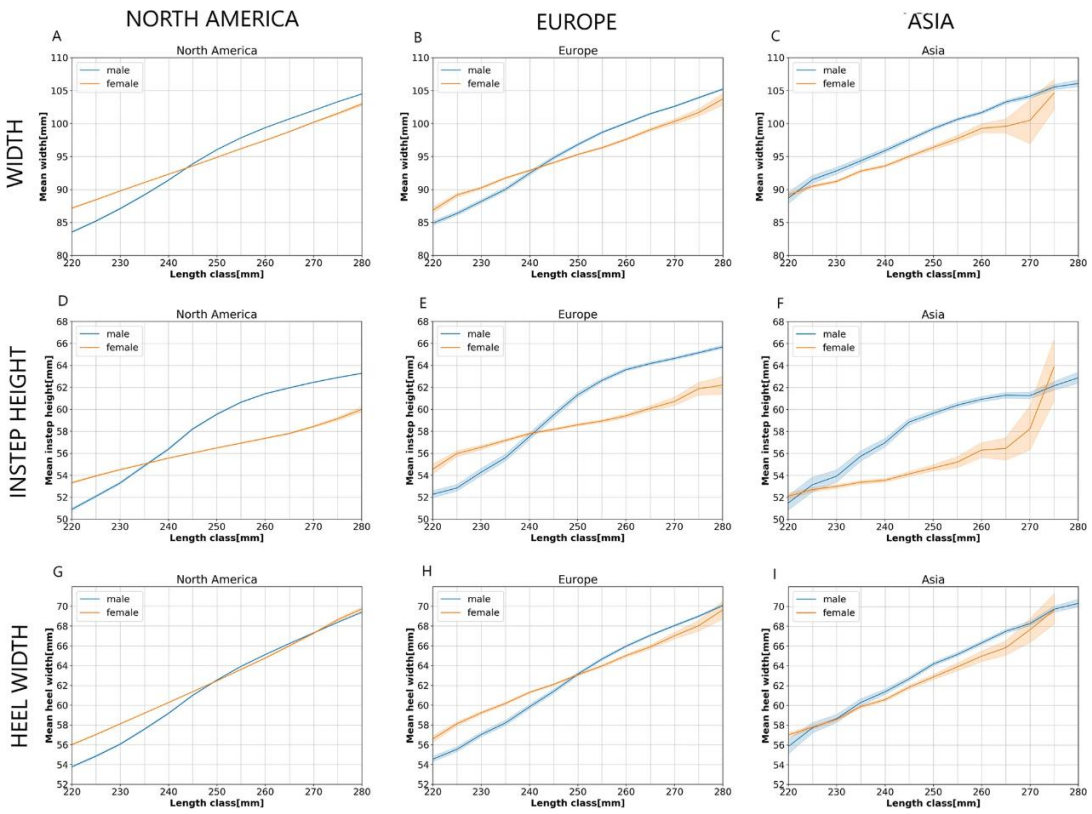

Figure 1.2.1 Comparison of male and female foot dimensions across North America, Europe, and Asia.(A–C) Mean foot widths; (D–F) mean instep heights; (G–I) mean heel widths, presented separately for each region.[19]

Traditional mold-based manufacturing also entails high fixed costs and limited flexibility. Once a mold is produced, even minor design modifications may require weeks or months to implement, which constrains rapid iteration and hinders personalized optimization. This rigidity not only restricts product diversity but also makes it difficult to meet the growing demands in sports and rehabilitation for rapid adaptation and precise individual fit. Moreover, conventional shoemaking typically involves dozens of components and multiple material classes, including rubber, EVA, and various textiles. These materials are often difficult to disassemble and recycle, resulting in low rates of circular reuse. The production process is additionally associated with considerable carbon emissions and waste generation, highlighting clear limitations from a sustainability perspective[21].

1.2.2 Advantages of 3D Printing in Footwear

One of the most significant advantages of 3D printing is its ability to overcome the geometric constraints inherent in traditional mold-based manufacturing, thereby enabling highly complex and finely detailed structural designs[22]. Geometries that are difficult or impossible to fabricate using conventional techniques—such as hollow honeycomb architectures or auxetic (negative Poisson's

ratio) unit cells—can be readily produced with additive manufacturing. These structures offer programmable mechanical properties and, through spatial variation in their configuration, can deliver region-specific cushioning, support, and ventilation. Such capabilities allow footwear to satisfy the distinct functional requirements of different plantar regions.

Compared with the mold-development cycle of traditional footwear manufacturing, which often spans several weeks or even months, 3D printing can complete the entire process from design to fabrication within a matter of hours. This rapid-iteration capability enables “on-demand” personalization based on individual foot-scan data and gait measurements. Parameters such as arch height, metatarsal morphology, and plantar pressure distribution can be directly mapped onto the geometry of insoles or midsoles, thereby substantially enhancing individual fit. For athletes and rehabilitation patients, such personalized solutions strikingly improve the balance between comfort and functional performance, while greatly increasing the efficiency of customization and structural optimization[20].

Commonly used materials for 3D-printed footwear include thermoplastic polyurethane (TPU), polyamide (PA12), photopolymer resins, and various composite formulations. Among these, TPU offers excellent elasticity and abrasion resistance, making it well suited for midsole lattice structures. Composite materials combine low weight with high mechanical strength and therefore exhibit superior structural efficiency. Several multi-material printing technologies, such as PolyJet and dual-extrusion FDM, further enable gradients or spatial transitions between rigid and compliant regions within a single component. These capabilities enhance the stability of arch support while improving overall fit and comfort[23, 24]. As shown in Figure 1.2.2, TPU-based footwear prototypes can be fabricated using FDM technology.

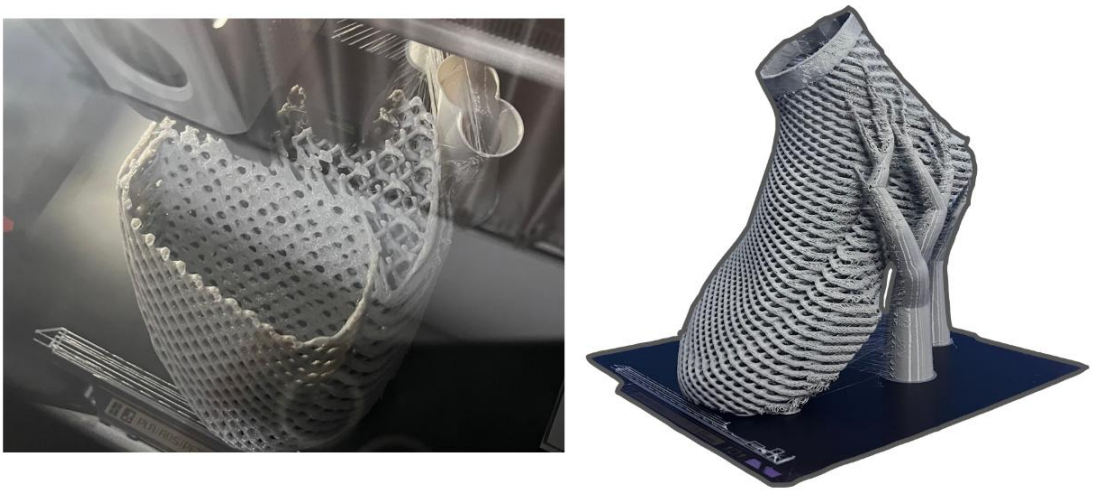

Figure 1.2.2 3D printing process and final output of a full-lattice shoe upper fabricated with TPU material.

Studies have shown that the production of conventional running shoes can generate approximately 16–21 kg CO_2eq per pair. In contrast, 3D printing can substantially reduce emissions and material waste through on-demand fabrication, decreased component counts, lower transportation requirements, and minimal reliance on adhesives. For example, a report from HILOS indicates that its 3D-printed footwear achieves a roughly 48 percent reduction in carbon emissions and a 99 percent decrease in water usage[25]. Moreover, 3D printing eliminates the need for large-scale factory infrastructure and supports small-batch and distributed manufacturing. This shift not only enhances sustainability but also opens new opportunities for innovation in footwear production and commercialization models.

1.2.3 Current Applications of 3D Printing in Footwear

In recent years, 3D printing has been increasingly integrated into the development of athletic midsoles. Compared with conventional foam materials, 3D-printed midsoles can employ parametrically designed lattice architectures to deliver region-specific cushioning and support. For example, low-modulus lattice units can be placed in the heel to enhance impact absorption, whereas higher-stiffness units may be deployed in the forefoot to improve propulsion. Such zonal configurations not only enhance energy-return efficiency but have also been shown to improve running economy and athletic performance to a measurable degree. A representative example is the Futurecraft 4D (also branded as 4DFWD) developed jointly by adidas and Carbon[26, 27]. Using a digital light synthesis process, this design fabricates a lattice midsole engineered with directional mechanical responses that provide targeted energy return and impact attenuation (Figure 1.2.3). The structure is parametrically tuned based on athletic motion data and is considered capable of improving gait efficiency and overall performance. The emergence of such midsole architectures signifies a broader transition within footwear manufacturing from standardized production toward data-driven, functionally optimized design paradigms.

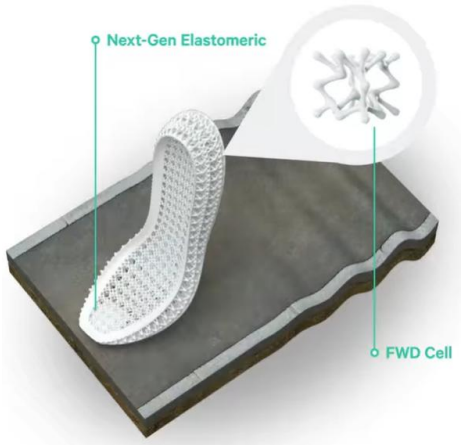

Figure 1.2.3 4D-printed lattice midsole of the adidas Futurecraft 4D.[26]

In medical and rehabilitation contexts, 3D printing likewise demonstrates substantial potential for precision customization. By integrating three-dimensional foot scanning with gait analysis, individualized insoles can be generated to correct foot deformities or reduce localized high-pressure regions. For example, a study involving individuals at high risk for diabetic ulceration employed Kelvin and related lattice structures to design personalized insoles that redistributed plantar pressure and effectively reduced high-risk loading zones[28].Assistive devices such as ankle–foot orthoses (AFOs) and arch supports have also been rapidly customized through 3D printing. These technologies not only improve clinical fitting efficiency but also enhance long-term comfort compared with conventional products[29].

Major athletic brands such as Adidas, Nike, New Balance, and Reebok have released multiple limited-edition products incorporating 3D-printed components, including the Adidas Futurecraft 4D, Adidas Climacool, and New Balance TripleCell[30], demonstrating considerable commercial potential. Meanwhile, emerging companies such as HILOS and Zellerfeld are exploring full-shoe 3D printing with an emphasis on sustainability and circular manufacturing. Despite these advances, most 3D-printed footwear products remain in the stages of small-scale production or experimental deployment. Key challenges persist, including low manufacturing throughput, high production costs, and insufficient long-term durability validation. In academic research, efforts are increasingly focused on mechanical-performance optimization, multifunctional material development, and frameworks for personalized design. These investigations are driving progress in functional materials, lattice-structure engineering, and individualized fabrication workflows, with the aim of enabling large-scale clinical applications and further enhancing athletic performance.

1.3 Data-Driven Parametric Lattice Structures and Programmable Mechanical Properties

1.3.1 Fundamentals of Lattice Architectures

Lattice structures are composed of periodic or quasi-periodic unit cells that together form a three-dimensional geometric framework. Unlike traditional solid or foam materials, the mechanical behavior of lattices is governed predominantly by their geometric characteristics rather than by the intrinsic properties of the base material. This "structure-driven performance" endows lattice architectures with the features of programmable materials, allowing their macroscopic mechanical responses—including stiffness, strength, energy absorption, and deformation modes—to be tailored through adjustments to microscopic geometric parameters[31].

Lattice unit cells exhibit a high degree of geometric diversity. Conventional cubic and honeycomb configurations are widely used due to their regularity and ease of fabrication. Topologies such as body-centered cubic (BCC) and face-centered cubic (FCC) provide favorable mechanical isotropy under multiaxial loading. Re-entrant geometries and other auxetic (negative Poisson's ratio) unit cells contract laterally under compression, which markedly enhances energy absorption and impact-mitigation capabilities[32]. With advances in CAD modeling and additive manufacturing, numerous new lattice topologies have been developed in recent years. These innovations enable continuously graded lattice designs in which unit-cell parameters vary spatially within a single component, allowing region-specific tuning of mechanical performance. Such capabilities offer a powerful structural design pathway for addressing complex functional requirements[33].

1.3.2 Mechanical Characteristics of Lattice Structures

Lattice structures, owing to their distinctive unit-cell geometries and programmable nature, are widely regarded as materials that can be "designed on demand." In contrast to conventional homogeneous materials, their macroscopic mechanical behavior is influenced not only by the intrinsic properties of the base material but also by the topology of the unit cells, geometric parameters such as strut thickness, porosity, and cell size, and the spatial arrangement of the lattice network[32]. This high degree of tunability confers unique advantages in lightweight design, impact attenuation, energy absorption, and structural support. It also opens new avenues for the functional zoning of footwear components.

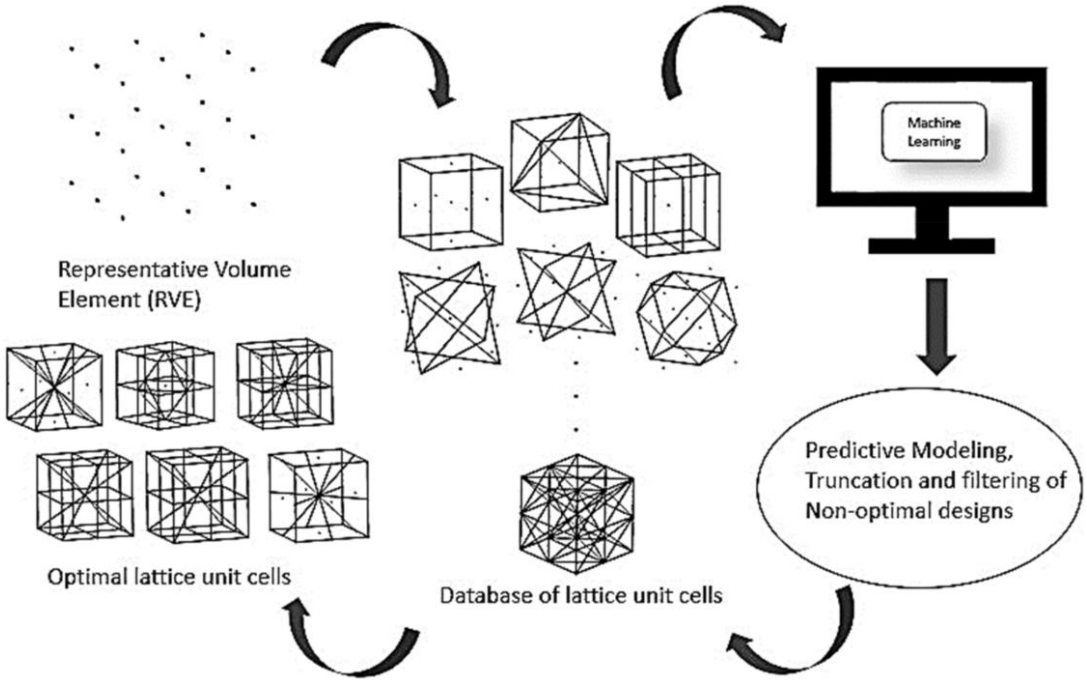

Figure 1.3.1 Machine-learning-assisted workflow for lattice structure design and optimization.[34]

By modulating porosity or strut thickness, lattice structures can span a wide spectrum of mechanical responses, ranging from soft, low-modulus behavior to high stiffness and high modulus. Both finite element analyses and experimental studies have shown that structural stiffness and strength decrease following a power-law relationship as porosity increases[35], whereas energy-absorption capacity is substantially enhanced. When applied to footwear design, these principles imply that high-porosity, low-stiffness lattice units may be deployed in the heel region to achieve effective impact cushioning, while low-porosity, high-stiffness configurations can be assigned to the arch and forefoot to provide essential support and propulsive capability. In this way, lattice architectures can be tailored to meet the distinct biomechanical requirements of different plantar regions.

In certain contexts, lattice structures exhibit superior energy-absorption performance under dynamic loading compared with conventional foams and honeycomb architectures. Studies have shown that well-designed functionally graded lattices can achieve approximately 20–30 percent greater cumulative energy absorption under compression than uniform lattices[32]. Truss-based lattices maintain good structural stability at high strain rates, whereas surface-based TPMS architectures, such as Gyroid structures, demonstrate more uniform stress distributions and higher buckling resistance under large deformations[35]. Recent computational and experimental investigations further indicate that truss lattices employing nonuniform topologies or inverse-designed configurations can achieve 30–90 percent improvements in buckling strength relative to traditional or bioinspired structures[36]. Certain specialized topologies, including re-entrant cells and rotating-honeycomb geometries, exhibit auxetic behavior (negative Poisson's ratio), contracting laterally

under axial compression[37]. This characteristic enhances lateral conformity and promotes efficient energy dispersion, allowing the structure to mitigate localized peak pressures and reduce the risk of stress-related injury. In footwear applications, auxetic structures are particularly advantageous in high-load regions such as the arch and forefoot, where their lateral expansion under compression improves comfort and enhances cushioning performance.

Beyond the tuning of individual mechanical properties, regional and graded design strategies in lattice architectures are essential for achieving multi-objective optimization. For example, implementing a longitudinal gradient in which stiffness transitions from high to low within a single midsole enables an effective balance between structural support and impact cushioning. Transversely, combining different topologies can accommodate diverse gait characteristics, such as excessive pronation or supination. Such spatially differentiated performance distributions are particularly critical in personalized footwear design and rehabilitation interventions, where localized geometric modulation can produce targeted functional responses.

1.3.3 Applications of Lattice Structures in Footwear Design

With the rapid maturation of additive manufacturing technologies, 3D-printed footwear has been gradually transitioning from proof-of-concept demonstrations to practical applications. Early studies primarily focused on showcasing the geometric complexity achievable through 3D printing, such as incorporating honeycomb or lattice architectures into insoles and midsoles to replace conventional foam materials. As both academia and industry began to recognize the advantages of additive manufacturing in lightweighting, regionalized design, and individualized customization, efforts increasingly shifted toward improving cushioning performance, optimizing plantar pressure distribution, and enhancing arch support. Recent systematic reviews have further noted that research on 3D-printed footwear has expanded from isolated structural testing to broader domains including performance enhancement, rehabilitation assistance, and sustainable manufacturing[22]. Thus, 3D printing is not merely an alternative fabrication method; it is emerging as a critical technological pathway for functional integration and personalized optimization in modern footwear design.

Improving impact attenuation is one of the most common objectives in applying lattice structures to footwear design. Previous studies have demonstrated that adjusting unit-cell size, porosity, and stiffness can substantially reduce heel-strike impact peaks while enhancing energy-absorption efficiency. For example, Geiger et al.[38] reported that insoles with appropriately tuned hardness can reduce peak heel pressure by approximately 37 percent and simultaneously improve forefoot load distribution. Leung et al.[39] designed a 3D-printed heel pad based on a re-entrant honeycomb topology for plantar protection in individuals with diabetes (Figure 1.3.2). Finite element simulations and in vivo testing showed that the heel-contact area increased by roughly 19 percent,

and peak heel pressure during gait decreased by approximately 33 percent, outperforming conventional PU foam insoles by a considerable margin.

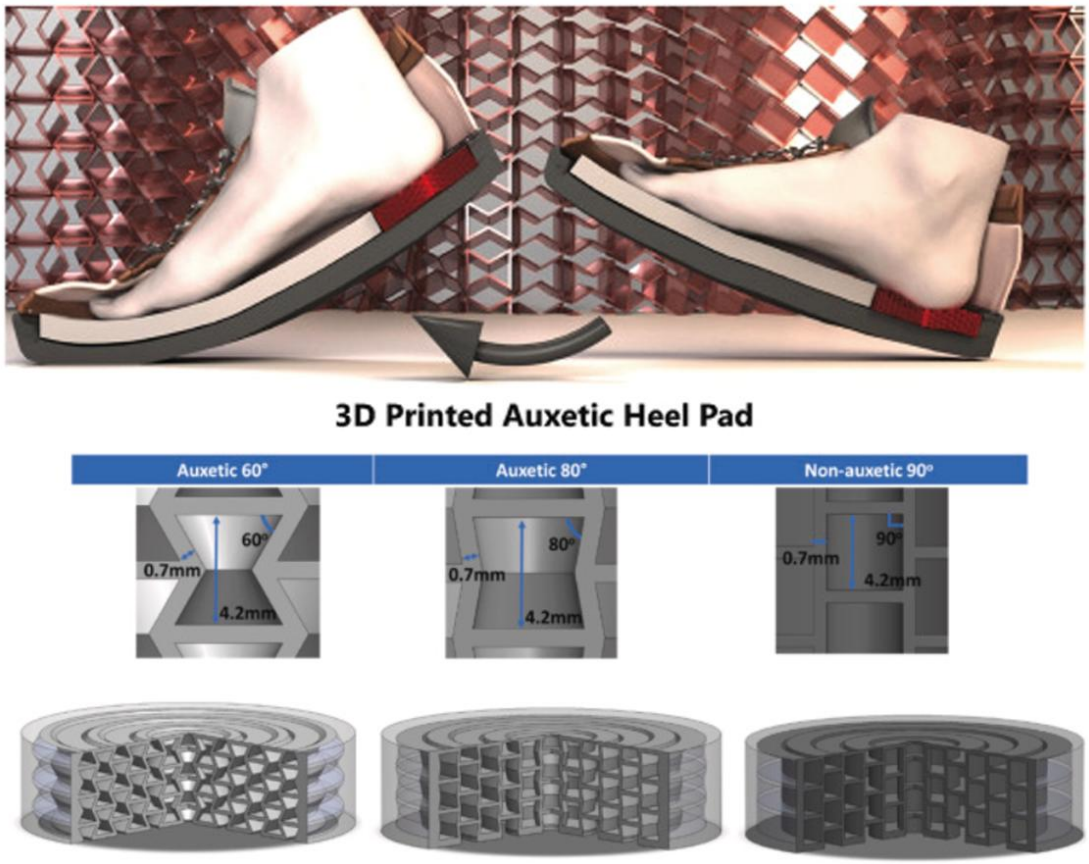

Figure 1.3.2 Design of a 3D-printed auxetic heel pad based on re-entrant honeycomb structures and its cushioning performance.[40]

Traditional insoles often suffer from either excessive or insufficient arch support, making it difficult to accommodate individual anatomical variability. With the advancement of 3D printing, lattice-based insole designs informed by foot scanning and gait analysis have gained prominence. Such approaches enable personalized arch parameters to be embedded directly during the design process, thereby improving midfoot stability and redistributing plantar pressure[41]. By tuning lattice fill density and unit-cell topology, the stiffness of the arch region can be selectively enhanced, allowing it to provide superior support under load. These design strategies not only improve comfort but also demonstrate greater stability and gait-correction efficacy than conventional orthotic insoles, particularly for individuals with pes planus or pes cavus. Systematic reviews further indicate that 3D-printed insoles positively influence pain reduction in flat-foot patients, increase arch stability, and improve gait dynamics, with benefits largely attributed to optimized arch-mechanics parameters achieved through personalization[41]. Compared with traditional plaster-mold customization, 3D printing offers clear advantages in fabrication precision and reproducibility. It also enables rapid

iteration of various support-height and stiffness configurations, substantially enhancing the efficiency and adaptability of rehabilitation interventions.

Moreover, the programmable nature of lattice architectures enables distinct functional roles to be assigned to different regions within the same sole. Low-modulus lattice units can be placed in the heel to enhance cushioning; high-stiffness units can be deployed in the forefoot to improve propulsive efficiency; and graded lattice configurations in the midfoot can reinforce overall stability. This zonal-support strategy transcends the inherent homogeneity of traditional foam materials and provides a novel structural pathway for achieving personalized footwear designs.

1.4 Applications of Finite Element (FE) and Machine Learning (ML) in Footwear Biomechanics

In footwear research, the finite element (FE) method is widely employed to construct coupled foot–footwear models[42]. Using medical imaging modalities such as CT and MRI, together with 3D foot scans, researchers can generate individualized anatomical models and integrate them with footwear structures. These models typically incorporate detailed geometries and material properties of bones, soft tissues, ligaments, fascia, and insole or midsole components. As a physics-based modeling approach, FE enables high-resolution mechanical analysis of the foot–footwear system and provides access to internal stress and strain fields that are difficult or impossible to measure directly in experimental settings.

1.4.1 Foot–Footwear Coupled Modeling

A central challenge in footwear biomechanics is understanding the coupled interaction between the foot and the shoe. As illustrated in Figure 1.4.1, finite element (FE) modeling has become an effective tool for simulating this interaction, as it can accommodate the complexity of foot anatomy, nonlinear material behavior, and detailed foot–shoe contact conditions. By constructing three-dimensional FE models of the foot–footwear system, researchers can analyze internal tissue loading and pressure distribution within the shoe during locomotion, thereby elucidating how different footwear designs influence foot biomechanics. Previous studies have developed coupled FE models to simulate heel-strike cushioning in athletic footwear, successfully capturing the stress distribution arising from foot–insole interaction and validating the model predictions against experimental measurements[43]. Such models have been widely applied to diverse footwear types, including high-heeled shoes and mountaineering boots, enabling the identification of key design parameters that most strongly influence foot mechanical responses and providing valuable guidance for functional optimization. It is important to note, however, that due to the high complexity of model construction, most foot–shoe FE analyses require certain simplifications. Current challenges include improving model accuracy and computational efficiency, obtaining high-quality geometric and material data for the foot, defining physiologically realistic boundary and loading conditions, and conducting rigorous validation. Despite these limitations, FE-based foot–shoe coupled analysis has become an indispensable tool in studies of injury mechanisms and in the optimization of footwear design.

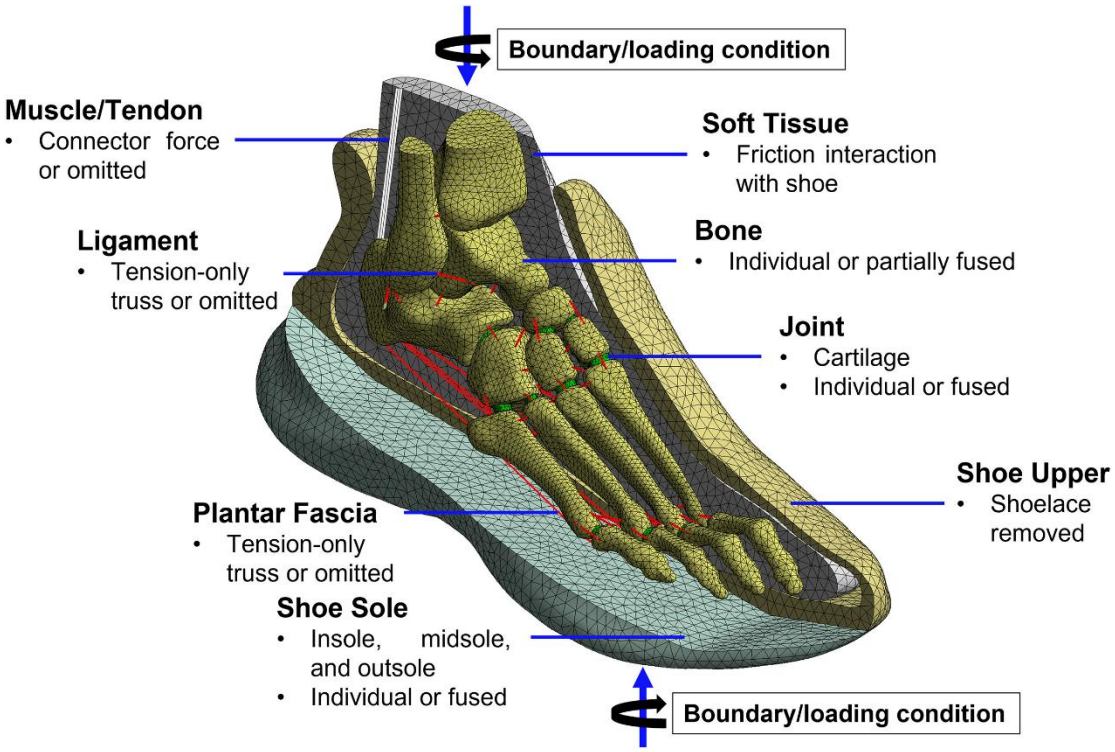

Figure 1.4.1 Schematic of the shoe–foot finite element model structure and mechanical boundary conditions.[42]

1.4.2 Prediction of Plantar Pressure and Tissue Stress

As noted previously, unfavorable concentrations of plantar pressure are closely associated with elevated risk of foot injuries, with abnormally high loads potentially contributing to conditions such as plantar fasciitis and diabetic foot ulceration. Traditionally, plantar pressure distribution is measured using pressure plates or instrumented insoles; however, FE simulation and ML-based prediction now provide powerful complementary tools for analysis and forecasting. The FE method enables mechanistic simulation of plantar-pressure formation based on the interaction between the foot and insole structures. For example, one study employed FE analysis to evaluate insole designs for patients with diabetic neuropathy, comparing materials and geometric configurations to determine their effects on peak stress[44]. Through virtual prototyping, the researchers identified customized designs capable of effectively reducing high-pressure regions. The findings demonstrated that FE simulation can accurately predict plantar pressure distribution and assess the efficacy of offloading interventions, thereby reducing the need for iterative trial-and-error approaches in clinical practice

On the other hand, machine learning methods have demonstrated strong data-driven advantages in the prediction of plantar pressure. As illustrated in Figure 1.4.2, Mun and Choi introduced a deep learning framework capable of reconstructing full plantar-pressure fields from a small number of

pressure sensors[45]. Using only nine sensing locations as input, their LSTM model predicted pressures at the remaining ninety points with a correlation coefficient of 0.98 and an error of approximately 7.9 percent. This approach opens the possibility for developing low-cost smart insoles that enable real-time plantar-pressure monitoring and early detection of abnormal loading patterns. Machine learning has also been applied to automated interpretation of plantar-pressure images. Deep convolutional networks have been used for regional segmentation and key-feature extraction from pressure heat maps, supporting the diagnosis of foot deformities and pathological gait patterns[46]. FE modeling and ML prediction offer complementary strengths. FE provides physics-based, high-fidelity computation of pressure distributions, allowing quantitative evaluation of how footwear modifies peak loads across plantar regions and enabling detailed assessment of stress in the plantar fascia, soft tissues, and articular cartilage. These capabilities are crucial for understanding the biomechanical implications of footwear design and its potential links to injury mechanisms. ML, in contrast, leverages large datasets to rapidly estimate pressure fields or classify foot conditions, offering efficient and practical tools for monitoring and assessing plantar-loading behavior.

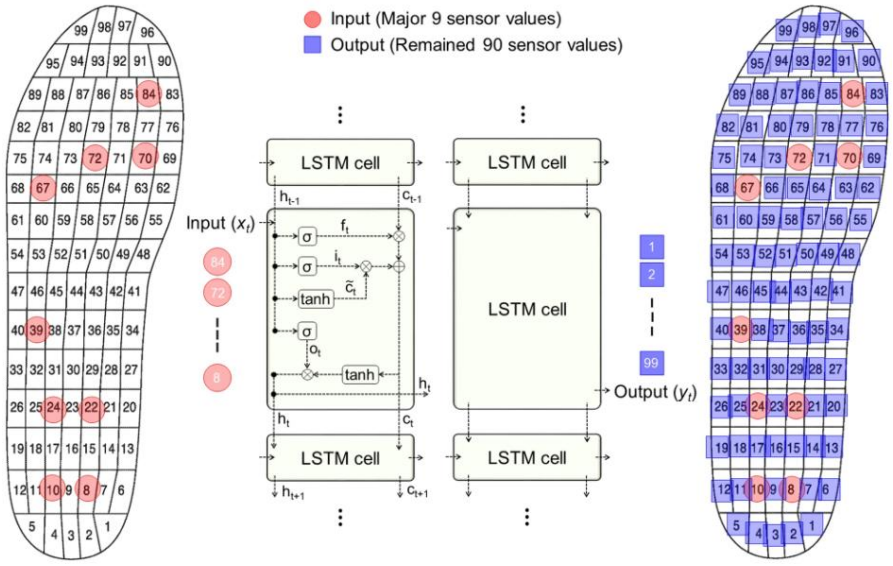

Figure 1.4.2 LSTM-based Deep Learning Model for Reconstructing Full Plantar Pressure Distribution from Sparse Sensors.[45]

1.4.3 Gait Simulation and Recognition

Gait simulation and gait recognition represent another key domain in footwear biomechanics research. FE modeling can be employed to simulate gait processes by integrating dynamic analyses or musculoskeletal models to evaluate how different footwear conditions influence walking and running mechanics. Such simulations enable assessment of how midsole stiffness and deformation

affect gait stability, energy expenditure, and overall locomotor performance. For example, engineers at the Massachusetts Institute of Technology developed a simplified modeling framework that uses human anthropometric data—such as height and body mass—together with midsole stiffness and elasticity to simulate gait patterns specific to a given shoe design[47]. The model predicts how footwear characteristics alter gait and identifies design configurations that may reduce metabolic cost or improve performance. This virtual testing approach provides valuable insights for optimizing midsole structures prior to physical prototyping.

Studies on gait stability have shown that reduced medial plantar pressure during walking may impair balance and increase fall risk in older adults[48]. Simulation-based analyses of how insole support influences arch loading can therefore provide valuable guidance for improving gait stability.

In contrast, machine learning offers clear advantages for gait recognition. ML models trained on wearable-sensor data or plantar-pressure distributions can automatically extract gait features for applications such as individual identification, gait classification, and abnormality detection[49]. For example, combining inertial measurement units with plantar-pressure arrays as model inputs enables classification of population-specific gait patterns or detection of pathological gait characteristics[46]. Other studies have applied deep learning to classify foot types (e.g., normal foot versus flat foot) from static plantar-pressure images, with ResNet-based models achieving markedly higher accuracy in detecting flatfoot compared with traditional footprint-index methods[50].

1.4.4 Data-Driven Optimization

Data-driven methodologies are rapidly emerging in footwear design and optimization, increasingly integrating with FE simulation to form intelligent design workflows. As noted earlier, traditional footwear development often relies on designer experience and iterative prototyping. The incorporation of FE analysis provides a quantitative foundation for parameter optimization, and the addition of ML techniques further accelerates this process.

In a series of studies published in Footwear Science, Material Strength and Applied Mechanics, npj Advanced Manufacturing, and the Journal of Biomechanics[44, 51–53], we proposed a personalized footwear design framework that combines FE simulation with machine learning. The approach begins by generating extensive mechanical-performance datasets for diverse 3D lattice midsoles or insole structures through FE simulation. These data are then used to train ML surrogate models, which, when integrated with FE outputs, enable rapid prediction and optimization of compressive behavior and deformation characteristics. This pipeline allows efficient exploration of the design space and identification of optimal structural configurations.

Similarly, other studies have employed genetic algorithms, particle swarm optimization, and related computational-intelligence methods to optimize insole or midsole structures, achieving objectives

such as reduced stress concentration and minimized structural mass[54].

Such digitally driven optimization exemplifies a “data-guided design” paradigm: ML models and optimization algorithms rapidly screen promising candidates within vast design spaces, while FE analysis provides high-fidelity evaluation of their mechanical performance. Together, these tools form a powerful framework for accelerating innovation in footwear engineering.

1.4.5 Advantages of FE and ML Methods and Their Integration Trends

The primary strength of the FE method lies in its explicit grounding in physical laws, which enables detailed mechanical characterization and produces results with strong interpretability. FE analysis can directly visualize how stresses within bones and soft tissues vary under different insole or footwear designs, thereby helping to elucidate injury mechanisms and guide design improvements. Unlike data-driven approaches, FE modeling does not require large volumes of prior data and can provide valid predictions even for new designs or extreme loading conditions. However, FE methods have notable limitations. Model construction and computation are resource-intensive, the workflow is complex, and predictions are highly sensitive to the accuracy of input parameters. Furthermore, FE results must be experimentally validated to ensure reliability.

The strength of ML methods lies in their ability to leverage large datasets and highly efficient algorithms, enabling rapid prediction and strong adaptability. Once trained, ML models can generate near–real-time outputs such as plantar-pressure distributions or gait classifications, which is of significant value for customized insole design and continuous gait monitoring. ML approaches can also capture complex nonlinear relationships and automatically extract patterns that are difficult for humans to discern, such as the combined effects of multiple parameters on foot loading. However, ML has inherent limitations. Its predictive performance depends heavily on the quality and diversity of the training data, and in the absence of physical constraints, it may yield unreliable or non-physiological predictions. Moreover, the internal mechanisms of many ML models function as a “black box”[55], making it challenging to interpret their biomechanical significance directly.

Integrating ML into the FE simulation workflow can substantially accelerate parameter identification and result processing. ML models may be used to rapidly fit material parameters or approximate portions of the simulation, thereby reducing computational time. Conversely, large-scale datasets generated through FE modeling can be used to train ML models, improving predictive accuracy in scenarios where extensive experimental data are unavailable. This synergy enables the development of digital twins that combine data-driven inference with physics-based modeling. In the context of 3D-printed footwear research, FE analysis can be employed to generate extensive

databases of midsole designs, while ML facilitates rapid performance evaluation and optimization. For smart insole applications, ML can adjust support characteristics in real time based on sensor data, whereas FE simulations can be used to assess the biomechanical consequences of such adjustments, enabling dynamically personalized protection.

The integration of FE and ML leverages the precision of physics-based modeling together with the efficiency of data-driven approaches, creating a complementary framework for footwear biomechanics research and application. This hybrid paradigm has the potential to advance intelligent footwear design and functional customization, providing a more robust scientific foundation for enhancing ergonomics and protecting foot health.

1.5 Research Objectives and Hypotheses

1.5.1 Limitations in Existing Research

Despite recent advances in the application of 3D-printed lattice structures for insoles and foot orthoses, several critical gaps remain in the current body of research.

Most existing studies on lattice-based footwear focus on localized pressure redistribution or the enhancement of single functional components, such as structural optimization for heel cushioning[38, 56] or arch support[23, 57], yet lack a comprehensive optimization framework that spans the entire plantar surface. This fragmented research approach limits the ability to account for interactions among different plantar regions, resulting in local improvements that often fail to translate into measurable enhancements in overall gait performance.

Moreover, many existing studies rely on static FE simulations or simplified experimental conditions[39], which limits their ability to capture the complex and time-varying plantar loading patterns that occur during gait. In my previous work[52], although we demonstrated that combined FE–ML modeling could achieve approximately a 44.45% reduction in plantar pressure, the optimization process was still based primarily on static loading scenarios and did not incorporate dynamic gait mechanics. In subsequent research[53], we proposed a metatarsal-pad design framework targeting forefoot overload and integrated dynamic biplanar X-ray imaging (DFIS, Taoimage, Shanghai, China) to achieve high-precision registration of bone and soft-tissue motion during locomotion, thereby improving the anatomical fidelity of the FE model under gait-relevant conditions. Although this study incorporated dynamic skeletal postures, the FE simulations were still performed at discrete time points rather than across the full gait cycle.

A further limitation in 3D-printed footwear research lies in the restricted controllability of structural parameters. Conventional lattice studies are often constrained by fixed unit-cell geometries or narrow parameter combinations[39, 58], resulting in insufficient structural degrees of freedom and limiting the ability to achieve high-precision adaptation for individualized needs[52]. Although our earlier work demonstrated that a dual-layer lattice metatarsal pad could enhance local tuning capacity[53], its controllable parameter range still falls short of meeting the nonlinear mechanical demands across the entire plantar surface.

Furthermore, current research generally lacks a closed-loop cycle that integrates design, validation, and optimization. Neither the existing literature nor my prior work has fully achieved dynamic coupling among structural parameters, gait responses, and individualized mechanical feedback under authentic gait conditions. As a result, the optimization process still retains a degree of “trial-and-error” behavior, leaving considerable room for improvement in both efficiency and robustness. Thus, despite meaningful advances in programmable lattice architectures, data-driven parameter

prediction, and localized pressure offloading, significant limitations remain. These include insufficient sample diversity, restricted structural degrees of freedom, the absence of dynamic gait validation, and the lack of a coordinated whole-plantar optimization framework.

1.5.2 Overall Research Objective

The overarching objective of this study is to establish a data-driven optimization framework for personalized lattice footwear. By integrating three-dimensional foot scanning, gait-pressure data, FE analysis, and ML methodologies, the framework forms a closed-loop pipeline encompassing data acquisition, structural modeling, optimization, and experimental validation. The goal is to transcend traditional footwear design paradigms that rely heavily on empirical judgment and iterative trial-and-error, thereby advancing the field from “average-based” manufacturing toward genuinely personalized design.

1.5.3 Specific Research Objectives

This study first examines lattice behavior at the unit-cell level by developing a series of representative parametric lattice models encompassing both strut-based and surface-based topologies. Through FE analysis, the mechanical characteristics of these architectures are systematically quantified, with particular attention to the effects of geometric parameters—such as cell size, strut thickness, porosity, and topology—on effective modulus, energy-absorption capacity, and buckling stability. Standardized lattice specimens are then fabricated and subjected to compression and cyclic-loading experiments to validate the consistency between simulation and physical performance. This phase aims to establish a robust unit-cell database that provides the mechanical foundation for subsequent personalized footwear modeling and optimization.

Experimental and clinical data will be collected through participant recruitment. Each participant will undergo laboratory assessments that include plantar-pressure measurement, ground reaction force recording, and motion-capture–based kinematic analysis, as well as three-dimensional foot scanning and medical imaging (CT). Using these multimodal datasets, individualized finite element models of the foot will be constructed, enabling precise reconstruction of the geometry and material properties of bones, soft tissues, ligaments, and the plantar fascia. The objective of this phase is to provide personalized boundary conditions for subsequent footwear design and to reproduce realistic foot-loading characteristics within the simulation environment.

Building upon the individualized foot models, corresponding footwear models will be developed, with the midsole segmented into functional regions such as the heel, forefoot, arch, and lateral midfoot. Differential lattice-parameter configurations will be assigned to each region according to

its biomechanical requirements. For example, high-porosity structures will be deployed in the heel to enhance cushioning; low-porosity, high-stiffness architectures will be used in the arch to strengthen support; and high-stiffness topologies will be incorporated into the forefoot to improve propulsive efficiency. FE simulations will then be used to conduct multi-objective optimization and validation of these region-specific designs, followed by laboratory gait testing to evaluate their mechanical performance and stability. Through this process, targeted optimization of each functional midsole region can be achieved.

1.5.4 Research Hypotheses

H1: The parametric design of lattice structures can substantially modulate the mechanical performance of footwear. By adjusting unit-cell topology, strut thickness, and porosity, it is possible to achieve programmable trade-offs among cushioning capacity, structural support, and propulsive assistance.

H2: Finite element models constructed from individualized foot morphology and gait data can accurately predict plantar-pressure distribution and internal tissue stress, and can capture biomechanical differences across footwear conditions, thereby providing a reliable physical foundation for personalized footwear design.

H3: Regionally differentiated lattice configurations in footwear—targeting the heel, forefoot, arch, and lateral midfoot—can achieve function-specific optimization, leading to marked improvements in plantar-pressure distribution and overall gait stability.

H4: An optimization framework that integrates finite element modeling with machine learning can significantly enhance computational efficiency while maintaining predictive accuracy. By establishing explicit mappings between design parameters and mechanical performance, this framework enables rapid design iteration and supports individualized footwear recommendations.

H5: Lattice footwear designs generated through simulation-based optimization will reproduce their predicted benefits in real gait experiments and will demonstrate superior performance compared with conventional footwear in both athletic and rehabilitative contexts.

2. Materials and methods

2.1 Participant Recruitment and Clinical Data Acquisition

2.1.1 Participant Profile and Inclusion Criteria

Three participants were recruited in this study: a healthy adult male (age 27 years, height 174 cm, body mass 75 kg, European shoe size 41.5), a female participant presenting with severe flexible pes planus (age 25 years, height 163 cm, body mass 55.5 kg, European shoe size 37), and a male participant diagnosed with Becker muscular dystrophy (BMD) accompanied by pathological flatfoot (age 26 years, height 175 cm, body mass 60 kg, European shoe size 42). The healthy male (HM) participant reported no history of musculoskeletal disorders in the lower limbs, exhibited normal gait patterns, and showed no apparent deformities, enabling him to complete all gait experiments independently. The flatfoot female (FF) demonstrated clinically confirmed arch collapse without acute injury, and the BMD participant presented stable ambulatory function under medical supervision, enabling all participants to complete the required gait acquisition procedures independently.

The collected biomechanical data were used for subject-specific parametrized lattice design and multi-objective optimization of individualized footwear prototypes. The inclusion of healthy, flatfoot, and pathological cases enables the evaluation of the proposed framework across distinct biomechanical conditions rather than relying on a single representative morphology.

2.1.2 Ethical Approval and Informed Consent

This study was approved by the University Ethics Committee prior to commencement (Approval No. TY2025071). All experimental procedures adhered strictly to the principles of the Declaration of Helsinki and relevant ethical guidelines for human-subject research.

Before participation, the research team provided all participants with a detailed explanation of the study objectives, experimental procedures, potential risks, and anticipated benefits. Written informed consent was obtained after ensuring full comprehension of the study requirements. For individuals with impaired decision-making capacity or those requiring guardian authorization, the consent form would be co-signed by a legal guardian or family member.

To protect privacy, all personal information was anonymized, and only essential demographic variables (age, height, body mass, and shoe size) were retained for analysis. All experimental data were stored on encrypted drives and were accessible exclusively to authorized members of the research team for use within the defined scope of the study. No data were shared with third parties. Through these measures, the study fully complies with both international and domestic standards

for participant rights protection, privacy security, and ethical data management. All 3 participants underwent comprehensive baseline biomechanical assessments, including three-dimensional foot scanning, gait data acquisition, and subject-specific finite element simulation and multi-objective optimization procedures. However, due to safety considerations and the increased physical demands associated with dynamic wearable validation, the final 3D-printed footwear fabrication and laboratory-based gait testing were conducted exclusively with the HM participant.

2.1.3 Experimental Tasks and Testing Environment

All experiments were conducted in the Human Movement Biomechanics Laboratory at Ningbo University, following standard requirements for gait-analysis research. The laboratory was equipped with a three-dimensional motion-capture system (Vicon, Oxford Metrics, UK), embedded force platforms (AMTI, USA), and a plantar-pressure measurement system (PEDAR, Novel GmbH, Germany). The testing area featured a non-slip surface with controlled room temperature and appropriate lighting to ensure experimental stability and participant safety.

All participants completed two categories of testing tasks. Static standing test: used to obtain baseline plantar-pressure distribution and characterize arch morphology. Walking test: each participant walked back and forth along the walkway at a self-selected comfortable speed. Plantar pressure, ground reaction forces, and lower-limb kinematics were recorded.

Before formal data collection, each participant performed 5–10 minutes of light walking to acclimate to the environment and equipment. During testing, participants were instructed to maintain a natural gait and avoid intentional modification of movement patterns. All measurements were conducted under standardized conditions, with adequate rest provided beforehand to prevent fatigue. A tight-fitting sports outfit was worn to ensure accurate tracking of motion-capture markers. Rest intervals of approximately 2–3 minutes were scheduled between trials to minimize fatigue effects. Any trial exhibiting abnormal movement or equipment malfunction was discarded and repeated.

2.2 Foot-Shape Scanning and Gait Data Acquisition

2.2.1 Foot-Shape Scanning

To capture the geometric and anatomical characteristics of each participant's foot, this study employed a combination of three-dimensional external foot scanning and medical imaging. The external foot contour was acquired using a Foot Scanner (OrthoBaltic, Kaunas, Lithuania), which completes high-resolution scans within seconds and generates detailed point-cloud data for footwear modeling and shape matching (Figure 2.2.1). Internal anatomical structures were obtained via computed tomography (CT), enabling reconstruction of bones, joint surfaces, and soft-tissue morphology to support finite element model development. The CT scans were acquired with a slice thickness of 0.25 mm, ensuring high image quality and fine anatomical detail. All three-dimensional datasets were exported in STL format to facilitate integration with CAD platforms and downstream finite element modeling workflows.

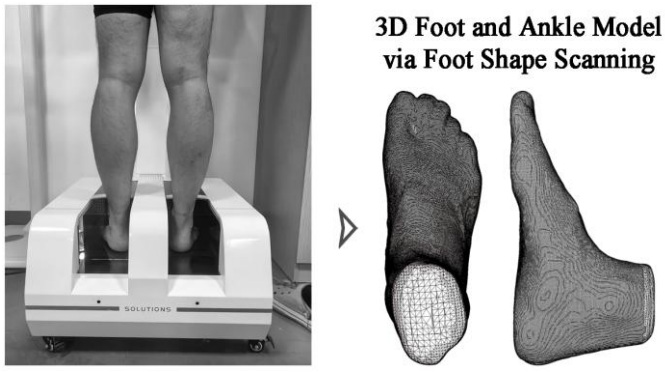

Figure 2.2.1 Applications of External Foot Scanning.

In determining the scanning posture, the substantial geometric differences of the foot under varying load-bearing conditions were taken into account[59]. Prior to formal data collection, three scanning conditions—non–weight-bearing, full–weight-bearing, and semi–weight-bearing—were compared. Although non–weight-bearing scanning (seated or with the foot elevated) captures the natural, unloaded morphology of the foot, it typically yields an artificially elevated arch height, which compromises fit accuracy[60]. Full–weight-bearing scanning, on the other hand, may underestimate arch height and midfoot curvature due to soft-tissue compression.

Balancing anatomical fidelity and measurement repeatability, this study adopted a semi–weight-bearing posture for foot scanning, with the participant standing naturally on both feet and distributing body weight evenly. This condition provides a realistic representation of foot geometry under typical daily loading.

2.2.2 Plantar Pressure Measurement

To characterize the dynamic loading patterns of the plantar surface during gait, plantar-pressure distribution was recorded using the PEDAR-X system (Figure 2.2.2). The system consists of ultra-thin flexible insole sensors connected to a portable data acquisition unit, allowing continuous measurement of plantar pressure under natural walking conditions. The PEDAR insoles incorporate capacitive sensing elements distributed across the major plantar regions and provide high flexibility and wearability, ensuring that the device does not interfere with each participant's natural gait.

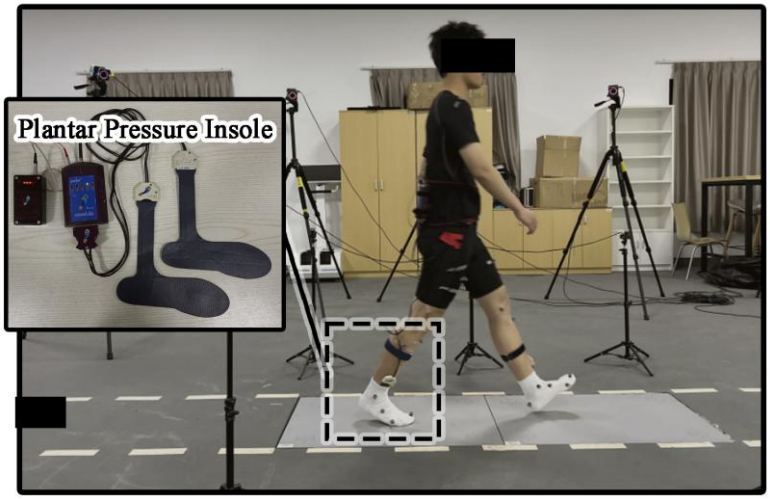

Figure 2.2.2 Plantar Pressure Measurement Using the PEDAR-X System and Experimental Gait Setup.

The system sampling frequency was set to 100 Hz to ensure sufficient temporal resolution for capturing walking dynamics and short-duration gait events. Prior to data collection, a two-step calibration procedure was performed. Zero calibration, conducted under no-load conditions to establish a baseline sensor output of zero. And load calibration, performed using standard weights applied at multiple points to align sensor output with actual pressure values and ensure measurement accuracy. To minimize sensor drift and environmental effects, calibration was repeated for each participant immediately before formal testing.

During the experiment, each participant wore standardized test shoes matched to foot size, with the PEDAR insoles placed inside the footwear. The participant were instructed to maintain a natural walking rhythm. A minimum of ten valid gait cycles was collected for each participant to ensure data representativeness and statistical reliability.

2.2.3 Gait Kinetics and Kinematics

Following previously published protocols[12, 61], reflective markers were placed on each participant's tight-fitting clothing and skin by an experienced researcher in accordance with the requirements of the OpenSim Gait2392 musculoskeletal model (Figure 2.2.3A). Each participant then completed approximately 5 minutes of warm-up walking at a self-selected comfortable pace to acclimate to the equipment and testing environment[62].

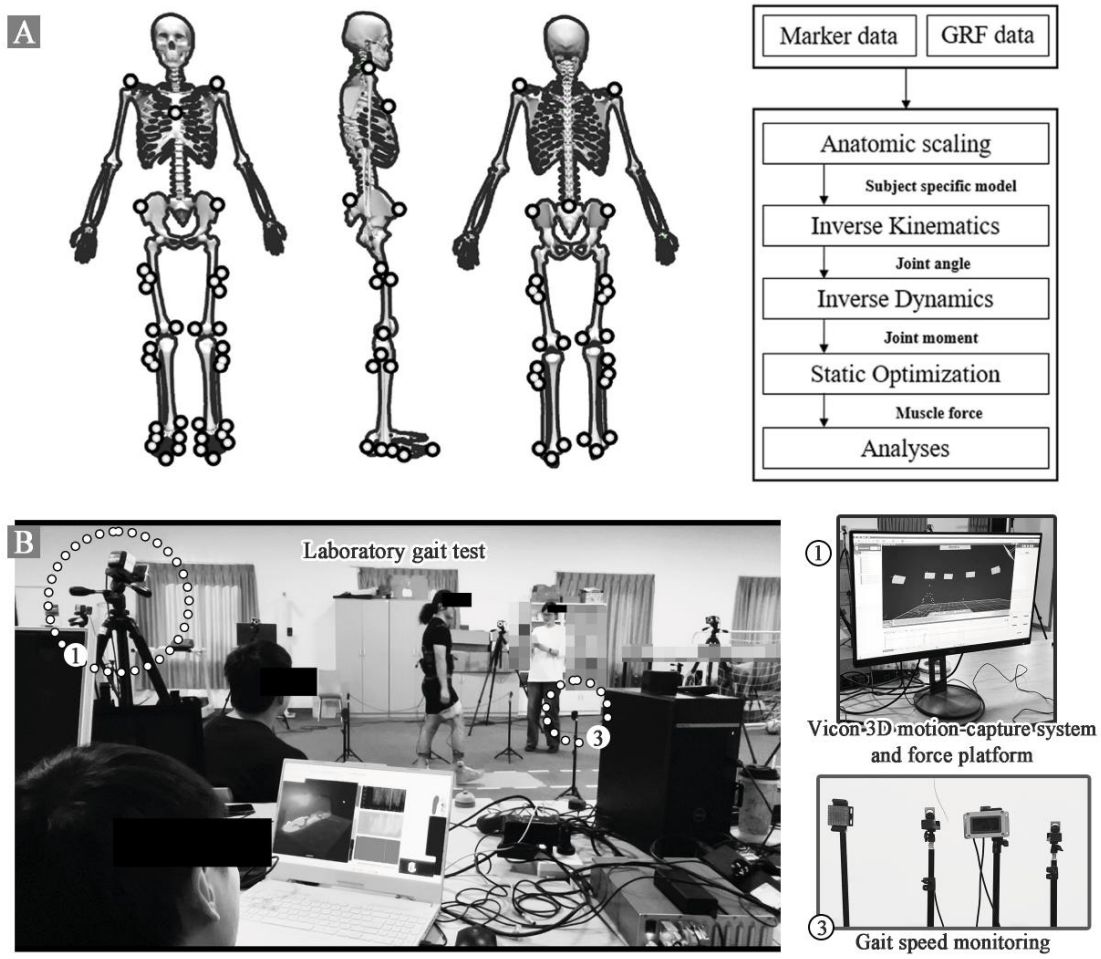

Figure 2.2.3 Workflow for Inverse Dynamics and Muscle Force Estimation and Experimental Gait Setup (A: Marker Placement and OpenSim Pipeline; B: Laboratory Gait Testing Setup).[12]

Ground reaction forces were recorded using two embedded three-dimensional force platforms at a sampling frequency of 1000 Hz, capturing vertical, anterior–posterior, and medial–lateral components of foot–ground interaction during walking. Simultaneously, kinematic data were collected using a 10-camera optical motion-capture system at 200 Hz (Figure 2.2.3B). Walking speed was self-selected and monitored using photocells positioned along the walkway. Each walking trial was repeated until a complete and valid dataset was obtained. A total of 30 valid gait cycles were collected for each participant. Of these, 80% were retained for analysis, while three trials with

relatively faster speeds and three with slower speeds were excluded to improve data consistency and reliability.

In OpenSim (version 4.5, National Center for Simulation in Rehabilitation Research, Stanford, USA), the musculoskeletal model was scaled by an experienced researcher using reflective marker trajectories and anthropometric measurements to match each participant's body dimensions. The maximum allowable deviation between experimental and virtual marker positions was set to < 0.01 m (Figure 2.2.3A). Inverse kinematics and inverse dynamics were subsequently solved, followed by static optimization—minimizing the sum of squared muscle activations—to estimate muscle forces[9, 12, 61]. For each participant, the time series of ground reaction forces and lower-leg muscle forces from 24 valid gait cycles were time-normalized to 0–100% of the gait cycle. The mean curves were then computed and used as boundary conditions for the subsequent finite element analyses.

2.2.4 Data Preprocessing and Normalization

The raw experimental signals inevitably contained noise and artefacts, which could introduce bias if used directly in subsequent analyses. Therefore, filtering and smoothing procedures were applied prior to data processing. Kinematic and kinetic signals were filtered using the built-in low-pass filters in OpenSim's Inverse Kinematics (default 6 Hz) and Inverse Dynamics tools, respectively, to attenuate high-frequency noise and improve the accuracy of joint-angle and joint-moment calculations.

Given the natural variability in gait cadence across participants and trials, all experimental data were time-normalized. Initial contact of the dominant foot was defined as 0%, and toe-off as 100%, standardizing the entire stance phase to a 0–100% scale. All kinematic, kinetic, and plantar-pressure signals were interpolated and resampled along this normalized time axis (standardized to 101 points), enabling consistent comparison and statistical analysis across participants and testing conditions.

To ensure consistency across multimodal datasets, the motion-capture system (200 Hz), force platforms (1000 Hz), and PEDAR plantar-pressure system (100 Hz) were synchronized during data acquisition. A unified trigger signal initiated all devices simultaneously, and post-processing alignment was performed using timestamps and trigger markers.

Data streams with differing sampling frequencies were resampled to a common temporal resolution of 100 Hz using linear interpolation. The resulting synchronized dataset—comprising joint kinematics, ground reaction force components, and plantar-pressure distributions—served as the consolidated input for subsequent finite element modeling, machine learning analysis, and experimental validation.

2.3 Parametric Lattice Footwear Modeling

2.3.1 Parametric Lattice Design

In this study, parametrized lattice architectures were incorporated into the full midsole as the primary load-bearing and functional-tuning structures. By exploiting programmable geometries, the lattice enables quantitative modulation of macroscopic cushioning, support, and propulsion properties—an approach described in our recent work[52, 53]. Lattice modeling was performed using nTopology 5.22.2 (New York, USA; hereafter referred to as nTop). As illustrated in Figure 2.3.1, all lattice configurations were constructed from cubic unit cells with dimensions of 10 × 10 × 10 mm. The geometry of each unit cell was governed by a set of adjustable parameters (A, B, T, P, θ). Parameters A and B control the spatial positions of key nodes that define the two-dimensional cross-sectional contour, with different combinations corresponding to distinct topological classes: A < B produces a honeycomb-like structure, A > B generates a re-entrant topology, and A = B yields a rectangular configuration.

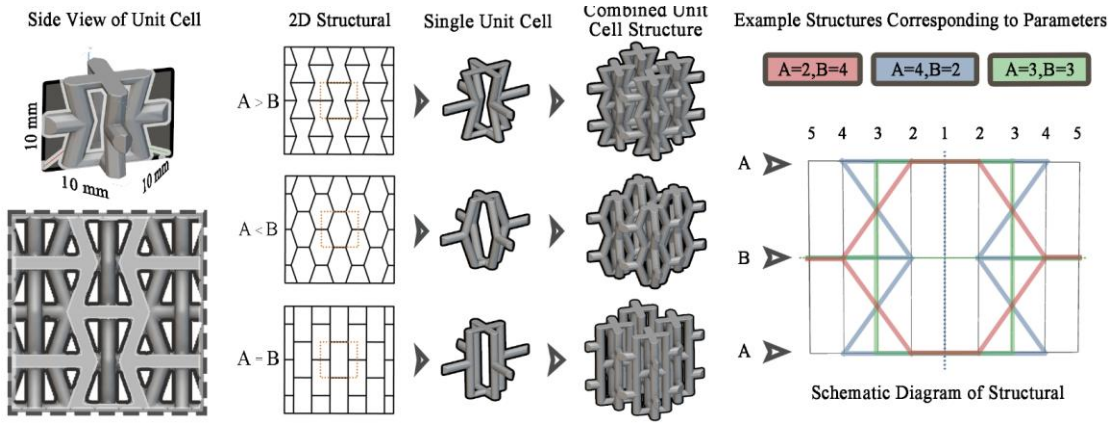

Figure 2.3.1 Topology Diagrams of Honeycomb, Re-entrant, and Rectangular Unit-Cell Structures Derived from A, B Parameters.

Honeycomb structures offer advantages in low weight and high specific strength, making them suitable for overall mass reduction. Re-entrant architectures exhibit negative Poisson's ratio behavior, undergoing lateral contraction under compressive loading, which enhances cushioning performance and conformability. Rectangular topologies, characterized by their geometric simplicity and regularity, facilitate controlled tuning and mechanical analysis. Incorporating different topologies into specific midsole regions enables targeted functional allocation. The thickness parameter (T) governs strut diameter, with increasing T yielding higher effective stiffness and load-bearing capacity. T also influences porosity (P), which reflects the void fraction of the

lattice and serves as a key determinant of lightweight performance and energy absorption. It is important to note that lattice structures are inherently anisotropic, exhibiting direction-dependent mechanical responses. Therefore, in this study, structural degrees of freedom were further expanded by rotating the unit cell—adjusting the orientation angle (θ) around the three spatial axes (Figure 2.3.2). By tuning A, B, T, P, and θ, the design space can theoretically span a broad continuum of mechanical behaviors, ranging from soft, highly compliant cushioning to stiff, supportive configurations.

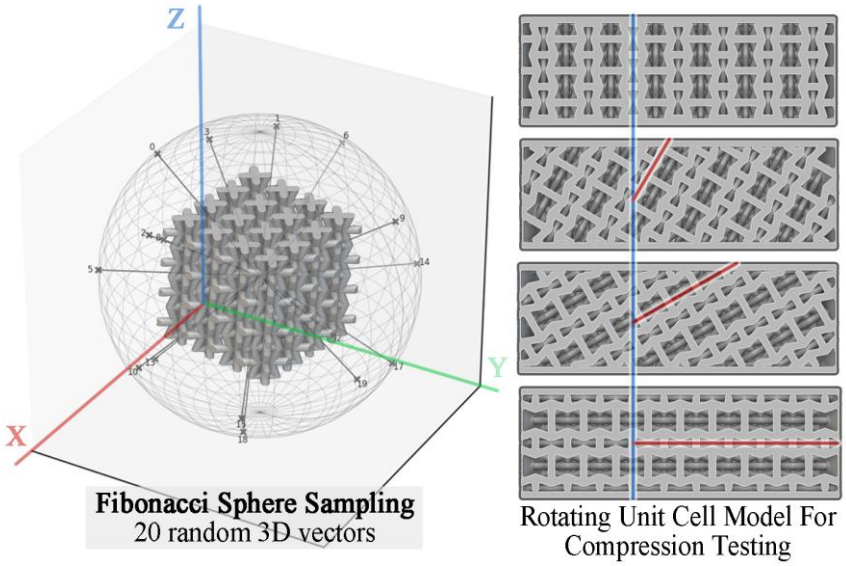

Figure 2.3.2 Fibonacci Sphere–Based Generation of 3D Orientations and Rotated Unit-Cell Models for Compression Testing.

2.3.2 Modeling Software and Design Workflow

Foot-shape STL data acquired under the semi–weight-bearing condition, together with CT-derived anatomical structures, were first imported into Geomagic Studio (Geomagic, North Carolina, USA) for surface reconstruction, defect repair, and topology inspection. Coordinate systems were unified, and self-intersections and mesh holes were eliminated to ensure geometric integrity. Subsequently, the processed foot geometry was imported into SolidWorks (Dassault Systèmes, Massachusetts, USA) to generate a conforming exterior shell and assembly interfaces. As illustrated in Figure 2.3.3, the baseline midsole model was reconstructed directly from a 3D scan of a standard running shoe. The geometry was then scaled to match each participant's foot length and width. During this process, non-essential geometric features unrelated to midsole mechanics—such as decorative patterns and outsole tread details—were removed, retaining only the core contours of the midsole and outsole as the boundary framework for lattice infill. To establish medial-arch support, the midsole geometry was locally thickened along the medial plantar curve extracted from each participant's semi–weight-

bearing foot scan. Specifically, reinforcement was applied along the normal direction from the navicular region to the proximal first metatarsal, forming a continuous structural support foundation for the arch.

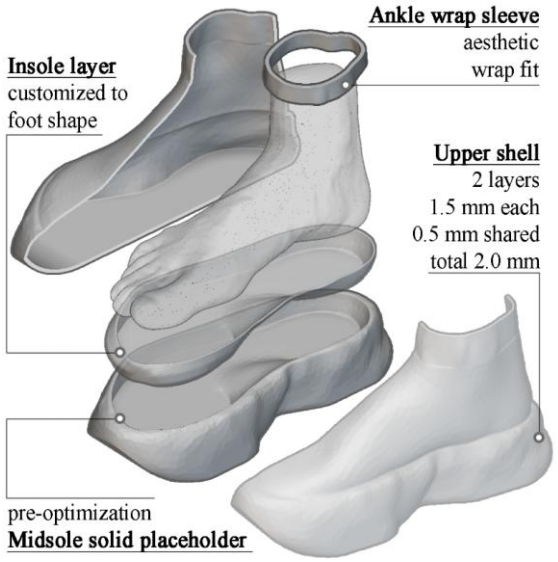

Figure 2.3.3 Layered Structure of Upper Shell, Insole Layer, and Pre-Optimization Midsole Model.

The lattice infill was generated and parametrically assembled in nTop, after which the complete model was imported into Ansys Workbench (ANSYS, Inc., Canonsburg, Pennsylvania, USA) for finite element analysis. Where required, the FE simulations were subsequently integrated with machine learning models to enable surrogate modeling and optimization.

2.3.3 Functional Zoning of the Footwear Midsole

As illustrated in Figure 2.3.4, the full midsole was partitioned into four functional regions comprising the heel, medial arch, lateral midfoot, and forefoot. The partitioning was performed in a subject-specific manner based on anatomical landmarks and plantar-pressure distribution patterns obtained during baseline gait trials. The boundaries of these zones were determined using plantar-pressure heat maps together with anatomical landmarks, including the calcaneal tuberosity, navicular point, and the heads of the first and fifth metatarsals. Within the unified exterior shell, each region was assigned an independent set of continuous parameter fields (A, B, T, P, θ). The overall design followed a system-level objective of achieving cushioning, stability, and propulsion, with each zone contributing distinctly to these functional targets.

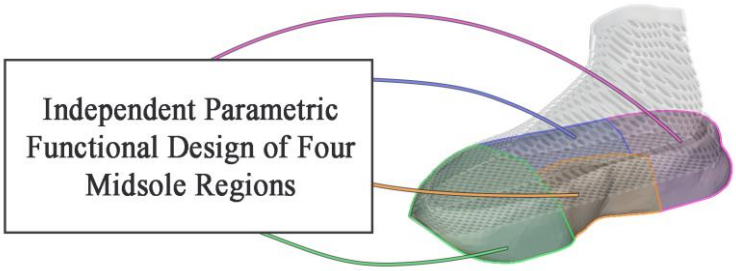

Figure 2.3.4 Parametric Design of Four Functionally Segmented Midsole Regions.

During the initial contact phase of gait, the heel region is primarily responsible for impact attenuation and is typically subjected to high peak pressures and elevated vertical loading rates. Inadequate cushioning can result in impact forces propagating proximally along the lower-limb kinetic chain, increasing instantaneous loads on the tibia and knee and potentially contributing to fatigue-related discomfort. Consequently, the structural parameters in this region must be configured to reduce peak pressure and modulate loading rate as much as possible, while maintaining adequate stability.

During late stance and toe-off, when force is transferred distally from the proximal segments, the forefoot plays a central role in propulsion. Accordingly, the structural design of this region prioritizes enhancing propulsive capacity. The relevant lattice parameters are optimized to improve energy storage–release efficiency and push-off performance; plantar pressure during this phase is not included as an optimization target.

The arch is essential for maintaining lower-limb stability and redistributing loads, and individuals at risk of arch collapse require additional structural support. The medial longitudinal arch bears load-sharing and elastic energy–storage functions during mid-stance; excessive collapse elevates plantar fascia tension and overloads medial structures. The lattice configuration in this region must therefore provide sufficient longitudinal support under compression while preserving necessary deformation to maintain conformity with the arch.

The lateral midfoot cooperates with the arch to provide mediolateral stability during gait, functioning as a “guiding rail” that limits excessive pronation or supination. If the structure in this region is either too compliant or too stiff, it may induce gait instability or exacerbate lateral deviation, increasing the control demands placed on the ankle joint. Thus, the lateral midfoot lattice must balance moderate flexibility with enhanced constraint against inversion–eversion, supporting whole-foot balance and reducing the risk of ankle-related injuries.

2.3.4 Sensitivity Assessment of Lattice Dimensions

To establish a mechanically reliable database of lattice structures with controllable geometric

parameters, this study used the unit cell as the fundamental module and constructed standardized hexahedral specimens. A peripheral bounding frame was added to each specimen to enhance numerical stability and mitigate edge effects. Because anisotropic unit cells exhibit markedly different external geometries depending on their orientation, using traditional “fixed-volume” samples would inevitably produce inconsistent distributions of effective material volume[63].

To ensure comparability across configurations, a “fixed cell count” modeling strategy was adopted. Specifically, a set of geometric parameters was randomly drawn from the parameter space, and a strut thickness was randomly assigned for sensitivity analysis. The specimen height was fixed at three unit cells (corresponding to a midsole thickness of approximately 30 mm), from which five lattice layouts were generated: 3×3×3, 4×4×3, 5×5×3, 6×6×3, and 7×7×3.

Recognizing that finite element results may be sensitive to mesh resolution, a two-factor experimental design was implemented to simultaneously evaluate the influence of cell count and mesh density on simulation outcomes.

2.4 Finite Element Modeling and Dynamic Gait Simulation

2.4.1 Finite Element Model of the Foot

As illustrated in Figure 2.4.1, each participant's CT images were imported into Mimics 21.0 (Materialise, Leuven, Belgium). Using grayscale thresholding, the images were segmented slice-by-slice to isolate the bony structures (including the metatarsals, phalanges, talus, calcaneus, etc.), soft tissues, ligaments, and the plantar fascia. The segmented anatomical components were then exported to Geomagic for surface smoothing and reconstruction, after which the processed geometries were reassembled in SolidWorks to generate the complete foot model.

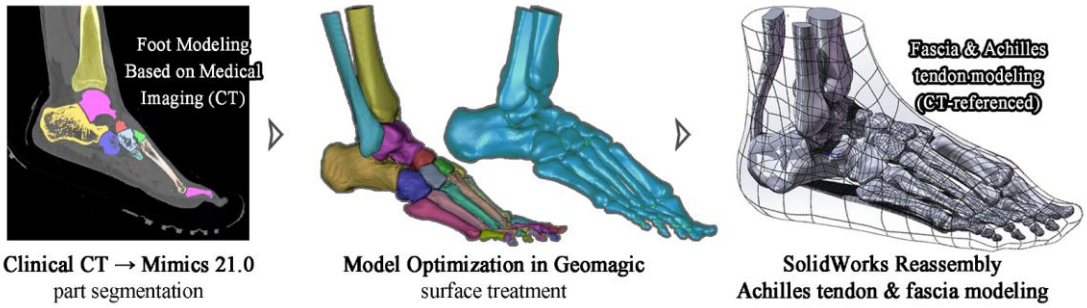

Figure 2.4.1 Segmentation, Optimization, and Reconstruction of the Foot FE Model from CT Data.

To simplify contact computations, the distal, middle, and proximal phalanges were modeled as a single rigid-body segment[53]. Following established literature[2, 64], ligament structures were incorporated into the foot model, and their attachment sites were manually adjusted with reference to each participant's CT images (Figure 2.4.2). Articular cartilage and connective tissues between adjacent bones were represented using solid elements with a thickness of approximately 2–3 mm. The plantar fascia and Achilles tendon were assigned thickness values of 3.3 mm[65] and 6.3 mm[66], respectively. Mesh generation for all anatomical components was performed in Ansys Workbench.

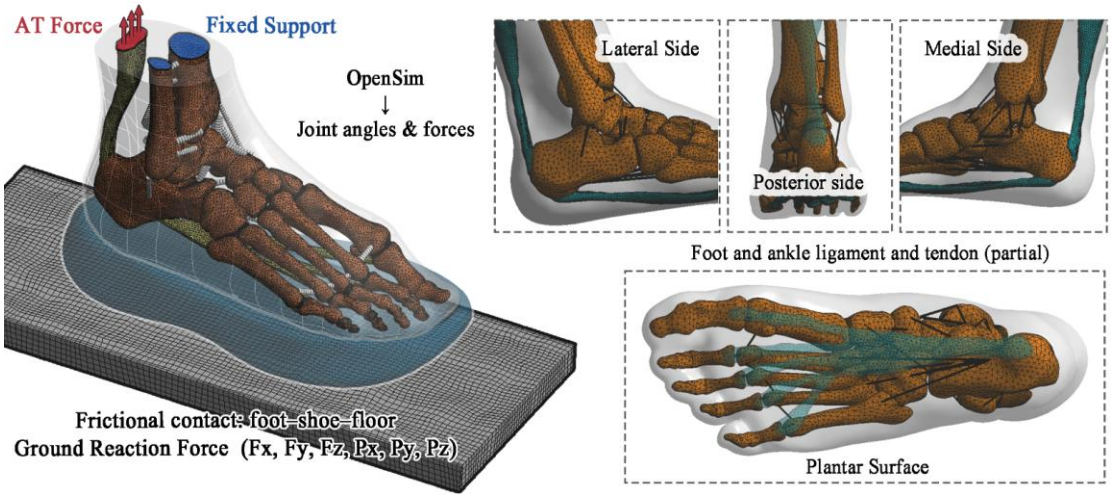

Figure 2.4.2 Schematic of Mechanical Boundary Conditions and Anatomical Structures in the Foot Finite Element Model.

Different tissues were assigned material properties representative of their biomechanical behavior. The bones were modeled as isotropic, linearly elastic materials, whereas the soft tissues, Achilles tendon, and plantar fascia were described using hyperelastic constitutive models to capture their large-deformation characteristics. Ligaments were represented using two-node, tension-only truss elements. Because bone stiffness is substantially higher than that of surrounding soft tissues, internal distinctions between cortical and trabecular bone have minimal influence on global mechanical responses; therefore, no differentiation between these bone types was made in this study[52]. A summary of the material parameters used in the model is provided in Table 1.

Table 2.4.1 Material Properties of Model Components.

Component	**Property**	**Nodes**
Bone[67, 68]	3D-tetrahedra; E: 17000 MPa; ν: 0.3; Density 1990 kg/m3	36576
Cartilage	3D-tetrahedra; E: 1 MPa; ν: 0.4	2463
Soft Tissue[57]	3D-tetrahedra; E: 0.15 MPa; ν: 0.45; Density 950 kg/m3	8760
Floor	3D-tetrahedra; E: 14200 MPa; ν: 0.1; Density 1000 kg/m3	5535

Footwear	3D-tetrahedra; Hyperelastic Material; eSun eTPU (95A)	5535
Primary Ligaments[69]: Anterior talofibular, Anterior tibiofibular, Calcaneofibular, Posterior talofibular, Tibionavicular, Spring ligament (plantar calcaneonavicular), Tibiocalcaneal, Anterior tibiotalar, Posterior tibiotalar	Two-node tension-only truss; Hyperelastic Material; Cross-section area: 1.5 - 5.91 mm2	-
Other Ligaments[67, 68]: Cervical ligament, Talonavicular, Posterior interosseous, Interosseous membrane	Two-node tension-only truss; Linear Elastic Material; E: 264.8 MPa; Cross-section area: 1.784 mm2	-
Plantar Fascia[67, 68, 70]	Two-node tension-only truss; Hyperelastic Material; Young's modulus: 0-700 MPa; Cross-section area: 290.7 mm2	3522

2.4.2 Finite Element Model of the Footwear

The core of the footwear FE model is the parameterized lattice embedded within the midsole, whose mechanical response governs the global cushioning and support characteristics. Following the geometric definitions and functional partitioning described in Section 2.3, spatial segmentation of the heel, medial arch, lateral midfoot, and forefoot regions was first performed in nTop. A cubic lattice cell with edge length 10 × 10 × 10 mm was adopted as the standard unit. The lattice domains were then Boolean-united with the outer shell to produce a closed, watertight, and mesh-compatible solid suitable for FE preprocessing (Figure 2.4.2).

The midsole was assigned the material properties of a flexible thermoplastic polyurethane (TPU 95A; eSun Industrial Co., Ltd.), with a density of 1.21 g/cm³ and an ultimate tensile strength of approximately 35 MPa. To accurately characterize the nonlinear behavior of the material under large deformations, uniaxial tensile and compressive tests were conducted to obtain the stress–strain response. The experimental data were subsequently fitted using a hyperelastic constitutive model, which was applied in the FE definition of the TPU material.

2.4.3 Foot–Footwear Coupled Model and Boundary Conditions

In the coupled FE model, surface-to-surface contact was defined between the plantar soft tissue and the footwear interface. To enhance numerical stability and better approximate in vivo contact behavior during gait, the plantar–insole friction coefficient (μ) was set to 0.5, consistent with previously reported measurements of barefoot–insole interactions[52]. A penalty-based contact

algorithm was employed, allowing limited tangential slip to realistically capture the relative motion between the foot and footwear throughout stance. Proximal constraints were imposed on the superior ends of the tibia and fibula, fixing all degrees of freedom. The ankle joint was modeled using frictionless contact to permit physiologic ranges of rotation. Bonded contact definitions were applied between bones and cartilage surfaces, as well as between ligaments and their anatomical attachment sites, ensuring structural coherence while representing the passive stabilizing role of joint and arch-supporting tissues during gait.

In the finite element model, surface-to-surface contact was defined between the plantar soft tissues and the footwear interface. To enhance numerical stability and better approximate in vivo contact mechanics during gait, the friction coefficient between the foot and the insole (μ) was set to 0.5, consistent with previously reported measurements from barefoot–insole interaction experiments. A penalty-based contact formulation was employed, permitting limited tangential slip to more realistically capture the relative motion occurring between the plantar surface and the footwear throughout stance. Proximally, the superior ends of the tibia and fibula were fully constrained, restricting all degrees of freedom. The ankle joint was modeled using frictionless contact to accommodate its physiological range of motion. Bonded constraints were applied between bones and cartilage, as well as between ligaments and their anatomical attachment sites, ensuring structural integrity while representing the passive stabilizing contributions of joint tissues and the medial arch during gait.

The dynamic loading conditions were derived entirely from laboratory measurements (Figure 2.2.3). The three-dimensional ground reaction forces recorded by the force platforms were applied to the inferior surface of the ground in a time-resolved manner, reproducing the interaction between the footwear and the floor during natural walking. Concurrently, a musculoskeletal model constructed in OpenSim was used to perform inverse dynamic analyses, yielding the forces of major muscle groups—including the resultant Achilles tendon force and the tibialis anterior force—which were subsequently mapped to their anatomical attachment sites within the finite element model. All time-series signals were aligned to gait events, normalized to the stance phase (0–100%), and resampled before being used to drive the transient contact analysis. Through the integration of these contact definitions, boundary constraints, and dynamic loading inputs, the coupled foot–footwear model was able to replicate the principal mechanical interactions occurring between the plantar tissues and the footwear throughout the gait cycle. This framework provides a robust computational platform for subsequent personalized optimization of lattice structures and for evaluating their functional effectiveness.

Through the integration of these contact definitions, boundary constraints, and experimentally derived dynamic loading conditions, the coupled foot–footwear FE model was able to reproduce, to

a substantial degree, the mechanical interactions between the plantar tissues and the shoe throughout the gait cycle. This model establishes a rigorous computational foundation for the subsequent personalized optimization of the lattice midsole structures.

2.4.4 Dynamic Biplanar X-ray Registration

To enhance the anatomical accuracy of bone positioning in the foot model, dynamic biplanar fluoroscopy (DFIS) was used to capture images of each participant's foot during standing and walking. As illustrated in Figure 2.4.3, key anatomical features were extracted via image segmentation and edge detection, and the three-dimensional foot model was subsequently registered to the coronal and sagittal plane projections. Fine manual adjustments of bone and soft-tissue geometry were performed to ensure spatial consistency within the global coordinate system. This DFIS-based registration technique is widely regarded as the gold standard for tracking in vivo bone motion and provides critical support for the validation and refinement of finite element models[68].

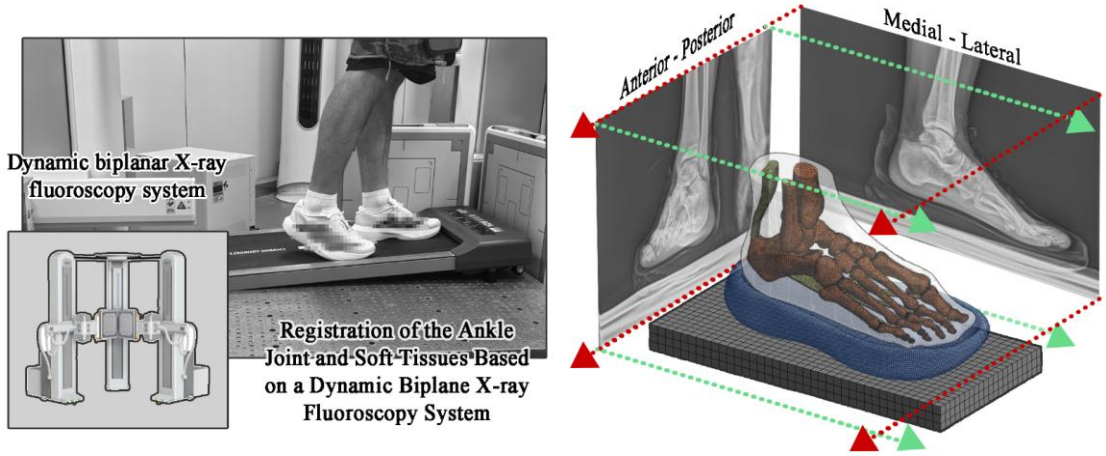

Figure 2.4.3 3D Registration of the Ankle Joint and Soft Tissues Using a Dynamic Biplane X-ray Fluoroscopy System.

2.4.5 Mesh Convergence and FE Model Validation

To ensure the stability and reliability of the FE analyses, a mesh convergence study was conducted. The element density within the lattice structures and the plantar soft tissues was progressively refined, and the corresponding variations in peak plantar pressure were evaluated across mesh configurations. Convergence was deemed achieved when the change in peak pressure fell below 5%, after which a mesh resolution balancing computational efficiency and numerical accuracy was selected. This procedure ensured that the dynamic gait simulations were both computationally tractable and biomechanically credible.

For external validation, experimental measurements were compared against model predictions. Dynamic plantar pressure distributions were recorded using the PEDAR system while each participant walked in standard footwear, and the resulting pressure maps were contrasted with those obtained from the FE simulations. This comparison enabled quantitative assessment of the model's predictive accuracy.

2.5 Machine Learning–Based Footwear Parameter Optimization

2.5.1 Design Variables and Optimization Objectives

The geometric attributes of the parameterized lattice structures served as the primary design variables, defining the search space for exploring their influence on overall footwear performance. As illustrated in Figure 2.5.1, midsole optimization was structured around three functional objectives: cushioning, stability, and propulsion. Cushioning performance was quantified by the peak equivalent stress within the heel soft tissues predicted by the FE simulations. Stability was assessed using the calcaneal pitch angle[71, 72], defined as the angle between the calcaneal longitudinal axis and the ground; a larger angle indicates reduced arch collapse and enhanced medial–longitudinal-arch support. Propulsive capability was evaluated using the peak ground-reaction force at the tibial cross-section during the push-off phase derived from the FE model, representing the effectiveness of forefoot energy transfer.

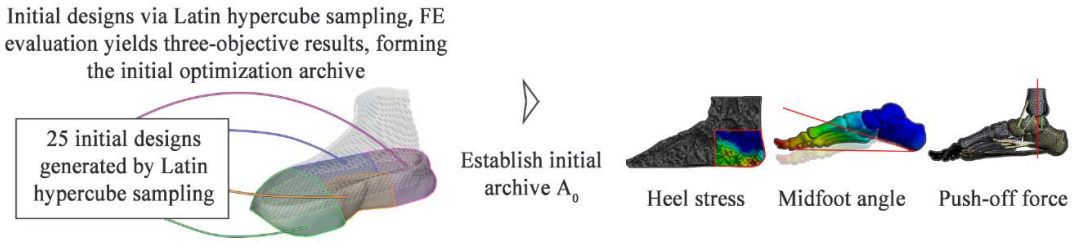

Figure 2.5.1 Initial Designs via Latin Hypercube Sampling and Three-Objective Finite Element Evaluation Workflow.

2.5.2 Lattice Property Dataset and Structure–Performance Prediction Model

The outputs of the FE simulations served as the performance indicators describing the mechanical behavior of each lattice configuration under compressive loading. The primary metrics extracted were structural deformation measures—including vertical displacement and lateral expansion—which characterize the morphological response of the lattice during compression. To construct a mechanics-informed database linking controllable geometric parameters to structural performance, a series of hexahedral “material blocks” composed of lattice unit cells were first generated in nTopology. A boundary encapsulation frame was added around each block to enhance numerical stability and mitigate edge effects. This design ensured that the recorded responses predominantly reflected the intrinsic mechanical properties of the lattice topology rather than artifacts induced by

boundary irregularities.

A mapping was established between the geometric parameters and the deformation-based performance metrics, forming the foundational dataset for subsequent machine-learning modeling and optimization. Because the raw samples were obtained only at discrete parameter values (e.g., A, B ∈ {1, 2, 3, 4, 5}), additional random sampling within the continuous parameter ranges was performed to achieve a more uniform distribution of data. As illustrated in Figure 2.5.2, and following our previously published workflow[53], a two-stage Gaussian Process Regression (GPR) framework was adopted. In the first stage, the geometric parameters (A, B, T) were mapped to the resulting porosity (P). In the second stage, (A, B, P) together with the lattice rotation angle θ (about the three principal axes) were used as input features to independently train predictive models for the vertical displacement (Dz) and lateral deformation (Dx, Dy) under compressive loading. Trained on the FE-generated dataset compiled during the initial phase, this approach yielded a comprehensive and well-balanced database encompassing diverse topologies and parameter combinations. The resulting surrogate models demonstrated strong generalization capacity and provided a robust basis for downstream optimization of personalized lattice-based footwear structures.

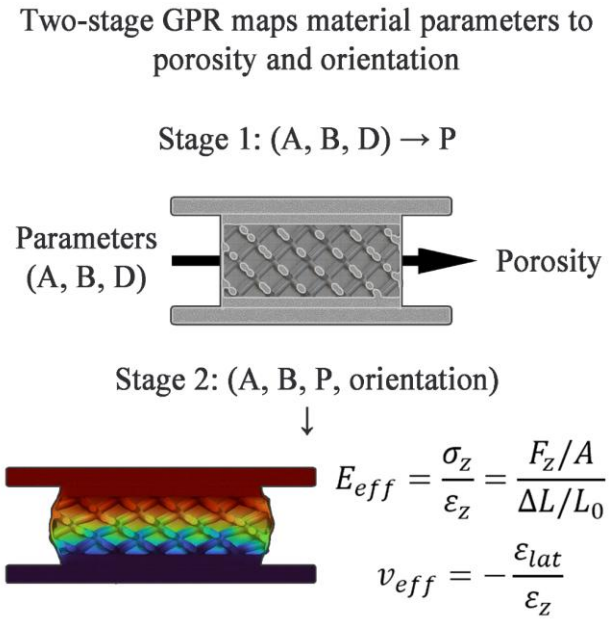

Figure 2.5.2 Two-Stage GPR–Based Surrogate Modeling Workflow for Mapping Lattice Parameters to Mechanical Responses.

Building upon the lattice property dataset and the trained surrogate models, a machine-learning–based optimization framework was developed for footwear parameter tuning. The optimization employed a two-stage GPR strategy analogous to the lattice-level modeling: the first stage learned the geometric mapping (A, B, T) → P, while the second stage implemented a hybrid neural

architecture—combining a convolutional neural network (CNN) to extract local patterns from the compressive response curves and a fully connected neural network (FCNN) to encode parameter features. Using (A, B, P, θ) as inputs, the model independently predicted the mechanical responses (Dx, Dy, Dz). Model uncertainty and predictive accuracy were evaluated through cross-validation across the full workflow. Additional data augmentation was then incorporated to regularize the parameter space, after which the surrogate models were retrained to improve stability and generalization performance.

2.5.3 Footwear Parameter Optimization

To enable systematic optimization of the multi-region midsole design, a formal parameterization of the footwear structure was established. Let the midsole design vector be defined as:

$$x = \{x_{heel}, x_{arch}, x_{midfoot}, x_{forefoot}\} \tag{1}$$

Each regional parameter set is defined as:

$$x_{(.)} = (A, B, T, P, \theta) \tag{2}$$

For each participant, a subject-specific multi-objective optimization problem was formulated within a unified computational framework, while allowing the objective functions to reflect individual biomechanical priorities. For the HM and FF participants, the optimization simultaneously minimized peak equivalent stress in the heel soft tissues, maximized midfoot stability (quantified by the calcaneal pitch angle), and maximized forefoot propulsive capacity (represented by the peak anterior component of the tibial reaction force during push-off). In contrast, for the BMD participant, the third objective was redefined as minimizing peak forefoot stress rather than maximizing propulsion, in order to reduce excessive localized loading under pathological constraints. The formal optimization problem is expressed as:

$$\text{HM\&FF: } min_x[\sigma_{heel}^{max}, -R_{force}^{max}, -Stablize] \tag{3}$$

$$\text{BMD: } min_x[\sigma_{heel}^{max}, \sigma_{forefoot}^{max}, -Stablize] \tag{4}$$

The optimization workflow adopted a closed-loop strategy that combined surrogate-based pre-screening with multi-objective Bayesian iterative refinement. For each participant, an initial set of 25 full-foot design samples was generated using Latin hypercube sampling. Their geometric and material parameters were evaluated through FE simulation, and the resulting outputs were used to

construct the initial database. As illustrated in Figure 2.5.3, each subsequent iteration proceeded as follows: a candidate pool was assembled through hybrid sampling that drew both from the vicinity of the current Pareto front ("local neighborhood sampling") and from the unexplored global design space. Candidates were then ranked according to their mean hypervolume contribution (HVC_mean), and the top five designs were selected for FE evaluation. After simulation, these new samples were added to the archive, and both the Pareto front and the uncertainty field were updated. The optimization terminated once no measurable hypervolume improvement was observed over three consecutive iterations (15 newly evaluated samples). Upon convergence, a subject-specific final design was chosen from the resulting Pareto-optimal set according to the study's performance priorities—maximizing propulsion while balancing heel cushioning and midfoot stability. The corresponding continuous parameter fields (A, B, T, P, θ) were extracted for all four functional regions of the midsole, followed by cross-region smoothing to ensure manufacturability and mechanical coherence. This workflow enabled efficient exploration of the high-dimensional design space with a limited number of FE evaluations, avoiding the prohibitive cost of exhaustive search while ensuring simultaneous gains in functional performance and engineering feasibility.

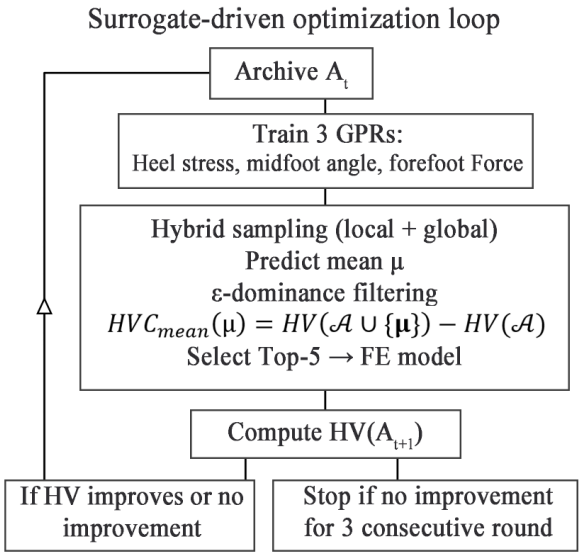

Figure 2.5.3 Surrogate-Driven Multi-Objective Optimization Workflow for Midsole Parameter Design.

2.6 Experimental Validation: Compression Testing and Gait Experiments

2.6.1 Material Mechanical Testing

To characterize the mechanical properties of the printing material and to provide constitutive inputs for the finite element model, uniaxial tensile tests were conducted on thermoplastic polyurethane (TPU; eSUN, Shore 95A). All specimens were fabricated using a Bambu Lab X1 Carbon printer (Bambu Lab, Shenzhen, China), which employs fused deposition modeling (FDM). The printer operates with nozzle temperatures up to 300 °C and a heated bed maintained at 110–120 °C. Equipped with a high-speed Core-XY motion system and an integrated micro-LiDAR module for in-process inspection, the device offers automatic bed-leveling, filament-runout detection, and power-loss recovery—capabilities essential for reliably producing the lattice-based footwear components required in this study.

After printing, the specimens were allowed to cool to ambient temperature and were lightly finished to remove surface irregularities and minimize residual stresses, ensuring geometric consistency across samples. All specimens were prepared in accordance with the ASTM D638 Type V standard for tensile testing of plastics. Tests were performed at a loading rate of 5 mm/min on four samples, and the full force–displacement response was recorded, including tensile strength, yield stress, and elongation at break. These experimental data provided the basis for calibrating the hyperelastic constitutive model of TPU, enabling the FE simulations to more accurately capture the material's mechanical behavior under large deformation and cyclic loading conditions.

2.6.2 Lattice Specimen Fabrication and Testing

Following the calibration of material-level mechanical properties, experimental validation was extended to the lattice-structure level. Representative geometric configurations—spanning combinations of control points (A, B), strut thickness (T), the resulting porosity (P), and the unit-cell rotation angle (θ)—were selected from the design space and fabricated as physical lattice specimens for compression testing. As illustrated in Figure 2.6.1, our previous work involved printing two sets of lattice samples with randomly selected parameters and subjecting them to compression tests[52, 53]. All specimens were printed using the FDM-based Bambu Lab X1 Carbon system. Compression tests were conducted on a universal testing machine at a loading rate of 5 mm/min under displacement control (maximum displacement: 5 mm). In the present study, the structural characterization was further expanded to accommodate the increased geometric resolution required for midsole-specific lattice configurations.

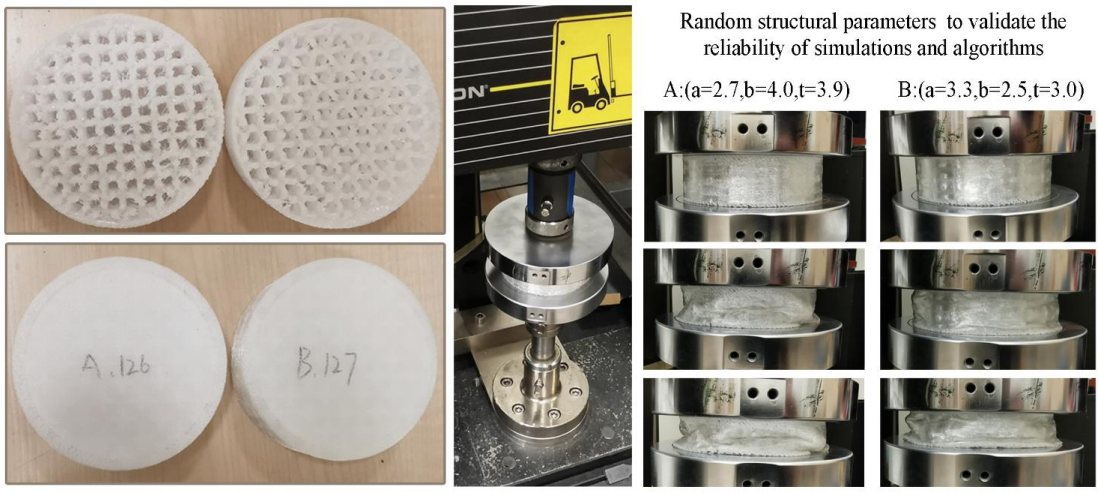

Figure 2.6.1 Compression test samples and procedures of randomly parameterized lattice structures (adapted from our previous published study) for validating the reliability of simulations and algorithms. [52, 53]

As noted earlier, the structural hierarchy in the present work was expanded to accommodate the finer spatial resolution required for midsole-specific lattice design. Although the lattice unit-cell size was refined from 15 mm in prior studies to 10 mm here, the overall parameterization framework and material system remained unchanged. Given that our earlier work had already conducted comprehensive experimental validation for this class of lattice–material combinations—with both numerical accuracy and physical reliability rigorously demonstrated—material-level testing was not repeated in the current study.

2.6.3 Prototype Footwear Fabrication

Based on the optimal design obtained from the parameter-optimization stage for the HM participant, the final parameter fields for the four functional regions—heel, medial arch, lateral midfoot, and forefoot—were imported into nTop. Boolean operations were then applied to generate a continuous, manufacturable lattice structure embedded within the midsole shell. After performing standard manufacturability checks (including manifold integrity, minimum strut diameter, and overhang-angle constraints), the completed midsole geometry was exported as an STL file for slicing. Importantly, the lattice porosity–stiffness gradients in this study were derived entirely from the optimization-driven explicit geometric design. Therefore, no slicer-based infill functions (e.g., “infill density,” “honeycomb infill,” or other software-defined internal patterns) were used. This ensured that the printed lattice faithfully reproduced the optimized geometry without unintended secondary modifications introduced during slicing.

All wearable components were fabricated using flexible TPU 95A, consistent with the hyperelastic material model employed in the finite element simulations. Printing was performed on a Bambu Lab X1 Carbon system (FDM process) with a layer thickness of 0.2 mm. During slicing, build orientations were selected to minimize support usage while preserving strut continuity within the lattice. A unified contour-first slicing strategy was applied across boundaries between functional regions to ensure that the optimized cross-regional geometric gradients were faithfully and smoothly reproduced in the printed structure. Upon completion of printing, the lattice midsole was allowed to cool naturally for approximately 30 minutes before support removal and minor edge finishing, ensuring structural integrity and safe wearability.

2.6.4 Gait Testing

To systematically evaluate the mechanical performance of the lattice-based footwear under realistic gait conditions and to validate the FE predictions, comprehensive wear tests were conducted exclusively with the HM participant in the gait laboratory. The HM participant completed the experimental protocol under three conditions: wearing the 3D-printed lattice footwear, wearing a control shoe (a commercially available casual athletic shoe), and walking barefoot.

The testing procedure followed the protocol described in Section 2.2.3 and was conducted within the same laboratory environment and instrumentation setup. To minimize the influence of first-time wear on gait behavior, a 5-min accommodation walk was administered prior to each condition, allowing the participant to fully adapt to the footwear and testing context (see Figure 2.2.3). All conditions were administered in a randomized, counterbalanced order to avoid sequence and learning effects. The participant walked at a self-selected comfortable speed, which was continuously monitored by photoelectric timing gates positioned along the walkway to ensure consistency across trials. For each condition, 30 valid gait cycles were collected. Data were deemed valid if the target foot made a complete and stable strike on the force platform, if PEDAR plantar pressure signals were fully synchronized with motion-capture data, and if trigger timestamps were aligned without evidence of sensor drift or data loss. Two trained researchers supervised the entire experiment, monitored fatigue, scheduled rest periods when necessary, and documented subjective comfort feedback and any occurrence of discomfort. To reduce confounding effects associated with speed fluctuations, the fastest and slowest three gait cycles for each condition were excluded. The remaining cycles were averaged within subject and used for subsequent statistical analyses and for comparison with finite element model predictions.

Throughout the experiment, two trained researchers supervised the protocol, monitored the participant’s fatigue level, scheduled rest periods when necessary, and documented subjective comfort ratings as well as any reported discomfort. To minimize the influence of gait-speed

variability, the three fastest and three slowest gait cycles within each condition were discarded. The remaining cycles were averaged within subject and used for subsequent statistical analyses and for comparison with the finite element model predictions.

2.6.5 Outcome Measures

The performance of the personalized lattice footwear for the HM participant was evaluated comprehensively across three domains: plantar pressure distribution, dynamic gait parameters, and subjective user assessment.

The first outcome metric was peak plantar pressure, used as a primary indicator of load alleviation and cushioning performance. Peak pressure represents the maximum instantaneous pressure experienced by a given plantar region during the gait cycle and is one of the most direct and widely adopted measures of local load concentration and structural shock attenuation. In addition to reflecting the magnitude of applied load, it is strongly influenced by regional contact area and therefore provides an effective assessment of a shoe's ability to redistribute pressure, reduce tissue stress, and improve contact mechanics. Persistently elevated peak pressures in specific regions are associated with increased risk of soft-tissue overload, metatarsalgia, stress fractures, and high-pressure ulceration in individuals with diabetes. Accordingly, the maximum equivalent stress in the heel soft tissue was used as the primary cushioning metric in the finite element simulations, and the corresponding plantar-pressure measurements from the gait experiments were used for empirical validation.

With respect to dynamic gait parameters, the analysis focused on how the footwear modulated gait stability and propulsive performance. In the finite element model, the calcaneal pitch angle was used to assess whether the footwear altered the participant's subtalar inversion–eversion tendency (Figure 2.6.2), as this angle reflects changes in medial–longitudinal-arch stability. In parallel, the anterior component of the tibial reaction force during push-off served as an indicator of propulsive efficiency, quantifying the extent to which the footwear enhanced forward propulsion. During subsequent laboratory gait testing, three-dimensional motion-capture data were used to compute ankle kinematics, including inversion–eversion angles, while synchronized ground-reaction-force measurements enabled calculation of peak anterior force during the propulsive phase. These experimental metrics were then compared against the FE predictions for validation. By benchmarking the lattice footwear against both the control shoe and the barefoot condition, the study provided a multidimensional evaluation of its performance—encompassing mechanical response, gait control, and subjective experience—thereby offering comprehensive evidence for the effectiveness of the personalized lattice-structure design.

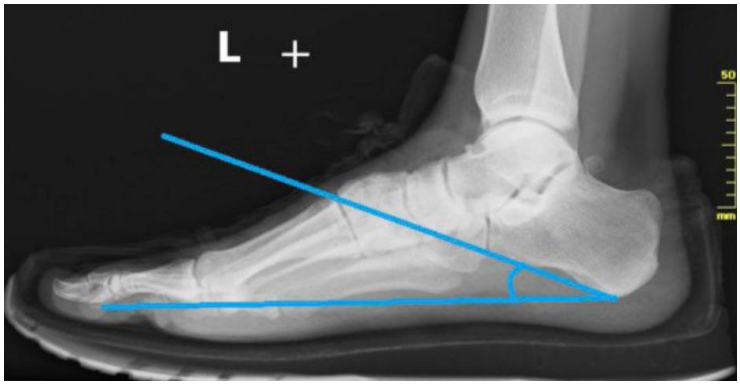

Figure 2.6.2 Calcaneal pitch angle measurement for assessing subtalar inversion–eversion. [73]

To complement the objective kinematic and kinetic metrics, this study further incorporates subjective perceptual evaluations as an additional assessment dimension. After completing each footwear condition, the HM participant rated their overall wearing comfort using a Visual Analog Scale (VAS, 0–10). With its high sensitivity and intuitive format[74], the VAS captures participant's immediate perceptions of fit, cushioning, stability and gait naturalness. Integrating these subjective ratings with objective measurements such as plantar pressure distribution, gait control metrics and propulsive performance provides a more comprehensive understanding of footwear function in realistic use contexts, and compensates for perceptual aspects that may be overlooked when relying solely on instrumented data.

2.7 Statistical Analysis

2.7.1 Statistical Methods

This study employed a single-subject repeated-measures design comprising three footwear conditions (3D-printed shoe, barefoot, and conventional shoe), with 24 valid gait cycles retained for each condition.

For continuous variables, the stance phase of each gait cycle was first time-normalized to 0–100%. Point-wise mean curves and standard deviations were then computed across the 24 cycles for joint angles, joint moments, ground reaction forces and ankle joint reaction forces, allowing the characterization of waveform patterns and inter-cycle consistency. Scalar parameters—including peak joint angles, peak joint moments, peak joint reaction forces and peak vertical ground reaction forces—were subsequently extracted from each cycle, and their means and standard deviations were calculated.

For each discrete metric, a one-way permutation test was conducted to assess overall differences among the three conditions, serving a role analogous to ANOVA (number of permutations $\geq$ 10,000; $\alpha = 0.05$). When a significant effect was detected, pairwise permutation tests were performed (3D-printed shoe vs. barefoot; 3D-printed shoe vs. conventional shoe; conventional shoe vs. barefoot). For all comparisons, estimated values (mean $\pm$ standard deviation) and the corresponding permutation-based p-values are reported.

3 Results

3.1 Material Testing and Model Validation

3.1.1 Uniaxial Tensile Testing

Flexible thermoplastic polyurethane (eSUN TPU 95A; eSun Industrial Co., Ltd.) was selected as the testing material. According to the manufacturer's specifications, the material has a density of 1.21 g/cm³ and an ultimate tensile strength of approximately 35 MPa. Its uniaxial tensile behavior was characterized following the ASTM D638 standard, which is widely employed to evaluate the mechanical response of polymers under tensile loading. The test protocol provides key parameters such as tensile strength, yield strength, ultimate strength and elongation at break. Specimens were fabricated in the Type V geometry defined by ASTM D638 (Fig. 3.1.1), a configuration suitable for thin-sheet materials and additively manufactured flexible polymers. These measurements supplied reliable foundational data for subsequent hyperelastic material calibration in the finite element modeling process.

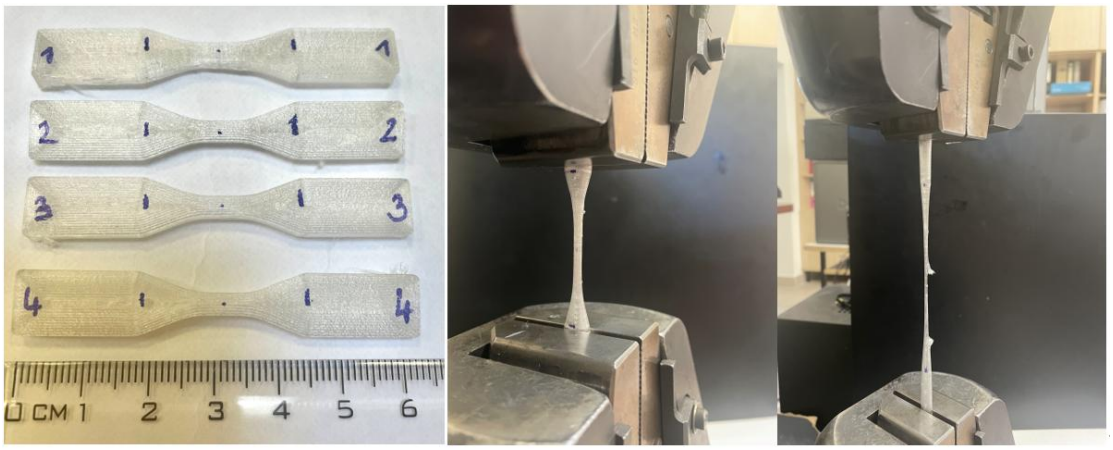

Figure 3.1.1 Appearance of Tensile Specimens and Their Deformation During Tensile Testing.[52]

Four specimens were subjected to uniaxial tensile testing at a constant loading rate of 5 mm min^{-1}. Throughout the test, tensile strength, yield strength and elongation at break were recorded to obtain the material's principal mechanical parameters. The averaged properties across the four specimens were subsequently used for material calibration in the finite element analysis. Figure 3.1.2 illustrates the force–displacement curves of the four samples.

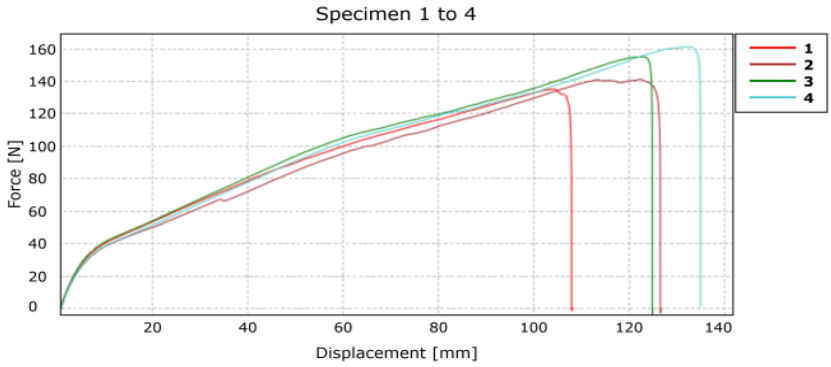

Figure 3.1.2 Force–Displacement Data Obtained from Tensile Tests of TPU Specimens.[52]

3.1.2 Sensitivity to Cell Count and Mesh Size

To systematically evaluate how modeling parameters influence the structural mechanical response, a two-factor sensitivity analysis was conducted by varying the number of lattice cells (from 3×3×3 to 7×7×3) and the mesh element size (0.4–1.0 mm). The corresponding effective Young's modulus was computed for each configuration (Fig. 3.1.2). The results indicate that both parameters exert a pronounced effect on the predicted structural stiffness.

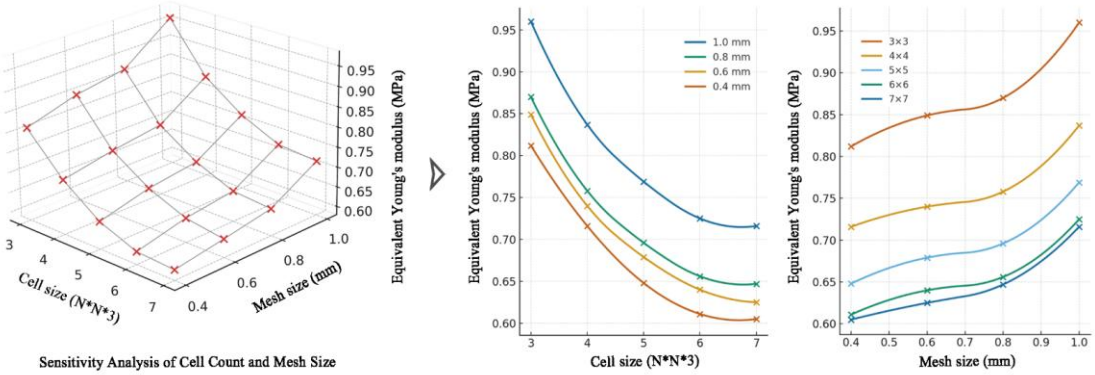

Figure 3.1.3 Effects of Unit-Cell Number and Mesh Size on the Effective Young's Modulus of the Equivalent Structure.

With respect to mesh discretization, reducing the element size from 1.0 mm to 0.4 mm produced a marked increase in the effective modulus, indicating that coarse meshes fail to adequately capture the geometric intricacies of the lattice and its localized mechanical response. Once the mesh size decreased below 0.6 mm, the rate of change in modulus fell to within 3%, and the curve gradually approached a plateau. This trend suggests that the simulation had essentially converged within this resolution range. Further refinement offered only marginal gains in accuracy while substantially increasing computational cost.

Regarding the number of unit cells, the effective modulus consistently decreased as the lattice dimensions expanded from 3×3×3 to 7×7×3. This behavior is largely attributable to boundary effects: smaller arrays contain a higher proportion of edge struts, whose additional constraint and reinforcement artificially elevate global stiffness. As the lattice size increases, the relative contribution of interior cells grows, diminishing boundary influence and allowing the mechanical response to approach the intrinsic behavior of an infinitely periodic lattice. When the array size reached 6×6×3 or larger, the change in effective modulus dropped below 5%, indicating that the model scale was sufficient to represent the characteristic mechanical performance of the periodic architecture.

Taken together, mesh resolution and cell count exert critical influence on the accuracy of the simulated mechanical response. Balancing numerical convergence with computational stability, this study adopted a 7×7×3 lattice array and a 0.4 mm mesh size for subsequent analyses, ensuring reliable and well-converged predictions of structural performance.

3.1.3 Finite Element Validation of the Lattice Architecture

The lattice design framework employed in this study builds upon the authors' previous work, with an extended hierarchical structure tailored to accommodate the refined spatial resolution required in localized regions of a footwear midsole. Although the unit-cell size was reduced from 15 mm to 10 mm, the overall structural morphology remained consistent with the established parametric design methodology, and the material system was unchanged. Since the prior study had already provided comprehensive experimental validation for this class of structures and materials, demonstrating both simulation accuracy and physical fidelity[52], repeated material-level testing was deemed unnecessary.

To evaluate the reliability of the lattice finite element simulations, cylindrical compression specimens were designed for comparative testing (Fig. 3.1.3). Two sets of structural parameters were generated programmatically in Python, and physical samples were fabricated using additive manufacturing. Compression experiments followed the ASTM D575 standard for assessing the compressive behavior of elastomeric materials. Because the standard specimen dimensions could disrupt lattice continuity, the geometry was modified to a diameter of 120 mm and a height of 30 mm to ensure structural integrity and uniform load distribution.

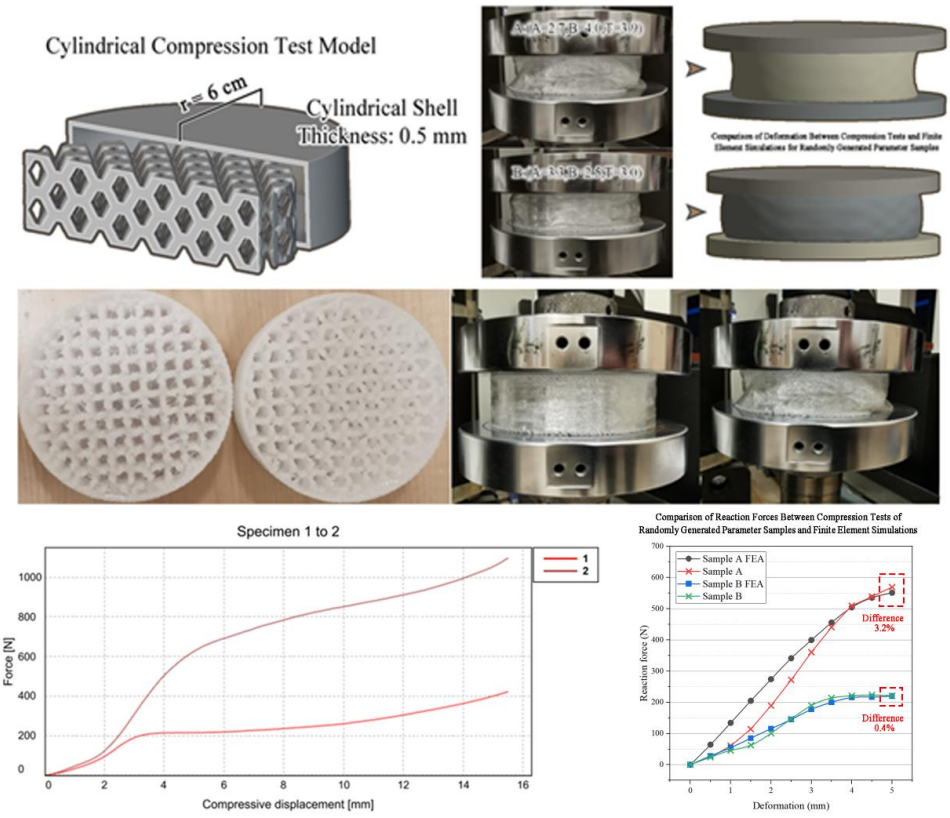

Figure 3.1.4 Comparison Between Compression Tests and Finite Element Simulations of Unit-Cell Structures.[52]

During the compression tests, no evident local damage was observed at a displacement of 5 mm, indicating that the specimens remained within the elastic deformation regime. The overall deformation patterns closely matched the finite element predictions (Fig. 3.1.2). The deviations between the experimental reaction forces and the simulated values were 3.2% for Sample A and 0.4% for Sample B. These results confirm that the finite element model developed in this study provides robust and reliable predictions of the lattice mechanical response.

3.1.4 Validation of the Foot Finite Element Model

As described earlier, plantar pressure data were collected under laboratory conditions during barefoot walking and compared with the predictions of the FE foot model to assess its validity. The results demonstrated strong agreement in both peak magnitudes and primary load-bearing regions. Across the three key phases of gait, the deviations in peak pressure were maintained at approximately 5% relative to the insole measurements: +3.4% at heel strike, –1.9% at mid-stance, and –5.5% at push-off. The locations and spatial patterns of pressure hotspots were also consistent with the experimental observations. These findings indicate that the FE foot model accurately captures the plantar loading characteristics of real gait, thereby providing a reliable foundation for subsequent footwear simulations.

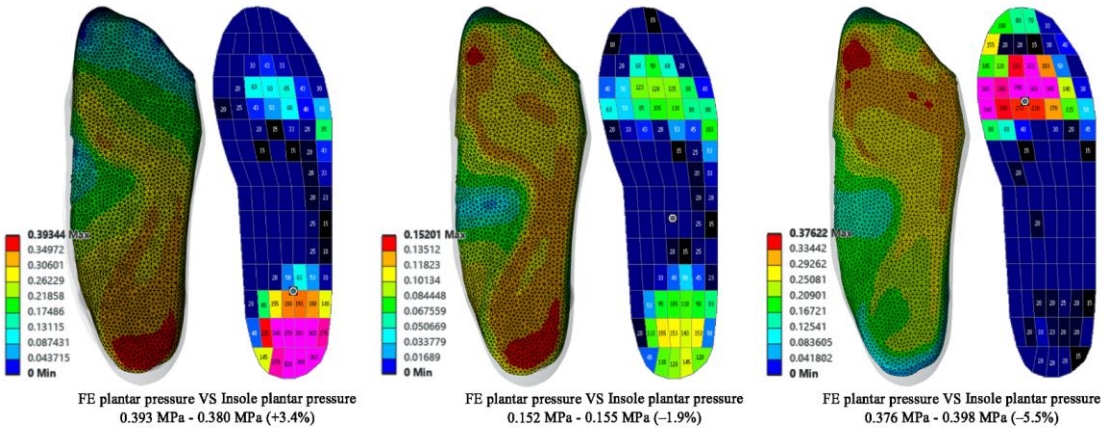

Figure 3.1.5 Comparison Between FE-Predicted Plantar Pressure and Insole-Measured Plantar Pressure.

3.2 Parametric Outcomes of the Lattice Structures

3.2.1 Deformation Modes of Representative Unit Cells

As described in Section 2.3.1, variations in structural parameters yield three principal categories of unit-cell architectures: honeycomb, re-entrant, and rectangular configurations (Fig. 3.2.1A). Under compressive loading, the honeycomb and rectangular lattices typically exhibit a positive Poisson's ratio, expanding laterally as axial compression increases. In contrast, re-entrant lattices are theoretically capable of displaying an auxetic response, characterized by lateral contraction during axial compression.

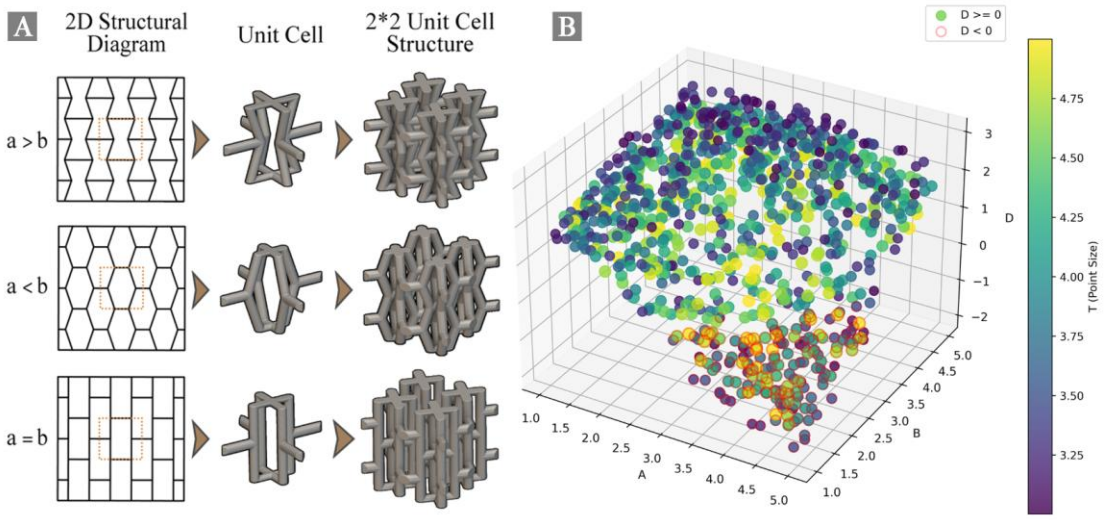

Figure 3.2.1 Deformation Modes of Typical Unit-Cell Structures (A: Three Types of Unit Cells; B: Distribution of Expansive/Contractive Behavior).

In practice, however, the effective Poisson's ratio is governed not only by the topological form but also by porosity. When struts are overly thick or porosity is insufficient, internal contact between cell members may occur, preventing the lattice from manifesting its intrinsic auxetic behavior even if the underlying topology is re-entrant. This phenomenon has been systematically analyzed in the authors' previous work[52]. As shown in Fig. 3.2.1B, without rotational modulation of the unit cell, 83.10% of parameter combinations produced lateral expansion under compression, whereas only 16.90% exhibited a negative Poisson's ratio.

3.2.2 Machine-Learning Training and GPR-Based Dataset Expansion

In this study, the initial simulation dataset derived from FE analyses was expanded through Gaussian Process Regression (GPR) sampling, after which the predictive models for lateral deformations (Dx and Dy) under compressive loading were evaluated following the authors' previously established procedure[52]. Figure 3.2.2 illustrates the correspondence between predicted and ground-truth values, together with the residual distributions.

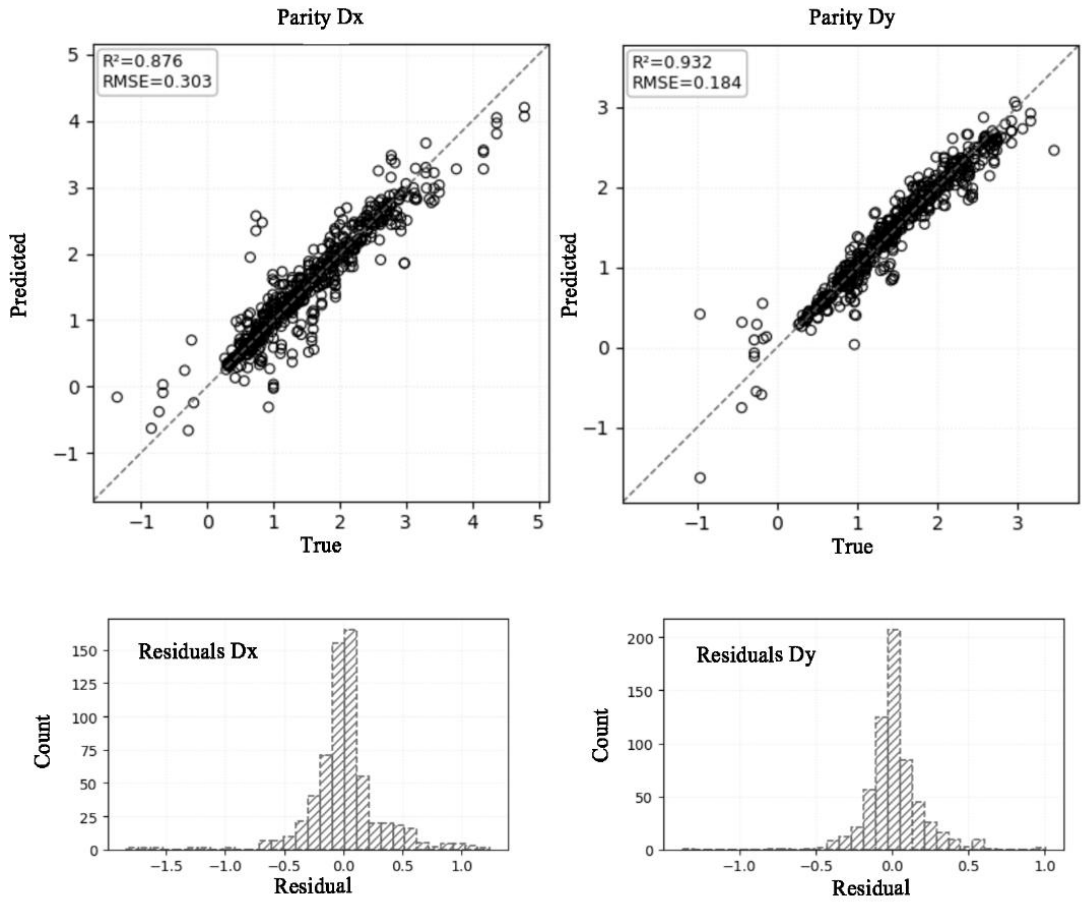

Figure 3.2.2 Fitting Accuracy and Residual Statistics of the GPR Model for Predicting Lateral Deformations.

Overall, the fitted models achieved high predictive accuracy in both deformation directions. The coefficient of determination reached 0.876 for Dx and 0.932 for Dy, with corresponding RMSE values of 0.303 and 0.184. The residuals in both directions were symmetrically distributed and tightly clustered, with the majority falling within ±0.5. These results indicate that the models exhibit no meaningful systematic bias and provide reliable predictions of lateral deformation behavior.

3.2.3 Influence of Structural Parameters on Mechanical Performance

Portions of the analyses presented in this section have been published in the authors' previous work[53], from which the relevant figures and conclusions are reproduced here. As shown in Fig. 3.2.3, the reaction forces generated under compressive loading (F1–F5) increase monotonically with structural diameter, corresponding to larger values of parameter T and reduced porosity. This trend indicates that higher T generally yields a stronger mechanical response. At the same time, parameters A and B modulate this increase in distinct ways, suggesting that they influence the lattice mechanics through different mechanisms. For example, under the combination A = 5 and B = 1, the reaction force exhibits the steepest rise with increasing T.

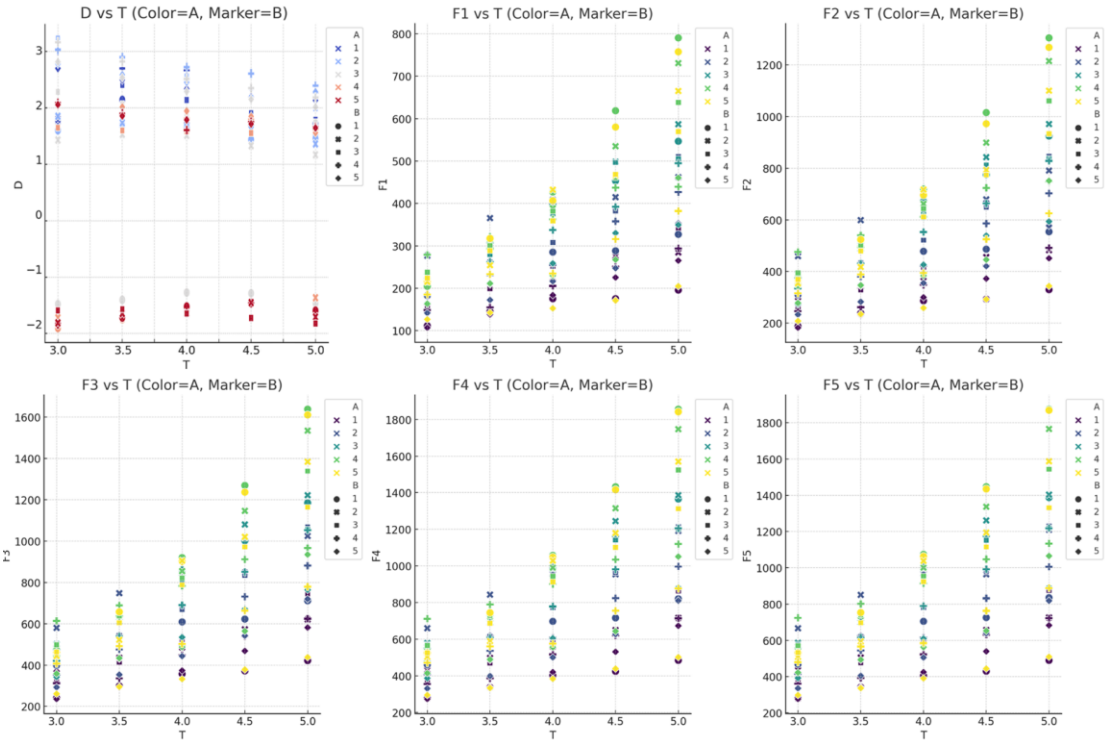

Figure 3.2.3 Influence of Structural Parameters on the Variation Trends of Mechanical Metrics.[53]

In contrast, the lateral deformation (denoted as D in the figure) displays a more complex dependence on the A–B parameter combinations, revealing pronounced nonlinear coupling. These observations imply that the geometric parameters interact with one another, jointly shaping the deformation behavior and mechanical performance of the lattice architecture.

3.3 Finite Element–Based Structural Optimization

Building on the initial database of 25 samples for each participant, a multiobjective optimization framework was developed to iteratively refine the midsole architecture. The overall iterative behavior is shown in Fig. 3.3.1A. After approximately 8–10 iterations, the growth rate diminished and gradually approached a plateau, indicating stabilization of the Pareto set. Although the absolute HV magnitudes differed among participants—reflecting differences in feasible objective ranges—the temporal convergence behavior remained consistent, demonstrating the robustness of the optimization framework under heterogeneous individual constraints.

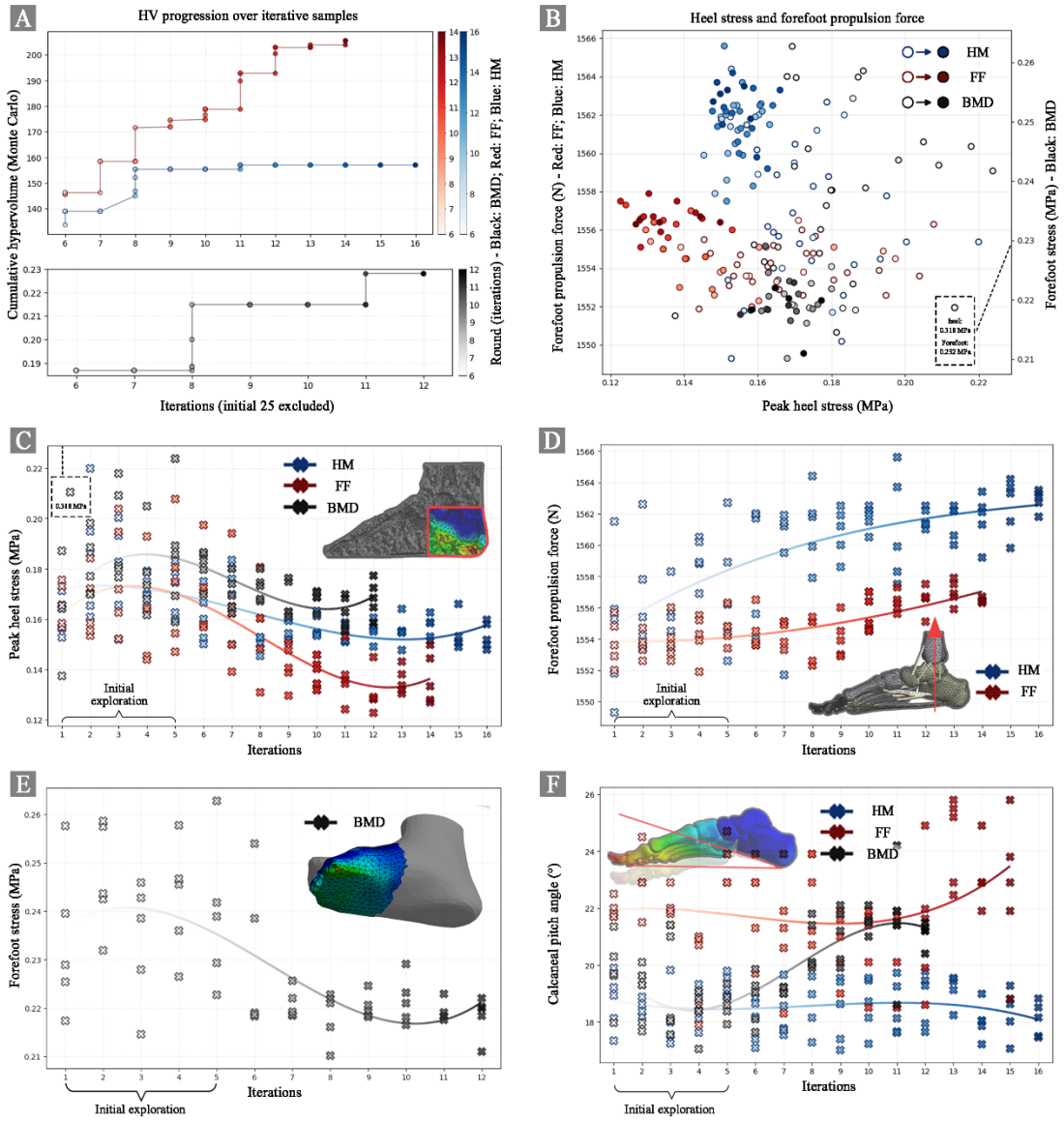

Figure 3.3.1 Subject-Specific Multi-Objective Optimization and Evolution of Biomechanical Metrics (A: Hypervolume progression and convergence behavior for HM, FF, and BMD; B: Objective-space distribution of heel stress and forefoot response; C: Iterative evolution of peak

heel stress; D: Iterative evolution of forefoot propulsion force; E: Iterative evolution of forefoot stress; F: Iterative changes in calcaneal pitch angle across participants.)

Figure 3.3.1B presents the distribution of evaluated samples within the objective space. For the HM and FF participants, the trade-off between peak heel stress and forefoot propulsion force is shown. As iterations progressed (color transition from blue to red), the samples migrated toward regions characterized by reduced heel stress and enhanced propulsion. The density of high-performing solutions increased markedly in the later rounds, indicating effective mitigation of the classical cushioning–propulsion trade-off. For the BMD participant, the objective space was defined by peak heel stress and peak forefoot stress rather than propulsion force. The optimization process progressively shifted the solutions toward a low-stress domain for both regions, reflecting constrained but stable improvement within pathological biomechanical limits. Although calcaneal pitch angle was retained as a stability-related objective during optimization, its variation across iterations remained relatively small, suggesting limited sensitivity to the explored parameter range. Consequently, while midfoot stability was monitored throughout the process, it was not treated as the dominant criterion during final solution selection.

The iteration-wise evolution of the primary objectives is shown in Fig. 3.3.1C–F. For heel stress (Fig. 3.3.1C), all three participants demonstrated a general downward trend during optimization. The FF participant exhibited the most pronounced stress reduction, decreasing from approximately 0.18–0.20 MPa in early iterations to around 0.13–0.14 MPa in later rounds. The HM participant stabilized near 0.15 MPa, while the BMD participant converged within a relatively higher but controlled stress band, consistent with pathological loading constraints. For propulsion performance (Fig. 3.3.1D), both HM and FF participants showed gradual increases in peak forefoot propulsive force over iterations. HM exhibited the largest absolute propulsion values, reaching above 1564 N, while FF demonstrated moderate yet consistent gains. These trends confirm that lattice parameter modulation effectively enhanced forward energy transfer without compromising heel cushioning. For the BMD participant (Fig. 3.3.1E), forefoot stress decreased progressively across iterations, approaching a stable minimum near 0.22 MPa. The absence of propulsion maximization for this participant reflects the clinically oriented objective prioritizing load alleviation. The calcaneal pitch angle (Fig. 3.3.1F) exhibited subject-dependent modulation. FF and BMD participants showed slight increases in midfoot stability over iterations, whereas HM demonstrated minimal variation. Unlike the earlier single-subject analysis, midfoot stability was retained as an active objective component in the multi-subject framework.

For each participant, the final design was selected from the converged Pareto set using a Utopia-closest criterion after normalization of objectives. For propulsion-oriented participants (HM and FF), compromise solutions preserved high propulsion while maintaining low heel stress. For the

BMD participant, the selected design minimized both heel and forefoot stress while maintaining stable arch geometry. The resulting subject-specific optimal parameter sets were subsequently used to generate the final midsole geometries for simulation evaluation. Physical fabrication and laboratory gait validation were conducted exclusively for the HM participant, as described in Section 2.1.2. The resulting optimal compromise solution achieved a rearfoot pressure of 0.151 MPa and a propulsive force of 1565.6 N. Notably, while maintaining the highest propulsion performance, its pressure level exceeded the minimum-pressure configuration by only about 3.7%. The optimized parameter set was then used to generate the final midsole structure, which was fabricated using a Bambu Lab X1C additive manufacturing system.

3.4 3D-Printed Footwear and Gait Testing

3.4.1 Fabrication of the Prototype Footwear

To assess the manufacturability of the parametric lattice design and its structural integrity under realistic use conditions, prototype footwear was fabricated using fused deposition modeling (FDM) (Fig. 3.4.1). All components were printed with TPU elastomer (Shore 95A), a material chosen for its flexibility, toughness and fatigue resistance, ensuring that the midsole could withstand repeated compression and rebound during gait.

Figure 3.4.1 Schematic of the 3D Printing Process for the Prototype Footwear.

To ensure accurate reproduction of lattice strut dimensions, porosity, and regional transitions, a fine-printing mode with a 0.2 mm layer height and a 0.2 mm first-layer height was employed. This resolution allows reliable fabrication of lattice struts approximately 0.8–1.2 mm in diameter while maintaining continuous deposition of TPU, thereby preserving geometric fidelity at both the macro- and micro-scales. The line width for the outer and inner walls was set to 0.42–0.45 mm to ensure stable formation of the hollow lattice cell boundaries and to prevent geometric deviations caused by excessive extrusion. The same line-width range was used for top surfaces and sparse infill, which enhances interfacial bonding between the lattice and the enclosing shell. For geometric detailing, the slicer was configured with a 0.012 mm resolution and a 0.049 mm compensation radius for inter-layer spacing. These settings effectively reduce local errors in high-curvature regions, improving the accuracy and surface conformity of complex anatomical features such as the arch and metatarsal areas.

Because the lattice architecture is inherently hollow, two perimeter walls were applied to ensure sufficient structural strength at the interface between the external shell and the internal lattice. The top and bottom surfaces were reinforced with five and three solid layers, respectively, providing the necessary compressive resistance and durability during initial heel contact. To emulate the graded mechanical response characteristic of TPU midsoles in real use, a sparse infill density of 15% was adopted, with a printing orientation of 45°. A minimum infill area constraint of 15 mm² was enabled

to guarantee stable fabrication of locally small geometric features within the lattice. This strategy achieves an effective balance between lightweight construction and structural resilience, particularly benefiting regions such as the forefoot and arch where nonlinear mechanical behavior is essential.

Because TPU is prone to stringing at high printing speeds, a progressive overhang slow-down strategy was implemented to dynamically adjust the print speed across different overhang angles, thereby preventing deformation of the lattice cantilever structures. The travel speed was set to 500 mm s^{-1} to maintain printing efficiency while minimizing excessive filament stretching during rapid retraction. To further enhance deposition continuity, the general printing acceleration was set to 10,000 mm/s^2, with a reduced acceleration of 5,000 mm/s^2 for the outer walls. The lattice regions employed percentage-based acceleration control (100%), enabling a balance between structural stability and printing throughput.

For multi-zone lattice midsoles with complex internal cavities, support generation is particularly critical. A tree-support strategy (automatic mode) was employed, offering low material usage and easy removal, making it well suited for flexible, porous structures. Because TPU is susceptible to edge warping, a brim attachment mode was applied with a 5 mm boundary width and a 0.1 mm offset between the model and brim to improve adhesion stability while facilitating post-processing removal.

To prevent material accumulation along intersecting extrusion paths, the reduced infill retraction and outer-wall wipe features were enabled, ensuring smoother filament deposition. These settings were especially effective in high-porosity regions, reducing surface defects and improving overall print fidelity.

The printing time for each shoe was approximately 50 hours. After printing, the parts were allowed to rest for about 30 minutes to ensure adequate cooling before support removal and edge finishing.

3.4.2 Plantar Pressure

As shown in Fig. 3.4.2, a one-way permutation “ANOVA-like” test (sum of squares as the test statistic, 10,000 permutations, $\alpha = 0.05$) was conducted on the peak plantar pressure in the rearfoot region during the loading response phase. The analysis revealed a significant main effect of condition ($p = 0.0001$). Subsequent pairwise permutation comparisons indicated that the barefoot condition exhibited significantly higher peak pressures than both the 3D-printed shoe ($p = 0.0001$) and the conventional shoe ($p = 0.0001$), whereas no significant difference was observed between the 3D-printed and conventional footwear ($p = 0.8060$). Analysis of peak rearfoot pressure at initial contact yielded a similarly significant main effect ($p = 0.0001$). Pairwise tests showed significant differences across all three comparisons—3D-printed vs. conventional ($p = 0.0001$), barefoot vs. conventional ($p = 0.0001$), and 3D-printed vs. barefoot ($p = 0.0001$). Overall, the 3D-printed shoe demonstrated the most effective cushioning performance in the rearfoot region.

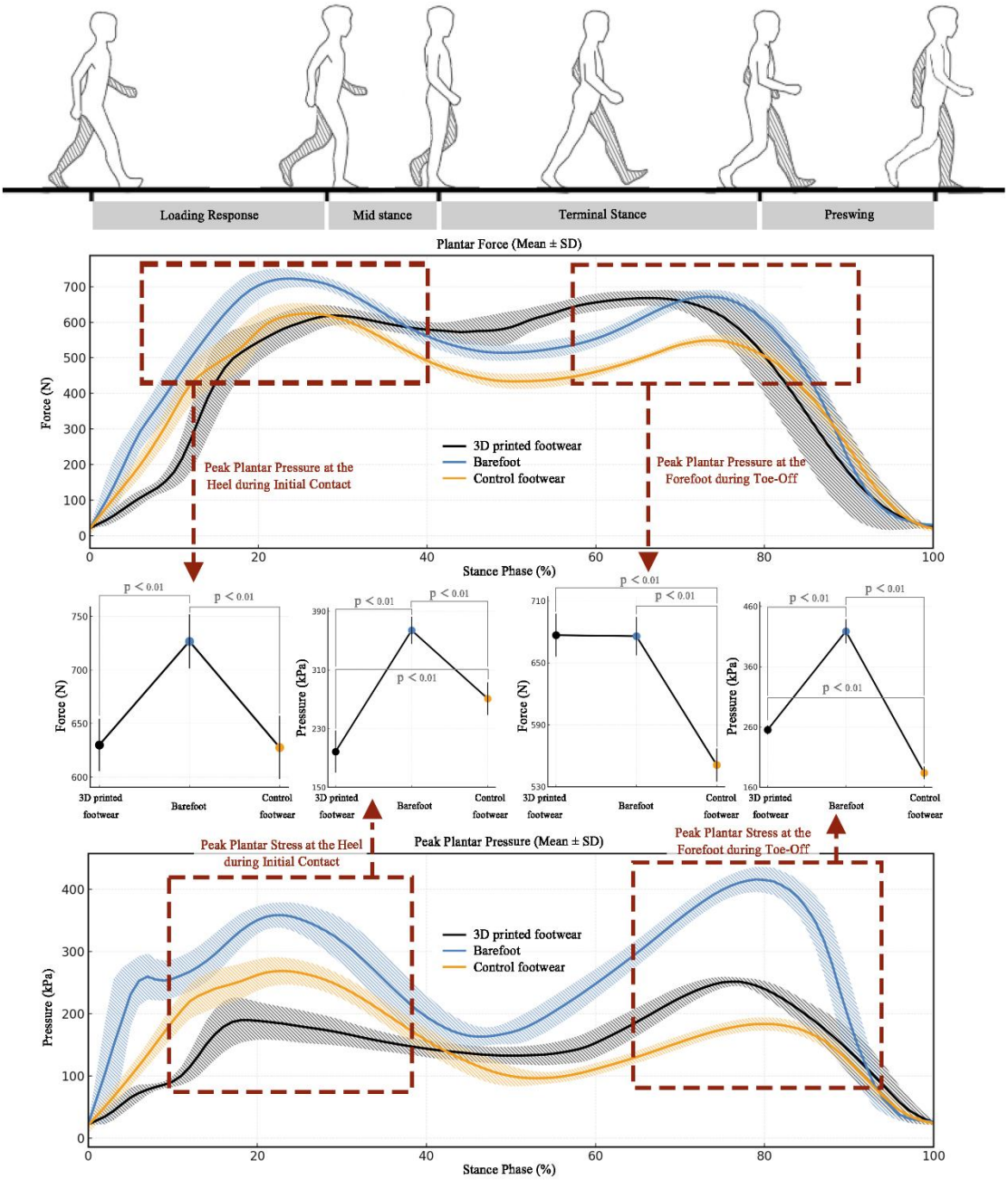

Figure 3.4.2 Comparison of Peak Plantar Pressure and Peak Plantar Stress at Heel Strike and Forefoot Toe-Off during the Gait Cycle.

During the push-off phase, the permutation-based "ANOVA-like" test for peak forefoot plantar pressure also revealed a significant main effect of condition ($p = 0.0001$). Pairwise comparisons showed significant differences between the 3D-printed and conventional shoes ($p = 0.0001$) as well as between the barefoot and conventional conditions ($p = 0.0001$), whereas no significant difference was observed between the 3D-printed and barefoot conditions ($p = 0.8784$). This indicates that peak forefoot pressures in the 3D-printed and barefoot conditions were both higher than those in the conventional shoe (Fig. 3.4.2).

A parallel analysis of peak forefoot pressure (expressed as pressure magnitude rather than total force) likewise demonstrated a significant main effect ($p = 0.0001$). Follow-up permutation tests confirmed significant differences across all three comparisons: 3D-printed vs. conventional ($p = 0.0001$), barefoot vs. conventional ($p = 0.0001$), and 3D-printed vs. barefoot ($p = 0.0001$). The overall pattern showed the highest pressures in the barefoot condition, intermediate pressures in the 3D-printed shoe and the lowest pressures in the conventional shoe.

These findings suggest that during push-off, the 3D-printed shoe delivers a forefoot propulsive performance comparable to barefoot walking while maintaining a moderate pressure level, thereby achieving a balance between propulsion enhancement and pressure management.

3.4.3 Gait Kinematics and Kinetics

As shown in Fig. 3.4.3, the joint kinematic and kinetic profiles across the three conditions exhibited broadly similar cyclical patterns, yet discernible differences emerged at specific phases of the gait cycle.

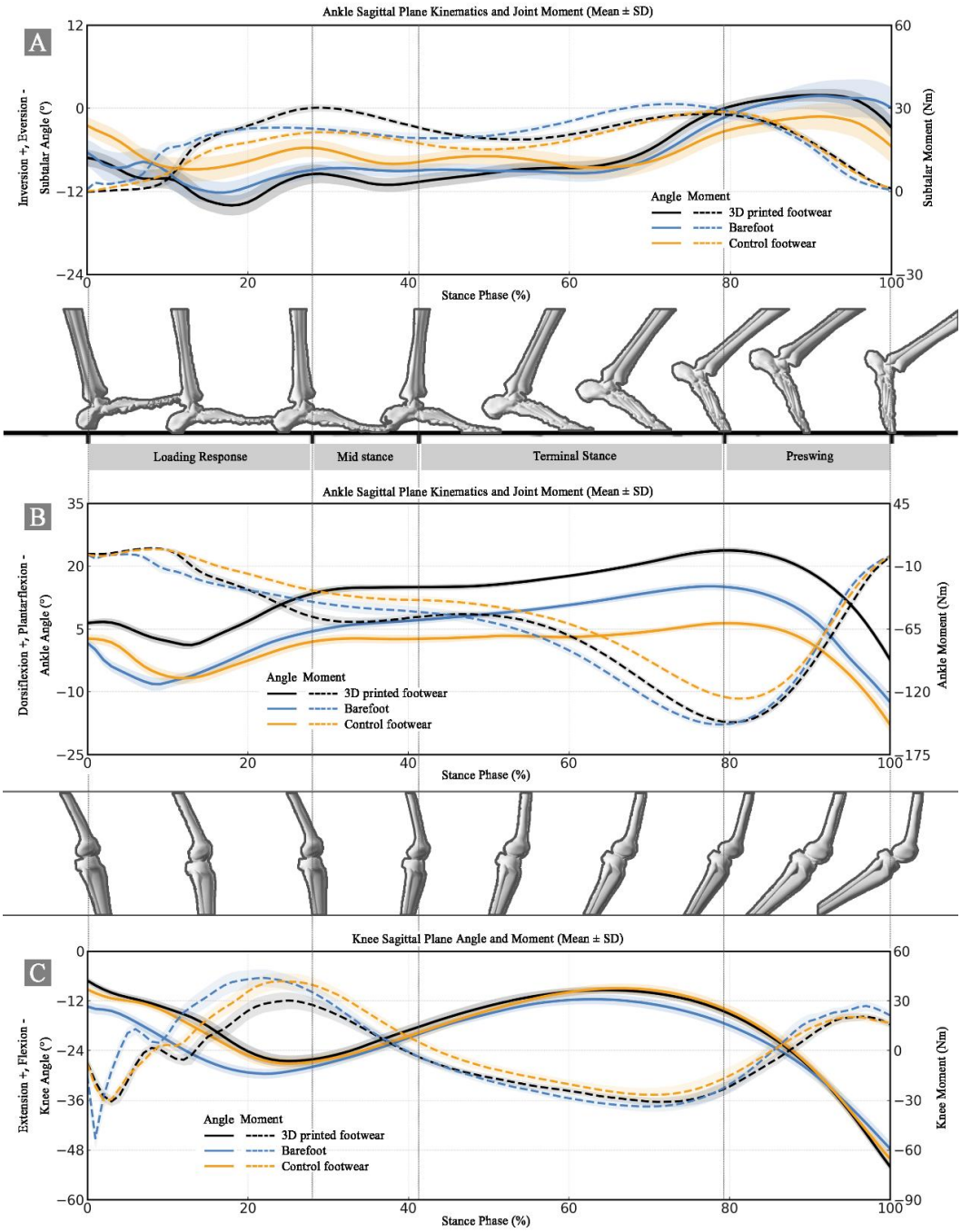

Figure 3.4.3 Comparison of Lower-Limb Joint Kinematics and Kinetics across Three Footwear Conditions (A, Subtalar; B, Ankle; C, Knee Joints).

In the subtalar joint (Fig. 3.4.3A), the 3D-printed shoe exhibited a more pronounced inversion during the loading response, closely resembling the barefoot condition. As the gait progressed into mid-stance, the joint angles across all three conditions converged. During terminal push-off, both the barefoot and 3D-printed conditions returned to near-neutral alignment, whereas the conventional shoe remained in a sustained inverted position. The corresponding moment profiles showed similar distinctions. The 3D-printed shoe produced a higher early-stance moment peak, the barefoot condition generated the highest moment during push-off and the conventional shoe maintained the flattest and least variable trajectory across the cycle.

In the ankle joint (Fig. 3.4.3B), all three conditions displayed the characteristic plantarflexion–dorsiflexion pattern. However, the 3D-printed shoe maintained a consistently greater dorsiflexion angle from initial contact through push-off. The barefoot and conventional conditions showed similar behavior during initial loading, whereas the barefoot condition exhibited a larger dorsiflexion excursion during push-off. Regarding joint moments, differences among conditions were minimal during the loading response. In the push-off phase, however, both the 3D-printed and barefoot conditions demonstrated higher moment peaks compared with the conventional shoe.

In the ankle joint (Fig. 3.4.3B), all three conditions exhibited the characteristic plantarflexion–dorsiflexion cycle, yet notable differences emerged in amplitude. The 3D-printed shoe maintained a consistently greater dorsiflexion angle from initial contact through push-off. The barefoot and conventional conditions behaved similarly during early stance, while the barefoot condition showed a larger dorsiflexion excursion during push-off. Joint moment patterns were comparable across conditions during the loading response. In contrast, the push-off phase revealed clear divergences, with both the 3D-printed and barefoot conditions generating higher moment peaks than the conventional shoe.

In the knee joint (Fig. 3.4.3C), all three conditions demonstrated a consistent flexion–extension pattern. The barefoot condition exhibited greater flexion during the loading response, whereas the 3D-printed and conventional shoes followed more similar angle trajectories. As stance progressed, differences among the three conditions diminished, particularly in the mid-to-late stance phases. For knee joint moments, the 3D-printed shoe produced a smaller peak moment during the loading response, while the barefoot condition generated higher moments in both early and late stance.

Building on the waveform patterns shown in Fig. 3.4.3, the discrete joint parameters further quantified the differences among conditions (Table 3.4.1). Both the 3D-printed and barefoot conditions exhibited greater subtalar joint mobility. For peak eversion angle, the 3D-printed shoe (14.11° ± 1.40) and barefoot condition (12.32° ± 1.43) were significantly higher than the conventional shoe (9.79° ± 1.16, $p < 0.01$). A similar pattern emerged for ROM, with the 3D-printed shoe showing the largest excursion (16.17° ± 1.39), followed by barefoot (14.56° ± 2.11) and the

conventional shoe presenting the smallest ROM (9.18° ± 1.53, $p < 0.01$). Peak inversion angle was lowest in the conventional condition (–0.61° ± 1.55, $p < 0.01$), reinforcing its more restrictive influence on subtalar motion. For joint moments, the barefoot condition exhibited the highest peak inversion moment during push-off (31.67 ± 1.36 Nm), whereas the conventional shoe showed the lowest (28.94 ± 1.04 Nm, $p < 0.01$), with the 3D-printed shoe falling between the two.

Table 3.4.1 Key kinematic and kinetic discrete parameters of the subtalar, ankle, and knee joints across the three conditions (mean ± SD).

	Metric	3D-Printed Shoe	Barefoot	Conventional Shoe	p
Subtalar	Peak inversion angle	2.05±0.91⁂	2.23±2.27⁂	-0.61±1.55*‡	< 0.01
	Peak eversion angle	14.11±1.40‡⁂	12.32±1.43*⁂	9.79±1.16*‡	< 0.01
	ROM	16.17±1.39‡⁂	14.56±2.11*⁂	9.18±1.53*‡	< 0.01
	Peak inversion moment	30.46±1.18‡⁂	31.67±1.36*⁂	28.94±1.04*‡	< 0.01
Ankle	Peak dorsiflexion Angle	23.79±0.74‡⁂	15.26±0.89*⁂	6.42±0.69*‡	< 0.01
	Peak plantarflexion Angle	2.25±1.11‡⁂	12.53±2.08*⁂	17.82±2.00*‡	< 0.01
	ROM	26.04±1.34‡⁂	27.78±2.10*⁂	24.24±1.90*‡	< 0.01
	Peak dorsiflexion moment	5.92±0.29‡⁂	0.85±0.58*⁂	5.12±0.69*‡	< 0.01
	Peak plantarflexion moment	146.82± 2.53‡⁂	148.92± 3.18*⁂	126.13±2.28*‡	< 0.01
Knee	Minimum extension angle	7.08±0.82‡⁂	11.46±1.09*⁂	8.55±1.01*‡	< 0.01
	Peak flexion angle	52.04±1.01‡⁂	47.70±1.76*⁂	50.15±1.54*‡	< 0.01
	ROM	44.97±1.00‡⁂	36.23±2.01*⁂	41.60±1.64*‡	< 0.01
	Peak extension moment	30.45±5.01‡⁂	44.28±5.12*	42.24±5.04*	< 0.01
	Peak flexion moment	32.96±2.60‡	52.97±6.06*⁂	31.85±2.23‡	< 0.01

Note: * Significant difference from the 3D-printed shoe condition. ‡ Significant difference from the barefoot condition. ⁂ Significant difference from the conventional shoe condition.

For the ankle joint, the 3D-printed shoe exhibited a markedly greater peak dorsiflexion angle during stance (23.79° ± 0.74), substantially exceeding both the barefoot (15.26° ± 0.89) and conventional shoe conditions (6.42° ± 0.69, $p < 0.01$), a pattern consistent with the larger dorsiflexion trajectory observed in the waveform analysis. In contrast, the barefoot and conventional shoes demonstrated greater peak plantarflexion angles during late stance (12.53° ± 2.08 and 17.82° ± 2.00, respectively;

both $p < 0.01$), reflecting the similarity in their push-off mechanics. For ankle joint ROM, the barefoot condition displayed the greatest excursion (27.78° ± 2.10), followed by the 3D-printed shoe (26.04° ± 1.34), while the conventional shoe showed the smallest ROM (24.24° ± 1.90). These findings suggest that the personalized lattice structure maintains functional modulation without restricting ankle mobility. In terms of kinetics, both the 3D-printed shoe and barefoot conditions generated higher peak plantarflexion moments during push-off (approximately 146–148 Nm), significantly exceeding those of the conventional shoe (126.13 ± 2.28 Nm, $p < 0.01$), indicating enhanced propulsive capability in the former two conditions. For peak dorsiflexion moment, the 3D-printed shoe exhibited the highest value (5.92 ± 0.29 Nm), whereas the barefoot condition produced the lowest (0.85 ± 0.58 Nm, $p < 0.01$). This suggests that the personalized lattice structure provides increased dorsiflexion support during early loading, thereby improving impact attenuation and the mechanical response at initial contact.

The discrete knee-joint parameters revealed clear differences in load-regulation strategies across the three gait conditions. During early stance, the barefoot condition exhibited the largest minimum extension angle (11.46° ± 1.09), followed by the conventional shoe (8.55° ± 1.01), whereas the 3D-printed shoe showed the smallest value (7.08° ± 0.82, $p < 0.01$). This indicates that, upon initial contact, the knee tends to adopt a more flexed posture when wearing the 3D-printed shoe, reflecting a more pronounced shock-attenuation strategy. Regarding peak knee flexion, the 3D-printed shoe again produced the highest value (52.04° ± 1.01), significantly exceeding both the barefoot (47.70° ± 1.76) and conventional shoe conditions (50.15° ± 1.54, $p < 0.01$). This suggests that the lattice-augmented midsole allows for greater flexion during mid-to-late stance, which may facilitate improved energy absorption and propulsion. A similar trend was observed for knee ROM: the 3D-printed shoe exhibited the largest range (44.97° ± 1.00), followed by the conventional shoe (41.60° ± 1.64), with barefoot demonstrating the smallest excursion (36.23° ± 2.01). These results indicate that the personalized lattice architecture expands functional knee mobility without imposing additional mechanical load, enabling a more “elastic” response pattern during stance. In terms of knee joint kinetics, the barefoot condition showed substantially higher peak flexion moments around push-off (52.97 ± 6.06 Nm, $p < 0.01$), reflecting the greater demand on active musculature in the absence of cushioning structures. In contrast, both the 3D-printed and conventional shoes produced lower flexion moments. Peak extension moment exhibited the opposite pattern: the barefoot and conventional conditions displayed higher values, whereas the 3D-printed shoe showed the lowest (30.45 ± 5.01 Nm, $p < 0.01$). This reduction in extension loading suggests that the personalized lattice midsole may optimize load transmission during mid-to-late stance, thereby reducing instantaneous demands on the knee extensors.

3.4.4 Subjective Feedback

To complement the objective biomechanical findings, subjective evaluations were collected after testing using a Visual Analog Scale (VAS, 0–10) to assess overall comfort, rearfoot cushioning, forefoot propulsion sensation, gait stability and arch support across the three conditions.

For overall comfort, the 3D-printed shoe received a score of 9. The participant reported that "the upper provides excellent containment, and the lattice structure creates a very soft interface between the foot and the midsole." The conventional shoe received a score of 8 and was described as "not soft enough in the midsole." The barefoot condition scored 6 due to its lack of cushioning, with the participant noting "a harder landing sensation and pronounced vibration."

Differences were most pronounced in rearfoot cushioning. The 3D-printed shoe received a perfect score of 10, described as "almost no impact at heel strike, as if cushioned by a cloud." The conventional shoe scored 7, while the barefoot condition scored 5 and was described as "heel pain with noticeable impact." These impressions align closely with the objective reduction in peak rearfoot pressure.

For forefoot propulsion sensation, the 3D-printed shoe received a score of 8. The participant reported "a smoother push-off and easier release of calf power." Both the conventional shoe and barefoot conditions received scores of 7, although the barefoot condition was described as having "direct power transfer but more concentrated pressure."

With respect to gait stability, the barefoot condition received the highest score (8), with the participant noting "a stronger sense of ground contact and more direct control." Both the 3D-printed and conventional shoes scored 7. For the 3D-printed shoe, the participant remarked that "the rearfoot feels slightly soft at landing, with moderate stability, but mid-stance and push-off remain very stable."

In terms of arch support, the 3D-printed shoe scored 8, with the participant noting that "the arch feels supported without being intrusive." The conventional shoe scored lower (6) due to its lack of dedicated arch structure. The barefoot condition was not applicable for this category.

4 Discussion

This study establishes a closed-loop footwear design framework centered on parametric lattice modeling, individualized gait data acquisition, finite element analysis, multiobjective optimization and dynamic experimental validation. Subject-specific simulations and optimization were performed for three participants, while laboratory-based wearable validation was conducted exclusively in the HM participant. The framework enables footwear structures to be shaped not by empirical material selection but through programmable geometries that allow targeted mechanical modulation, while incorporating subject-specific biomechanical information directly into structural generation and performance optimization. In doing so, it advances footwear design from traditional material-based approaches to structurally tunable systems, offering a new theoretical foundation and engineering pathway for footwear biomechanics and on-demand manufacturing.

4.1 Mechanical Expressiveness of Parametric Lattices and the Mechanisms Underlying Footwear Functional Reconfiguration

The multidimensional parametric lattice system developed in this study demonstrates that, even within a single material class, lattice architectures can achieve highly tunable and continuously predictable mechanical responses purely through geometric configuration. By introducing parameters such as topology type, strut thickness, porosity, unit-cell scale and spatial orientation, key structural properties—including effective elastic modulus, energy absorption capacity, buckling modes and lateral deformation behavior—can be modulated smoothly across a broad performance range. In contrast to traditional midsole design strategies that rely on altering material properties or foam densities, the present study adopts a geometry-driven approach to mechanical tuning, enabling substantial functional differentiation while maintaining an identical material system. This programmable, geometry-centered mechanical capability represents the foundational rationale for the long-term strategic value of lattice architectures in footwear design.

Through large-scale FE simulations combined with previously validated experimental data, this study establishes a continuous mapping between geometric parameters and mechanical responses, further elucidating the constitutive distinctions among different lattice topologies under compression. The results indicate that re-entrant architectures can reliably exhibit a negative Poisson’s ratio when designed within an appropriate porosity range, and their characteristic lateral contraction endows the structure with confinement and stabilization capabilities that are difficult to achieve with conventional materials. By contrast, honeycomb and rectangular topologies display typical positive Poisson’s ratio behavior, making them more suitable for energy absorption and compliant deformation scenarios, consistent with established findings in structural mechanics[75–

77]. The study also reveals that buckling onset, buckling mode and post-buckling behavior across these topologies are all highly controllable. Importantly, such behaviors are not governed by any single geometric attribute but instead emerge from coupled interactions among multiple parameters. For instance, minor adjustments in strut thickness can alter local buckling pathways, whereas porosity and unit-cell orientation predominantly shape the global stress-transfer mechanism. The diverse nonlinear deformation modes arising from these multi-parameter interactions render the lattice response under large deformation, transient impact and cyclic loading conditions more representative of the complex loading environment encountered during human gait. This enhanced mechanical plasticity provides a robust foundation for functional tuning of footwear across a broad range of use conditions.

The construction of this multidimensional geometric parameter space not only expands the expressive capacity of lattice architectures but also transforms structural response from a passive material outcome into a predictable and tunable engineering variable. The findings demonstrate that lattice structures are no longer merely lightweighting or energy-absorbing components; rather, they function as designable mechanical units with properties that can be prescribed independently of the base material. Their mechanical behavior becomes a deterministic function of geometry, thereby establishing the theoretical foundation for treating lattices as “programmable materials” in footwear design.

Another key finding of this study is the functional translatability of lattice structures within footwear. In conventional footwear, cushioning, support and propulsion capabilities are primarily governed by material constitutive properties and overall geometric form[78], leaving limited capacity for region-specific or phase-specific modulation throughout the gait cycle. In contrast, by tuning unit-cell topology, porosity and orientation, the present lattice system enables the midsole to exhibit markedly different mechanical responses across plantar regions, each aligned with the functional demands of distinct gait phases. For example, during heel strike, compliant lattice zones absorb impact energy and substantially reduce peak plantar pressure and soft-tissue stress. In the arch region, high-stiffness configurations restrain arch collapse and maintain a calcaneal pitch angle closer to its natural alignment. In the forefoot, directional control of lattice orientation enhances plantarflexion moment generation, thereby improving push-off efficiency. Through this mechanism, the lattice no longer serves a single localized purpose; instead, it forms a continuous functional chain across the gait cycle, enabling coordinated, region-specific mechanical regulation. This capacity for spatially and temporally differentiated response marks a higher-order mode of structural–functional expression in footwear design.

Moreover, this study shows that the regulatory effects of lattice architectures extend beyond local redistribution of plantar pressure and propagate along the lower-limb kinetic chain, altering the

kinematic and kinetic behavior of upstream joints such as the ankle and knee. Regional variations in midsole deformation influence not only the magnitude and direction of the ground reaction force but also the trajectory of its line of action, thereby reshaping joint load distribution and modulating the neuromuscular control strategies of the lower extremity. These findings indicate that the design of lattice midsoles transcends the domain of localized material engineering and instead constitutes a cross-regional, cross-joint and cross-system biomechanical coordination process. Consequently, this work provides a new theoretical perspective for future footwear optimization grounded in whole-chain dynamics and suggests that personalized footwear design should evolve from localized response tuning toward a framework of system-level locomotor modulation.

Most importantly, the lattice parameterization framework proposed in this study offers a fundamentally new mode of structural expression in footwear design, shifting the design paradigm from materials dictating function to structure dictating function. Within this framework, structure is no longer the passive outcome of material processing but emerges as a modelable, tunable and verifiable design variable. Through systematic modulation of topology, porosity, strut thickness and orientation, footwear performance can be predictably tailored within the geometric design space. This shift frees footwear design from the limited adjustability of traditional material formulations and foam densities, moving instead toward a programmable structural system driven by geometry and computational modeling. Such a system not only provides the engineering feasibility required for high-resolution functional differentiation but also lays the technological foundation for truly personalized footwear. As printable materials expand, manufacturing precision improves and the parameter space continues to grow[79, 80], lattice architectures are poised to become the core structural unit in next-generation footwear, propelling the field from empirically guided development toward a new engineering era of functionally controlled and computationally designed structures.

4.2 Functional Coupling and Regional Synergy of Zoned Lattice Midsoles

Human gait is intrinsically a spatiotemporally coupled dynamical process in which different plantar regions do not operate as isolated units but instead form a continuous and coordinated mechanical response through load transfer along the kinetic chain. Although each phase of the gait cycle imposes distinct functional demands on the foot, conventional footwear typically relies on uniform adjustments of material properties to accommodate these variations, leading to inherent limitations in local functional expression. For example, the material and structural characteristics of the rearfoot region influence not only lower-limb biomechanics but also stance duration[81], postural stability[82] and potentially spinal loading[83]. Forefoot stiffness directly affects propulsive efficiency, mechanical energy utilization and even injury risk[84]. Similarly, heel cups and lateral support structures have been shown to significantly modulate peak plantar pressure and postural control, respectively[85, 86].

However, most of these studies adopt a "single-structure–single-metric" analytical paradigm, producing region-specific functional interpretations that provide limited insight into how internal footwear structures coordinate across regions and across the entire gait cycle. As a result, the mechanisms by which footwear mediates multi-regional mechanical synergy during dynamic locomotion remain insufficiently understood.

Against this backdrop, the zoned lattice midsole model proposed in this study seeks to reconstruct the correspondence between plantar structure and function from a systems-level perspective. Geometrically, the midsole is partitioned into regions such as the rearfoot, arch, lateral midfoot and forefoot; however, these regions do not operate as independent modules. Instead, through parameter-continuous and topology-tunable lattice architectures, they maintain smooth spatial transitions and engage sequentially—"in relay"—to fulfill the functional demands of different phases of the gait cycle.

This design yields a continuous-field mechanical regulation system driven by structural parameters, enabling cushioning, stability and propulsion to emerge as dynamically coordinated, multi-regional responses across the entire gait cycle. Such a paradigm breaks from the traditional separation of regional functions in footwear design and offers a new theoretical framework for understanding how internal footwear structures exert system-level influence across the gait kinetic chain.

In the early stance phase, the compliant lattice in the rearfoot region serves as a critical "entry regulator" of the load pathway. Through nonlinear buckling and progressive compression, this lattice zone effectively reduces the initial slope of the ground reaction force curve, thereby lowering both impact peak magnitude and loading rate. This mechanical mechanism not only mitigates

transient stress concentration on the heel's soft tissues and fat pad but also provides a wider temporal window for the ankle joint and lower-leg musculature to respond and modulate loading. Unlike traditional midsoles that rely primarily on material damping to achieve cushioning, the compliant lattice implements a delayed-buffering strategy: its deformation pattern preserves the natural energy-absorption role of the calf musculature observed in barefoot locomotion, while avoiding the high impact and focal stress associated with barefoot heel strike. As a result of the smoother initial impact management, the line of action of the ground reaction force enters the midfoot phase more stably, establishing more favorable initial conditions for arch and lateral midfoot support. This reduces the likelihood of excessive pronation or compensatory muscular activity that can arise from insufficient rearfoot cushioning.

As the center of pressure migrates anteriorly, load is progressively transferred from the rearfoot to the midfoot complex. During this phase, the arch and lateral midfoot jointly function as a postural nexus: they must dissipate residual impact energy carried over from heel strike while simultaneously establishing a stable and advantageous geometric configuration for subsequent forefoot propulsion. In this study, the use of a higher-stiffness lattice in the arch region effectively constrained medial longitudinal arch collapse without eliminating the elastic deformation essential for shock attenuation and energy storage. This "elastic constraint rather than mechanical locking" enhances load-sharing efficiency while preserving the arch's intrinsic energy storage–release characteristics. Concurrently, the lateral midfoot region, governed by transverse lattice orientation and localized stiffness tuning, provides flexible restraint against excessive coronal-plane internal rotation, thereby maintaining the foot within a more physiologically stable postural corridor during mid-stance. Both FE simulations across participants and laboratory gait measurements in the HM participant indicated that the calcaneal pitch angle during mid-stance remained closer to its natural physiological range, while subtalar joint ROM—despite being slightly elevated at initial contact—converged toward the values observed in the conventional shoe during mid-to-late stance. This indicates that the midfoot lattice does not impose rigid corrective forces but instead employs a force-path–guidance mechanism that redirects stress flow while allowing controlled deformation. In essence, the midfoot lattice establishes an elastic field capable of both supporting and yielding appropriately, redistributing load along trajectories that favor efficient forefoot propulsion. This ensures a dynamically smooth transition from cushioning to propulsion, integrating the functional roles of adjacent regions into a coherent mechanical continuum.

This midfoot nexus generates regulatory effects that directly shape the structural–functional behavior of the forefoot during propulsion. The lattice topology and orientation in the forefoot region were designed to enhance effective sagittal-plane stiffness, enabling greater energy storage and return during push-off. At the same time, localized buckling modes increase the functional

contact area, thereby reducing peak forefoot pressure and producing a combined effect of efficient propulsion with moderated pressure distribution. Crucially, the improvement in propulsive efficiency does not arise from a simplistic amplification of local stiffness; rather, it is contingent on the mechanical preprocessing achieved by upstream regions of the kinetic chain. If rearfoot cushioning is insufficient, the midfoot must absorb more residual impact through pronounced postural compensation, distorting its geometric configuration and shifting load paths away from those that best facilitate propulsion. Under such unfavorable initial conditions, the forefoot is forced to generate push-off power with lower mechanical effectiveness, reduced energy return and increased risk of localized overload. The coordinated lattice design of the rearfoot and midfoot in this study effectively prevents these issues: the compliant rearfoot moderates and delays impact transmission, while the midfoot complex stabilizes arch height and coronal-plane posture through elastic constraint. Consequently, the forefoot enters the push-off phase in a configuration closer to natural gait, with improved alignment of load paths. Within this globally "pre-shaped" mechanical environment, the forefoot lattice is able to express barefoot-like propulsion characteristics—high energy return and effective moment generation—while avoiding the elevated local pressures typically associated with barefoot stance. This combination of barefoot-style propulsion and pressure-mitigated contact exemplifies the cross-regional synergy enabled by the zoned lattice architecture: each region does not merely execute an isolated local function but participates in a temporally sequenced relay of mechanical regulation across the gait cycle. Such multi-region coupling achieves system-level optimization that is difficult to realize with traditional homogeneous materials.

From a systems perspective, the cross-regional synergies demonstrated in this study are not merely post hoc interpretations of experimental observations but are outcomes actively discovered and exploited during the optimization process itself. Within the multiobjective optimization framework, each candidate structure is evaluated not on isolated metrics—such as rearfoot peak pressure, arch postural stability or forefoot propulsion—but on the combined performance of these metrics under dynamic gait loading. As a result, the optimization algorithm inherently "perceives" the coupling relationships formed through load transfer along the plantar kinetic chain, and subsequently leverages these interdependencies to enhance global performance during iterative search. Although the machine-learning surrogate model exhibits a degree of black-box behavior[55], limiting direct inspection of its internal input–output mapping, the evolutionary trajectory of the optimization reveals its implicit logic. Certain structural modifications—such as increasing arch stiffness or adjusting the transverse orientation of the lateral midfoot lattice—were retained in the final Pareto-optimal solutions not because they improved local deformation metrics in isolation, but because they altered stress-flow pathways, moderated the transmission of rearfoot impact, redirected midfoot

load trajectories and ultimately enhanced forefoot propulsive efficiency. In other words, the optimization process does not simply stack three local functions; rather, it uses the high-dimensional design space provided by the parametric lattice to autonomously discover a cross-regional, cross-phase coordination strategy. Because the midsole is a continuous structure, changes in local parameters propagate through geometric and mechanical fields, influencing dynamic behavior across the entire stance phase. The optimization framework leverages this property to regulate foot–shoe coupling at the system scale. This phenomenon not only reinforces the intrinsic system-level nature of gait as a linked kinetic chain but also illustrates that zoned lattice structures provide sufficient adjustable degrees of freedom for the algorithm to overcome the traditional linear logic of "material property, local function," enabling genuine system-level optimization at the structural level. Looking forward, incorporating multi-phase gait constraints, multimaterial combinations or musculoskeletal feedback would further amplify this capacity to "optimize through coupling," advancing footwear design from localized adjustments toward holistic regulation of the full-cycle kinetic chain.

In a recent review, Mohammadi et al. advocated for a stricter single-variable experimental paradigm in footwear biomechanics, recommending that researchers isolate one design factor—such as a localized outsole geometry or a single material component—by constructing simplified prototypes and elucidating their functional mechanisms through controlled mechanical testing[87]. This perspective is well grounded in materials science and structural engineering, where isolating variables can indeed facilitate clear causal inference. However, its marginal utility within footwear biomechanics is rapidly diminishing. The effects of numerous isolated variables—such as midsole thickness, heel geometry, forefoot stiffness, lateral stability features and material properties—have already been extensively characterized[88, 89]. Further repetition of single-variable studies often yields little more than confirmatory evidence for well-established phenomena, offering limited theoretical advancement. As discussed earlier, the influence of footwear on gait arises from cross-regional load transfer, structural coupling and neuromuscular regulation acting in concert. While single-variable designs allow experimental control, they inherently fail to capture these inter-regional interactions and cannot reveal the coordinated mechanisms that govern foot–shoe dynamics during locomotion. This limitation has become increasingly pronounced as modern footwear evolves toward multi-component, structurally integrated systems. What the field now urgently requires is not more granular single-factor experiments, but datasets of sufficient scale, ecological validity and population diversity to uncover cross-population, cross-task and cross-design regularities. Equally important are advanced modeling and optimization tools capable of systematically exploring vast, high-dimensional structural design spaces. This perspective aligns closely with the future research directions proposed by Steffen Willwacher and colleagues,90 who

highlight several key avenues for breakthrough: building large, representative real-world databases; leveraging 3D printing to enable structural freedom in experimental footwear; integrating FE, machine learning and gait dynamics into unified modeling frameworks; and strengthening interdisciplinary collaboration among materials science, engineering, biomechanics and data science. Taken together, the future of footwear research lies not in increasingly narrow single-variable validations, but in the development of research frameworks capable of uncovering system-level principles and multi-structure synergies.

Viewed against these emerging research trajectories, it becomes evident that traditional single-variable experimental paradigms can no longer meet the analytical demands of modern movement science, particularly when investigating complex structure–function relationships. The zoned, parameterized lattice framework proposed in this study addresses this gap by enabling simultaneous modulation of mechanical properties across the entire midsole. This allows footwear structures to be modeled, optimized and interpreted as an integrated system rather than as an assemblage of isolated components. Through multiobjective optimization and a unified FE–ML surrogate modeling approach, the present study evaluates the systemic impact of structural variations on plantar pressure distribution, foot postural control and propulsive dynamics under dynamic gait conditions. This moves beyond the conventional logic of linking a local structure to a single outcome measure and instead captures the interconnected nature of foot–shoe mechanics. The value of the zoned lattice midsole does not lie in merely mapping the rearfoot, arch and forefoot onto traditional functions—cushioning, support and propulsion. Rather, its programmable architectural design organizes these functions into a temporally and spatially continuous sequence of coordinated behaviors. The structure becomes a mechanical field that evolves with gait events, engaging in dynamic relays among impact attenuation, posture regulation and energy return. Such a synergy-centered structural logic enables a system-level reinterpretation of the structure–gait relationship. By integrating structural programmability with biomechanical coherence, this work establishes both the structural foundation and the biomechanical rationale for transitioning footwear design from traditional “component-stacking” paradigms toward holistic, field-driven design. This perspective aligns with the broader shift in movement science toward understanding locomotion as an emergent property of coordinated, multi-scale interactions rather than isolated mechanical events.

4.3 Dynamic-Gait–Driven Multiobjective Structural Optimization and Its Implications

Conventional approaches to footwear structural design and optimization typically rely on static loading conditions, homogeneous materials or limited parameter adjustments, with research objectives often centered on a single functional outcome[22]. Such methods fail to capture the complexity of real locomotion, including the multi-peaked nature of ground reaction forces, the time-varying deformation of plantar soft tissues, the phase-dependent modulation of joint posture and the shifting coordination among musculoskeletal elements across gait phases. Critically, different plantar regions undertake distinct mechanical roles during stance, and their functional demands evolve continuously over time. As a result, any optimization based solely on static conditions or isolated time points is intrinsically constrained.

By integrating FE simulation, a GPR-based surrogate model and multiobjective Bayesian optimization, this study establishes a closed-loop structural generation framework that links data, modeling, optimization and validation into a unified pipeline. This framework allows subject-specific gait characteristics to directly inform the search and convergence of lattice parameters. In contrast to traditional design workflows driven largely by expert intuition, the proposed method uses quantifiable data as the primary driver, autonomously exploring a high-dimensional structural space and iteratively approaching solutions that best satisfy individual functional requirements. This transition from experience-driven to data-driven design endows footwear structures with system-level adaptivity and personalization for the first time, laying the technical foundation for truly functional, individualized customization.

The scientific significance of dynamic-gait–driven optimization lies in its ability to align structural regulation directly with real usage conditions. Variations in rearfoot soft-tissue stress are evaluated using the actual time course of the ground reaction force during gait, capturing changes in impact peak magnitude and loading rate at initial contact. Arch stability is assessed through the dynamic evolution of the calcaneal pitch angle across the entire stance phase—rather than through static arch metrics commonly used in orthotic research—thereby reflecting the distinct stability requirements of the cushioning, transition and propulsion sub-phases. Forefoot propulsive performance is quantified by inverse dynamics at push-off, ensuring that the optimization target encompasses joint moment generation, gait rhythm and forward progression capacity. By incorporating these dynamic metrics into the optimization framework, structural tuning transcends traditional pressure-management or localized stiffness control and establishes a continuous, quantifiable linkage to whole-body locomotor performance. This transforms the relationship between footwear structure and the gait kinetic chain, yielding a new coupling logic that is inherently temporal, functional and

system-level.

At the level of optimization mechanics, the GPR model—trained on a large corpus of initial finite-element (FE) simulations—successfully captured the highly nonlinear mapping between lattice geometric parameters and their mechanical responses. While maintaining high predictive fidelity, the surrogate model markedly reduced computational cost: structural evaluations that would otherwise require numerous transient contact FE solutions were compressed to a negligible fraction of their original expense, thereby enabling Bayesian optimization to operate efficiently within a high-dimensional and continuous parameter space. Although similar surrogate-based approaches have been reported in computational materials and structural design[36, 90], they have largely remained confined to material property prediction or the validation of single configurations. Building upon a multilayered mapping across material behavior, structural topology, and mechanical attributes, the present study embeds the GPR surrogate model into the region-specific optimization of the midsole lattice, achieving cross-regional coordination that traditional FE frameworks cannot readily support. This system enables simultaneous evaluation of multiple functional attributes—including rearfoot cushioning compliance, arch-support stiffness, midfoot–lateral stability control, and forefoot propulsion enhancement—within a unified optimization cycle, ultimately constructing a Pareto front that reflects the intrinsic trade-offs among multi-objective performance targets. Notably, the optimization landscape exhibits characteristic conflicts: for example, excessive reduction in rearfoot pressure may diminish forefoot propulsive efficiency, whereas strengthening forefoot propulsion typically elevates local stress in that region. By quantifying predictive uncertainty, Bayesian optimization actively identifies, at each iteration, the candidate sample with the highest expected information gain, thus maintaining a principled balance between exploration and exploitation. Through this iterative process, the solution space progressively converges toward an optimal performance regime capable of satisfying the complex interplay among competing objectives.

It is worth emphasizing that the optimized designs demonstrated a high degree of consistency between FE-based predictions and experimental validations. This concordance serves not only as a conventional assessment of model accuracy, but more critically as compelling evidence for the feasibility of the dynamic-gait-driven optimization paradigm proposed in this study. Across plantar-pressure distributions, joint kinematic trajectories, and propulsive dynamics during toe-off, the experimentally observed trends closely mirrored the model predictions, indicating that the lattice structures, when implemented in real wearable conditions, faithfully reproduced the intended mechanical regulation mechanisms encoded in the simulations. Such cross-scale agreement—from the cellular architecture of the lattice, to the mesostructural configuration of the midsole, and further to whole-body locomotor behavior—signifies that the optimized structures transcend the theoretical

domain of numerical simulation and can be transferred with high fidelity to actual human movement. This multiscale coherence marks a conceptual shift: structure optimization informed by gait data is no longer a speculative or purely computational construct, but a design methodology with tangible engineering implementability.

Viewed from a broader perspective, the workflow established in this study represents an early prototype of future intelligent footwear design. Foot-shape scanning provides the geometric constraints; gait acquisition supplies physiologically realistic boundary conditions; and surrogate-assisted multi-objective optimization autonomously generates individualized lattice midsoles—eliminating the reliance on empirical parameter tuning or labor-intensive prototyping cycles. Such an end-to-end, data-driven generative framework lays a robust foundation for personalized, on-demand manufacturing systems and offers a highly scalable technological pathway for diverse applications, including injury prevention, rehabilitation support, pressure management, and performance enhancement.

More fundamentally, the concept of dynamic-gait-driven structural optimization extends well beyond the footwear domain, offering a new paradigm for designing human–equipment coupled systems. In principle, this methodology can be generalized to a wide spectrum of wearable or assistive devices: for instance, enabling the creation of phase-adaptive prosthetic footplates tailored to an individual's locomotor profile; achieving precise mechanical matching in orthotic devices to modulate local tissue loading; developing intelligent protective gear capable of redistributing pressure in real time; or advancing multi-objective mechanical design for full-body wearable systems. In this sense, the present work not only advances the field of footwear engineering but also provides a conceptual and methodological foundation for next-generation human–machine interaction systems, bridging disciplines through a unified structural design philosophy.

4.4 Multiscale Biomechanical Validation of Lattice Footwear and Its Engineering Prospects

The experimental findings obtained in the validation phase not only further corroborate the reliability of the prior model predictions, but also provide essential empirical support for the multiscale biomechanical chain that links microstructural regulation to macroscopic gait behavior. A defining feature of lattice architectures is that their mechanical performance is governed directly by geometry: the high-dimensional design space encoded by strut thickness, unit-cell topology, porosity, and orientation enables highly localized mechanical tuning at the microscale, while the resulting effects propagate through the soft tissues of the foot and the kinetic chain of the lower limb, ultimately manifesting in plantar-pressure redistribution, joint-posture modulation, propulsive dynamics, and even global gait patterns. Laboratory wearable trials conducted in the HM participant demonstrated that the local load-bearing behavior of the lattice structures closely reproduced the patterns predicted by finite-element analysis. Subject-specific simulations for the FF and BMD participants showed consistent directional improvements within the computational framework. This agreement extends beyond localized biomechanical indicators—such as peak pressures and stress trajectories—to higher-order functional responses, including midfoot postural stability and forefoot propulsive efficiency. More importantly, the consistency spans two fundamentally different evaluative dimensions: objective biomechanical measurements and subjective perceptual assessment. The HM participant's reported experiences of rearfoot cushioning, arch support, and forefoot propulsion aligned with the predicted functional trends, indicating that the influence of lattice architecture extends from the structural domain into perceptual and behavioral domains. This observation suggests that lattice structures possess not only the capacity to act as localized material substitutes, but also the system-level potential to modulate human movement patterns. Their geometric programmability enables coherent mapping across multiple scales: microstructural tuning, mesoscale tissue response, macroscale kinetic-chain behavior, and subjective experience. The continuity of this chain, verified experimentally in the HM participant and supported computationally in the other participant-specific simulations, establishes both the theoretical foundation and evidence necessary for developing structure-centered, personalized movement-intervention strategies in the future.

From a structural standpoint, the performance of the lattice midsole observed in the HM wearable experiment aligns closely with the predictions of the finite-element simulations. In the rearfoot region, the compliant lattice exhibited stable nonlinear compression under authentic gait-induced impacts, effectively reducing peak pressures and moderating the rate of impact rise—behaviors consistent with FE predictions. This agreement indicates that the intended mechanisms of localized

buckling and progressive collapse operate reliably under real loading conditions. The midfoot composite zone likewise demonstrated responses in accordance with model expectations; by modulating local stiffness and lateral deformation capacity, the lattice facilitated subtalar-joint posture transitions during stance that more closely resembled those of natural gait. In the forefoot region, the lattice architecture enhanced energetic return during toe-off through its tailored topology and orientation, yielding an increase in propulsive torque—a trend also mirrored in the simulated improvements in propulsion performance. Collectively, these findings confirm that, in the HM wearable validation, geometric tuning at the microscale can be translated in a stable and predictable manner into macroscale biomechanical effects; the corresponding simulation results suggest similar transferability for FF and BMD under subject-specific constraints. Structural modifications influence not only localized pressures and deformations but also foot posture and the broader behavior of the lower-limb kinetic chain. Taken together, the results demonstrate that parametric lattice architectures constitute not merely an alternative material system, but a functionally actionable structural mechanism capable of modulating whole-shoe and whole-gait performance. This capability establishes a solid foundation for deploying lattice structures as the core functional components of next-generation footwear systems.

What is particularly noteworthy is that the experimental results obtained in the HM wearable validation not only validated the mechanical predictions of the finite-element analyses but also demonstrated the stability and comfort of the lattice structures under real wearing conditions. The midsole lattice exhibited excellent deformation recovery during repeated loading–unloading cycles, with the FDM-fabricated spatial strut network achieving sufficient structural continuity, geometric accuracy, and regional transition quality to meet the mechanical demands of gait. Even under complex loading scenarios—including high strain gradients, localized buckling, and multiaxial loading—the lattice maintained a stable global configuration and reproduced the mechanical response patterns anticipated by the simulations. Subjective evaluations further reinforce these findings. The HM participant reported that the lattice-equipped footwear provided superior impact attenuation during landing, smoother forefoot rollover during toe-off, and a more natural overall gait compared with the control shoe. These perceptions suggest that the localized mechanical enhancements induced by microscale geometric tuning have translated into movement experiences recognizable by the neuromuscular control system. The convergence between structural performance and perceptual feedback thus offers compelling evidence for the broader applicability of lattice architectures in wearable systems.

The significance of this study extends far beyond validating the performance of a single footwear prototype. Its primary contribution lies in articulating a transferable, coupled design methodology that links structural regulation with functional expression. The parametric lattice–based midsole

design enables researchers to construct structural units with tunable mechanical properties through subtle adjustments to local geometric parameters. When integrated with gait-driven multi-objective optimization, these units can autonomously assemble into task-specific “functional formulations.” In running scenarios, for instance, the framework can enhance forefoot propulsion while simultaneously improving rearfoot energy absorption. In multidirectional sports such as basketball, local stiffness modulation along the lateral midfoot can increase transverse stability. In hiking or trail-running contexts, graded lattice architectures can be configured to improve impact attenuation and adaptability to uneven terrain. Compared with traditional midsole design approaches—typically constrained by material properties, localized thickening, or discrete functional components—the lattice methodology introduces a paradigm in which structure, rather than material, becomes the primary design variable. Function is expressed through geometry, while the material serves mainly as the substrate that enables its realization. This shift in design philosophy establishes a methodological foundation for future programmable footwear and structurally adaptive sports equipment across diverse use scenarios.

In rehabilitation and podiatric contexts, the potential value of lattice structures becomes particularly pronounced. For pathological foot conditions such as flatfoot, high-arched foot, and diabetic foot, conventional insoles or orthoses typically rely on regionally varied foam materials to provide localized support[91, 92]. However, such material-based zoning offers limited control over structural behavior and is insufficient for simultaneously modulating deformation modes, buckling pathways, transverse constraint, and energy-transfer characteristics—mechanical attributes that are essential for restoring or optimizing foot function. By contrast, lattice architectures enable systematic modulation of geometric parameters to redistribute stress peaks, alter soft-tissue deformation patterns, and influence plantar loading trajectories and postural control within localized regions. Because these adjustments arise from computationally defined and continuously tunable geometric inputs, the resulting interventions no longer depend on heuristic or experience-driven partitioning. Instead, they allow the formation of predictable, personalized support strategies[53, 93]. This capability provides a more engineered and reproducible pathway for customized orthotic design tailored to pathological foot types.

Looking further ahead, integrating lattice architectures with sensor networks and embedded electronic systems could transform footwear from a fixed-function passive structure into an actively responsive device[94, 95]. The intrinsic programmability of lattice geometry naturally provides the actuation units required for such systems. For example, regional stiffness could be modulated in real time based on continuous pressure feedback; in-shoe sensors could detect gait abnormalities and trigger localized structural responses; and support patterns could be adaptively adjusted during training or rehabilitation to accommodate changing load conditions, thereby enabling more precise

gait correction. Moreover, embedding miniature sensors within the lattice itself would allow for fatigue monitoring, pressure-pattern recognition, and motion-feature tracking, effectively enabling the midsole to undertake certain computational and actuation tasks typically associated with lightweight exoskeletal systems. Existing variable-stiffness footwear concepts already demonstrate the technical feasibility of this direction. ANTA's "Wolverine" system, for instance (Fig. 4.4.1), employs carbon plates, adjustable mechanisms, and sensor-driven control to dynamically tune longitudinal bending stiffness, thereby maintaining stable mechanical posture and joint power output during high-speed or high-load movements. Its design objective is to automatically compensate for the decline in propulsive stiffness that accompanies late-stage fatigue, thus sustaining athletic performance. Although such technologies remain in the exploratory engineering phase, they clearly illustrate an evolutionary trajectory in which footwear progresses from static structural optimization toward real-time, system-level regulation. This trajectory also provides a tangible reference for the deeper integration of lattice architectures with intelligent actuation mechanisms.

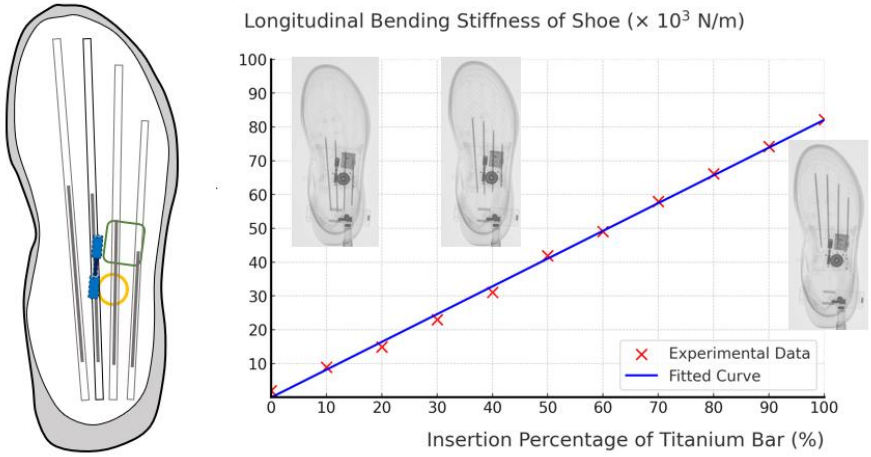

Figure 4.4.1 ANTA "Wolverine" Adjustable Bending-Stiffness Sole System and Its Longitudinal Stiffness Tuning Performance.

Furthermore, the overarching concepts advanced in this study—structural programmability, gait-driven design, and multi-objective optimization—are not confined to the footwear domain. Their essence lies in translating individual mechanical demands into computable and controllable structural parameters, and in establishing a stable multiscale mapping from microstructural geometry to macroscopic behavioral outcomes through systematic validation. This principle applies equally to a broader class of biomechanical devices, including prosthetic footplates, ankle–foot orthoses, and lower-limb exoskeletons, all of which fundamentally depend on mechanical controllability and individual-specific adaptation[96, 97]. Current approaches in these fields

typically rely on limited-dimensional adjustments—such as modifying material stiffness, altering global shape, or incorporating mechanical hinges—rendering it difficult to meet the dynamic, multi-regional, and multi-phase functional requirements inherent to human movement. In contrast, the lattice model and optimization framework developed in this study offer an extensible structural representation: local mechanical attributes can be directly governed through geometric parameters, and structural responses can be precisely matched to an individual's gait characteristics. This capability enables higher functional specificity and greater adaptability across user populations. The multiscale experimental validation further suggests that lattice architectures, beyond demonstrating stable and predictable regulatory behavior in footwear, hold promise for translation into more complex movement or rehabilitation scenarios. As a form of functionally programmable material, lattice structures transcend the intrinsic limitations of conventional materials, shifting equipment design away from isolated structural adjustments toward system-level control of movement. With continued advances in personalized scanning, real-time gait monitoring, and intelligent manufacturing, such architectures may become foundational elements of next-generation wearable systems—capable of autonomously adapting and actively regulating performance based on human biomechanical dynamics. In this sense, footwear design is transitioning from a traditional materials-centric paradigm toward a structurally oriented, dynamically informed era of intelligent performance. The structural logic developed here is poised to influence a much broader landscape within sports science and rehabilitation engineering.

4.5 Limitations

Despite presenting a relatively comprehensive framework for parametric lattice–footwear design, and achieving a coherent integration of structural modeling, finite-element analysis, dynamic gait validation, and multi-objective optimization, it remains necessary from a scientific perspective to acknowledge several limitations of this study. These limitations relate to the characteristics of the research participants, the constraints of the experimental design, the simplifying assumptions underlying the computational models, the materials and fabrication methods employed, and the overall scope of the methodological framework.

The experimental wearable validation phase relied on an in-depth single-participant case study (HM), while subject-specific modeling and optimization were performed across three participants. Although this design expands computational generalizability, the limited experimental sample size naturally constrains statistical inference. Foot biomechanics vary substantially across individuals, factors such as arch height, soft-tissue thickness, joint compliance, body-mass index, gait strategy, and neuromuscular control can all influence plantar-pressure patterns and lower-limb kinetic behavior. Yet under the requirement to maintain tight control of experimental variables and to preserve the integrity of the modeling–simulation–optimization–validation loop, a case-based approach offers unusually clean observational conditions. In contrast to large-sample studies where behavioral heterogeneity and gait variability often obscure underlying mechanisms, the single-participant design reduces noise stemming from inter-individual differences and allows the mechanical regulation pathways of the lattice structure to emerge with greater clarity. In this sense, although the sample size is limited, the value of the study does not lie in statistical inference. Rather, it resides in demonstrating how individual-level structural response mechanisms manifest consistently across geometric parameters, foot mechanics, and gait outcomes. This provides a verifiable conceptual foundation for future efforts aimed at personalized, structure-driven design.

Although the finite-element model used in this study was validated through material testing, parameter calibration, mesh convergence analysis, and comparisons with plantar-pressure measurements, it inevitably incorporates a number of simplifying assumptions. The soft tissues of the plantar region were modeled as homogeneous, isotropic, and time-independent; the plantar fascia was represented in a reduced form; and the modeling of inter-bone articulation, cartilage friction, and ligamentous constraints did not fully reflect anatomical detail. As a result, the model remains an approximation rather than a complete physiological replica, particularly when describing localized stress peaks, deep-tissue loading, or fine-scale behavior under complex boundary conditions. It is important to emphasize that such simplifications are not specific to this study but are characteristic of foot finite-element modeling more broadly. The foot is an inherently complex, multi-tissue, multi-material, and multi-joint system. Attempting to reconstruct every biomechanical

feature within a single model would dramatically increase dimensionality and computational cost, while also complicating parameter identification, numerical stability, and the interpretability of outcomes. In fact, most published foot FE studies adopt a comparable level of abstraction and tissue simplification, reflecting a consensus that, in engineering and biomechanical applications, the primary aim is not absolute physiological fidelity but rather the accurate capture of key mechanical mechanisms within a reasonable margin of precision[98, 99]. Despite its simplifications, the model developed in this study reproduced experimental trends in overall pressure distribution, regional loading differences, and the relative effects of structural modulation. This agreement suggests that the abstractions did not compromise its utility for mechanism analysis or structural optimization. From a methodological perspective, the modeling strategy should therefore be viewed as a pragmatic balance among problem complexity, computational feasibility, and research objectives. As advances in soft-tissue constitutive modeling, individualized imaging, and high-performance computing continue, the level of anatomical detail in foot FE models will undoubtedly increase. Yet for the present study's focus on structural regulation mechanisms and personalized optimization, the adopted modeling fidelity is sufficient to provide reliable, interpretable, and experimentally verifiable mechanical insight.

It should be noted that although the TPU 95A material used in this study is suitable for fabricating experimental midsole prototypes, its long-term service performance has not yet been systematically evaluated. Lattice architectures consist of slender struts and internal cavities, and in real-world use they must withstand high-frequency cyclic loading and complex gait conditions. Over extended periods of operation, phenomena such as material fatigue, shifts in buckling behavior, micro-crack initiation and growth, and accumulated damage at nodal connections may arise, ultimately leading to gradual reductions in structural stiffness and energy-absorption capacity. Such forms of degradation stem not only from the intrinsic properties of the material but also from common challenges faced by 3D-printed footwear research more broadly[100]. The experimental validation conducted here focused primarily on short-duration gait tests and limited repetitions of walking, which cannot fully capture the high-cycle, long-duration loading typical of everyday use. Consequently, any extrapolation to long-term reliability should be made cautiously. Yet this material-level limitation does not undermine the generality of the methodological framework proposed in this study. In the present context, TPU 95A serves as a manufacturable, testable, and reproducible structural carrier whose primary function is to realize the geometric expression and structural degrees of freedom required for parametric lattice design, rather than to dictate the success of the method itself. The framework centers on structural programmability, and its effectiveness arises from the ability of geometric parameters to regulate functional performance, rather than from the inherent qualities of any particular material. In fact, the replaceability of the material is one of

the strengths of the approach. As higher-performance materials become available, such as E-TPU with improved rebound properties, multi-phase elastomers with extended fatigue life, flexible thermosets with specialized response characteristics, and even programmable materials capable of time-varying stiffness[101, 102], the functional space of lattice structures will continue to expand. These materials promise not only greater energy return, fatigue resistance, and buckling stability, but also finer control and broader dynamic range in structural modulation. At the same time, advances in multi-material 3D printing will make it possible to combine soft and stiff phases, create continuous material gradients, and integrate responsive materials within a single midsole. Such capabilities offer a powerful technical platform for exploring more complex cross-regional mechanical interactions and multidimensional functional regulation.

The scope of the experimental scenarios and evaluation metrics adopted in this study also constitutes a surface-level limitation. The validation focused primarily on steady walking, a highly controllable task, and did not include more demanding activities such as running, abrupt stopping and turning, incline or decline locomotion, or traversal of irregular terrain. Similarly, the assessment metrics were restricted to mechanical quantities such as plantar pressure, joint kinematics, and gait dynamics, without consideration of higher-level physiological and behavioral indicators including metabolic cost, long-term comfort, muscle fatigue patterns, or injury risk. From the standpoint of comprehensiveness, these restrictions indeed limit the extent to which the performance of lattice structures can be extrapolated to more realistic and complex movement contexts. However, much like the simplifications inherent in materials selection and modeling assumptions, the constrained experimental scope should be understood as a necessary and rational abstraction during the early stages of methodological development. Steady walking, with its strong controllability, high repeatability, and minimal inter-individual variability, provides a clean environment in which gait-chain alterations induced by structural modulation can be identified and attributed with greater confidence. Likewise, focusing on core mechanical indicators allows the structure–function mapping and the optimization framework to be validated at their most direct and interpretable levels. In this sense, the objective of the present work is not to exhaust all possible application scenarios but to verify the feasibility of the fundamental mechanism—structure-driven regulation—and to establish a theoretical and methodological foundation that can be extended. As future experiments incorporate multi-scenario, multi-intensity, multi-terrain, and even fatigue-state gait conditions, the regulatory behavior of lattice structures across diverse contexts will become increasingly informative. The structure–gait coupling model, dynamic target-setting strategy, and multi-objective optimization procedures developed in this study provide an initial methodological platform for such expansion. Viewed in this way, the current “limitations” do not reflect shortcomings in the capability of the approach, but rather represent the foundational theoretical and experimental layer required

before moving into more complex locomotor ecologies. Building on this foundation, subsequent research will be able to explore, in a more systematic manner, the performance and adaptation mechanisms of lattice structures across a wide range of movement environments.

In summary, this study does present several limitations related to sample size, modeling assumptions, material durability, and the specificity of the experimental conditions. These limitations, however, arise largely from the level of abstraction and methodological choices required when studying foot biomechanics as a complex system, rather than from shortcomings in the approach itself. Given current technological and methodological constraints, any attempt to fully reconstruct the multi-tissue, multi-material and multi-joint physiology of the foot, or to design experiments encompassing the full spectrum of human movement, would inevitably encounter an unmanageable space of variables and substantial interpretive noise. The present work instead advances along a controlled, verifiable and traceable path. This strategy allows structural parameterization, mechanical prediction and gait-driven optimization to operate coherently within a unified framework, and enables the functional influence of lattice structures on plantar loading, joint posture and propulsive dynamics to be confirmed through experiment. Viewed in this light, the limitations identified here should be regarded less as boundaries that restrict the method and more as directions in which future work may grow. The concepts introduced in this thesis, including structural programmability, dynamic target setting, multiscale validation and multi-objective optimization, hold clear promise for extension to larger datasets, more demanding movement tasks, broader material systems and models that integrate multiple disciplinary perspectives. As imaging technologies, materials science, high-performance computation and intelligent wearable devices continue to advance, the framework developed in this study is likely to support applications across a far wider movement ecology. It may ultimately contribute to a shift in footwear design from localized structural adjustments toward a genuinely systemic, biomechanics-informed and individualized era of intelligent performance.

5 Conclusions and future works

5.1 Main Research Conclusions

This dissertation centers on parametric lattice architectures and establishes an integrated research framework that spans midsole structural design, numerical simulation and dynamic validation. The analysis focuses on three core functional demands of gait—cushioning, stability and propulsion. The main conclusions are as follows:

(1) The multidimensional parametric lattice system covers a broad mechanical spectrum ranging from compliant energy absorption to high-stiffness support.

Through systematic modulation of geometric parameters, including topology type, strut thickness, porosity, unit-cell scale and orientation, the lattice structures exhibit continuously tunable mechanical responses and enable pronounced functional differentiation within a single material system. The finite-element simulations align closely with existing experimental evidence, demonstrating that the system reliably and accurately maps microstructural geometry to macroscopic mechanical behavior.

(2) The region-specific lattice midsole, designed for gait tasks, enables coordinated regulation across both regions and gait phases.

The lattice configurations in the rearfoot, arch and forefoot perform distinct mechanical roles throughout the gait cycle. Rearfoot energy absorption, arch postural modulation, lateral midfoot constraint and forefoot propulsion enhancement act in sequence and are linked through force-chain transmission, forming a continuous and coordinated mechanism. The midsole therefore functions not as an assembly of isolated components but as a structurally programmable system that participates in the mechanical execution of the entire gait process.

(3) Gait-driven multi-objective optimization verifies the feasibility and effectiveness of personalized lattice design.

By integrating finite-element simulation, Gaussian Process Regression surrogate modeling and multi-objective Bayesian optimization, this study achieves, for the first time, structural parameter search using real gait dynamics as input. The optimal solutions exhibit consistent trends in both simulation and experiment, indicating that personalized lattice midsoles can simultaneously improve cushioning, stability and propulsion. This demonstrates the advantages of a structure–gait coupling approach.

(4) Multiscale validation confirms that microstructural modulation can be reliably translated into macroscopic gait improvement.

The fabricated prototypes and wear experiments show substantial reductions in rearfoot impact, improved arch stability, enhanced toe-off propulsion and clear subjective benefits. These findings

collectively demonstrate that geometric tuning at the microstructural level can meaningfully influence plantar-pressure distribution, joint kinematics and overall gait behavior, establishing lattice structures as an effective strategy for achieving multiscale functional regulation.

5.2 Contributions of This Thesis

(1) Methodological contribution: establishment of a complete and reusable lattice design framework. This study develops an end-to-end workflow that integrates parametric lattice modeling, finite-element simulation, structure–function mapping, gait-driven multi-objective optimization and experimental validation. The framework shifts footwear structural design from empirical parameter tuning toward data-driven and model-driven decision making. By combining surrogate modeling with Bayesian optimization, it enables efficient exploration of high-dimensional design spaces and provides a standardized pathway for implementing structural programmability.

(2) Theoretical contribution: formulation of the coordinated regulation mechanism of lattice structures within the gait kinetic chain.

The dissertation identifies how lattice architectures exert region-specific yet continuous regulation throughout the entire gait cycle. It elucidates how structural parameters in different foot regions influence load transfer, postural control and propulsive dynamics, and introduces the concept of a "structure–gait coupled regulatory chain." This mechanism demonstrates that a lattice midsole functions not as a local feature but as an integrated participant in dynamic force transmission, offering new theoretical insight into the coupling between footwear structures and the human locomotor system.

(3) Engineering contribution: development of a practical design and fabrication scheme for midsoles. The thesis implements parametric lattice midsoles through 3D printing and validates their performance in real gait conditions, extending the concept of structural programmability from simulation into wearable prototypes. The approach exhibits strong scalability and can be adapted to athletic footwear, rehabilitative footwear and plantar orthotic devices. It provides an engineering framework that supports on-demand manufacturing and personalized functional customization.

5.3 Future Research Directions

Although this dissertation establishes a relatively complete design framework for parametric lattice footwear, the complexity of foot biomechanics and the diversity of movement scenarios indicate that many avenues remain open for further investigation. The present study adopted an in-depth single-participant case approach, which ensured strong consistency between modeling, simulation and experimental validation, but inevitably limits the generalizability of the findings. Future work

should involve larger and more representative cohorts encompassing a range of foot morphologies, body weights, ages and movement habits. Such studies would help elucidate how lattice structures adapt to individual variability and would support the development of a dual-scale design paradigm that functions at both the population and individual levels.

A second direction concerns the finite-element modeling of the foot. In this study, necessary engineering simplifications were applied to tissue constitutive behavior, joint contact interactions and the representation of muscle forces. Although these abstractions did not impede the identification of the primary mechanical mechanisms, future work may progressively incorporate more realistic tissue properties and dynamic characteristics. Such enhancements would allow the model to approach physiological conditions more closely while remaining computationally tractable, thereby improving both the accuracy and interpretability of structure–gait coupling predictions.

At the material level, substantial opportunities for advancement remain. Although TPU 95A satisfies the requirements for prototype fabrication, its fatigue life, buckling stability and long-term performance are limited. With the rapid development of multi-material 3D printing, variable-stiffness elastomers, high-rebound polymers and responsive materials, future research may explore strategies that couple material selection with geometric design. Examples include embedding soft–hard gradients, multiphase compositions or programmable materials within a single lattice. Such approaches would allow the midsole to exhibit higher-dimensional mechanical behavior and enhance its capacity for energy management under complex gait conditions.

In terms of structural representation, this dissertation employs parameterized modeling based on predefined families of lattice topologies. This approach offers a clear and controllable design space, but it also constrains the diversity of attainable structural forms. Future work may incorporate topology optimization, TPMS-based architectures and generative geometric modeling to move beyond fixed unit types and expand the midsole design into a more continuous and unconstrained geometric domain. Such developments would allow finer coordination between small-scale and large-scale structural features and enable richer forms of multiscale mechanical regulation.

The experimental validation in this study focused primarily on steady walking, which offers a clean and controlled setting for identifying the dominant structural effects. However, this scope does not capture the multidirectional, high-intensity or inherently uncertain conditions characteristic of real-world movement. Future research should extend the investigation to a broader range of tasks, including running, directional changes, incline and decline locomotion, uneven terrain and fatigue-induced gait alterations, in order to assess the stability and robustness of lattice structures across diverse scenarios. With ongoing advances in wearable sensing, mobile motion capture and real-world data acquisition technologies, it will become increasingly feasible to validate and iteratively refine structural optimization strategies within natural movement environments, thereby bringing

the integration of modeling and experimentation closer to authentic ecological conditions.

Finally, as flexible sensors, miniature actuators and variable-stiffness materials continue to advance, lattice architectures hold the potential to evolve from static geometric structures into functional entities capable of real-time adjustment. Future systems may incorporate a closed-loop interplay among structural configuration, sensing and active modulation, allowing footwear to modify local stiffness or deformation patterns in response to pressure distribution, movement state or even fatigue level. Such developments would represent a substantive step toward truly intelligent structural systems. Beyond transforming the design paradigm of footwear itself, this trajectory may also exert significant influence on broader domains such as rehabilitation and orthotics, podiatric medicine, sports protection and lower-limb exoskeleton technologies.

Thesis points

1st Thesis point: Establishment of a Programmable Parametric Lattice Modeling Framework Enabling Multidimensional Control of Footwear Structural Mechanics

This dissertation introduces a programmable parametric lattice modeling framework tailored for footwear applications, in which key structural elements—including unit-cell topology (such as honeycomb, re-entrant and rectangular forms), strut thickness, porosity and spatial orientation—are unified within a multidimensional geometric design space. This framework enables continuous and precise control of lattice morphology and mechanical response, allowing structures generated from a single material system to span a wide spectrum of behaviors ranging from compliant energy absorption to high-stiffness support. Local adjustments can further be applied to satisfy region-specific functional requirements. Compared with traditional midsole design approaches that rely primarily on material properties or foam-density modulation, the proposed framework shifts the basis of mechanical performance from "material-determined" to "geometry-driven." This transition lays the foundation for programmable and functionally tunable footwear structures, offering a more versatile and controllable pathway for engineering next-generation midsoles.

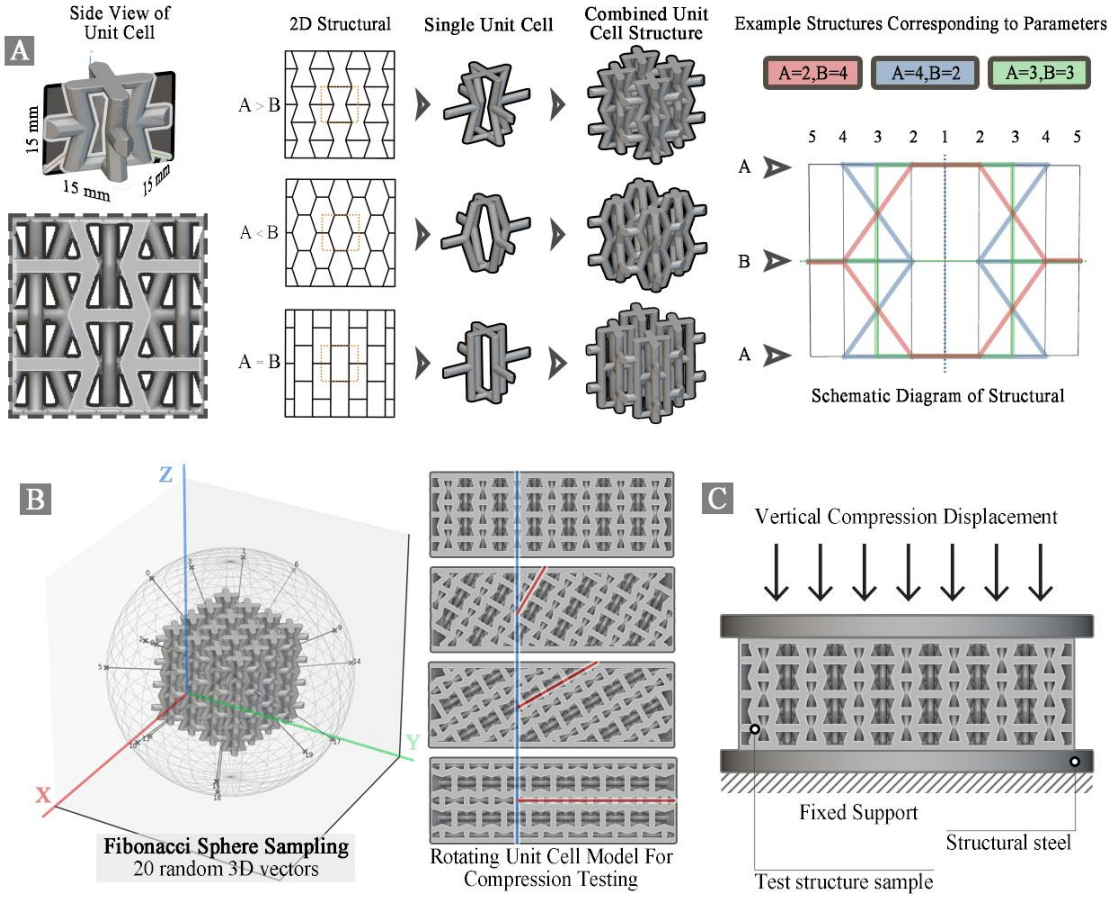

Building on a systematic suite of FE simulations, this study constructs a geometric–mechanical

mapping database that covers a broad parameter range and clarifies how different combinations of design variables influence structural stiffness, transverse deformation, energy absorption capacity and buckling response. The results demonstrate that lattice architectures can achieve predictable and continuously adjustable mechanical behaviors through geometric manipulation, exhibiting multidimensional, multi-stage and inherently designable mechanical modes. This programmable structural system frees the midsole from dependence on inherent material constitutive properties and instead enables fine-scale and region-specific performance configuration through geometry alone. It establishes a theoretical premise in which "structure defines function," and forms the methodological core for subsequent gait-driven optimization and personalized design.

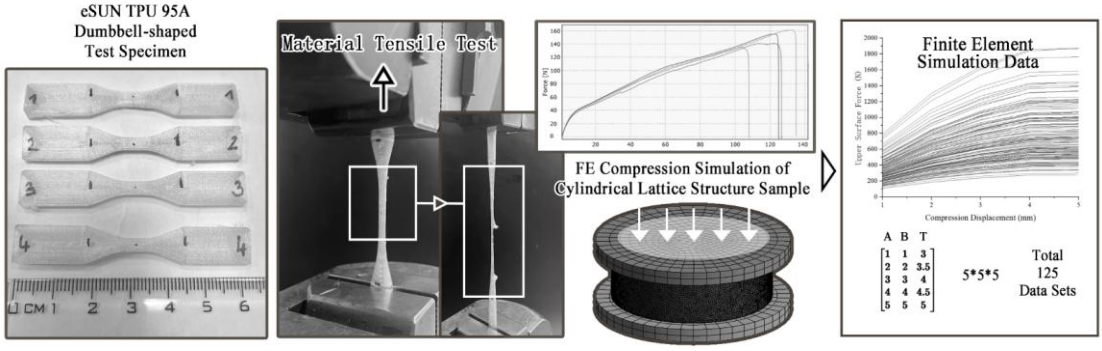

Related articles to the 1st thesis point:

1. **Z Lu**, X Li, D Sun, Y Song, G Fekete, A Kovács, Z Gao, J Zheng, L Xiang, Y Gu. (2025). Computationally tuned dual-layer lattice pads adapted to gait-induced pressure distribution. npj Advanced Manufacturing , 2(1), 43. **Nature Portfolio journal**.
2. **Z Lu**, X Li, D Sun, Y Song, G Fekete, A Kovács, K András, Y Gu. (2025). Parametric cushioning lattice insole based on finite element method and machine learning: A preliminary computational analysis. Journal of Biomechanics, 184, 112674. **IF: 2.4, Q1**.

2nd Thesis point: Development of a Region-Specific Lattice Midsole Design Method and Establishment of a Clear Coupling Mechanism Between Structural Regulation and Gait Function

This dissertation proposes and implements a region-specific lattice midsole design method informed by functional demands of the gait cycle. The midsole is partitioned into four major regions—rearfoot, arch, lateral midfoot and forefoot—each assigned lattice topologies, porosity levels and stiffness gradients tailored to its mechanical role. Through spatially continuous transitions and parametric geometric representation, the study constructs a "continuous functional chain" spanning the entire gait cycle, from initial contact to toe-off. The compliant rearfoot structures absorb impact and reduce vertical loading rates; the stiffer, orientation-specific architectures in the arch and lateral midfoot regulate medial collapse and coronal-plane posture; and the directionally reinforced forefoot lattices enhance plantarflexion torque and propulsive efficiency. More importantly, the work identifies the dynamic coupling mechanisms linking these regions. Rearfoot energy absorption alters the preparatory state of midfoot posture, midfoot stability directly influences forefoot propulsion efficiency and together they form an integrated force-transmission system that operates across regions and gait phases. This reveals that midsole design should not be conceived as a simple aggregation of local functional components. Instead, it should be understood as a system-level regulatory framework organized along the mechanics of the entire gait kinetic chain. The findings provide a new theoretical basis for understanding how midsole structures participate in and modulate the full gait process.

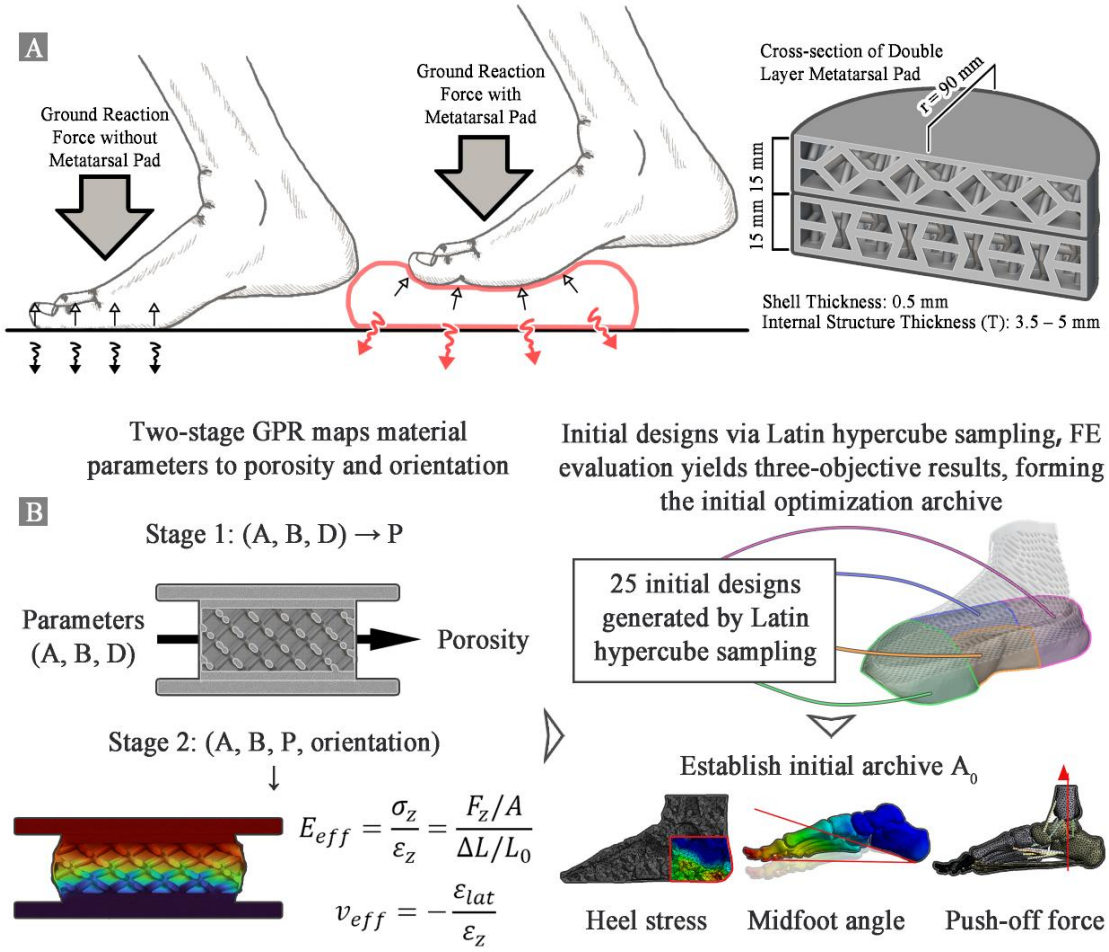

Related articles to the 2nd thesis point:

1. **Z Lu**, X Li, D Sun, Y Song, G Fekete, A Kovács, Z Gao, J Zheng, L Xiang, Y Gu. (2025). Computationally tuned dual-layer lattice pads adapted to gait-induced pressure distribution. npj Advanced Manufacturing , 2(1), 43. **Nature Portfolio journal**.
2. S Gao, Y Song, D Sun, X Cen, M Wang, **Z Lu**, Y Gu. (2025). Impact of Becker muscular dystrophy on gait patterns: Insights from biomechanical analysis. Gait & Posture. **IF: 2.4, Q1**.
3. Y Xu, C Zhu, Y Fang, **Z Lu**, Y Song, C Hu, D Sun, Y Gu. (2025). The effects of different carbon-fiber plate shapes in shoes on lower limb biomechanics following running-induced fatigue. Frontiers in Bioengineering and Biotechnology, 13, 1539976. **IF: 4.8, Q1**.
4. X Li, **Z Lu**, Y Song, M Liang, Y Yuan, G Fekete, A Kovács, D Sun, Y Gu. (2024). Pregnancy-induced gait alterations: meta-regression evidence of spatiotemporal adjustments. Frontiers in bioengineering and biotechnology, 12, 1506002. **IF: 4.8, Q1**.

3rd Thesis point: Development of a Dynamic-Gait-Driven Multi-Objective Optimization Framework for Personalized Lattice Structures Enabling Automated Functional Coordination

This dissertation establishes a multi-objective optimization framework for personalized lattice structures, driven directly by dynamic gait data. The framework integrates finite-element analysis, Gaussian Process Regression surrogate modeling and multi-objective Bayesian optimization into a unified system. For the first time, an individual's foot morphology and gait dynamics are incorporated directly into the structural parameter search, enabling simultaneous optimization of rearfoot impact attenuation, arch postural stability and forefoot propulsion efficiency.

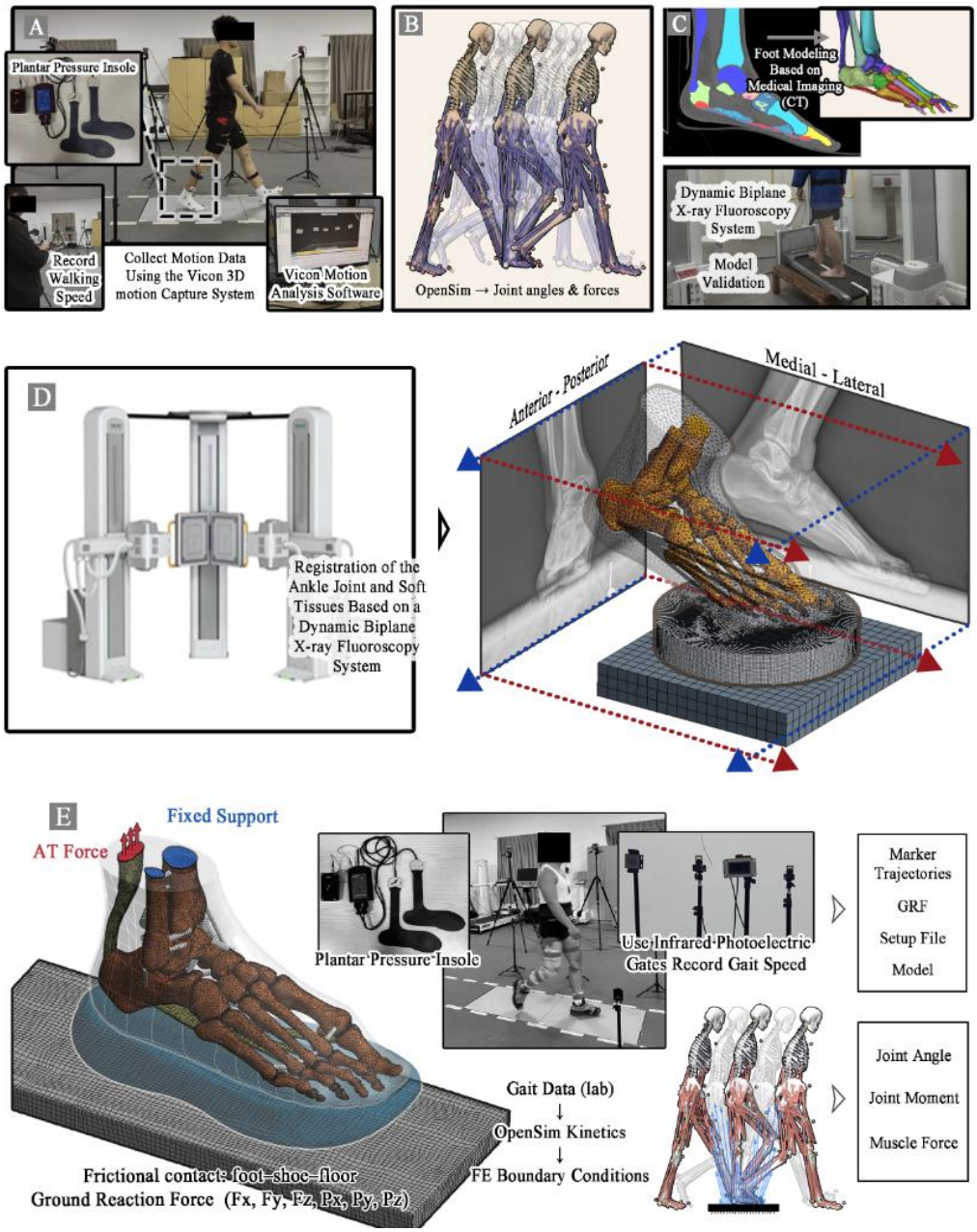

The optimization operates in a closed-loop sequence of model solving, surrogate learning, multi-

objective exploration and experimental validation. This process efficiently converges toward the Pareto front within a high-dimensional parameter space, shifting structural regulation from empirical trial-and-error to a computationally guided and automated reasoning procedure. The final designs not only exhibit marked improvements in impact reduction, postural control and propulsive enhancement in simulation but also successfully transfer to physical prototypes, where their performance is confirmed experimentally.

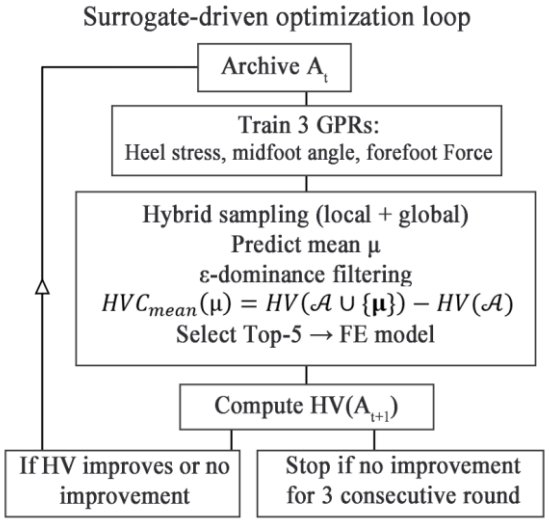

Related articles to the 3rd thesis point:

1. **Z Lu**, X Li, D Sun, Y Song, G Fekete, A Kovács, Z Gao, J Zheng, L Xiang, Y Gu. (2025). Computationally tuned dual-layer lattice pads adapted to gait-induced pressure distribution. npj Advanced Manufacturing , 2(1), 43. **Nature Portfolio journal**.
2. **Z Lu**, X Li, D Sun, Y Song, G Fekete, A Kovács, K András, Y Gu. (2025). Parametric cushioning lattice insole based on finite element method and machine learning: A preliminary computational analysis. Journal of Biomechanics, 184, 112674. **IF: 2.4, Q1**.
3. **Z Lu**, D Sun, B Kovács, Z Radák, Y Gu. (2023). Case study: The influence of Achilles tendon rupture on knee joint stress during counter-movement jump–Combining musculoskeletal modeling and finite element analysis. Heliyon, 9(8). **IF: 3.4, Q1**.
4. C Zhu, D Sun, Y Xu, **Z Lu**, C Hu, X Cen, Y Song, Z Gao, Y Gu. (2025). Integrating footwear features into fatigue prediction models for marathon runners: A hybrid CNN-LSTM approach. Proceedings of the Institution of Mechanical Engineers, Part P: Journal of Sports Engineering and Technology, 17543371251356133. **IF: 1.1, Q2**.
5. C Hu, X Cen, D Sun, **Z Lu**, Y Xu, C Zhu, Y Xu, Y Gu. (2025). Biomechanical effects of asymmetric backpack shoulder straps on the unilateral flatfoot: a finite element analysis. Computer Methods in Biomechanics and Biomedical Engineering, 1-11. **IF: 2.4, Q2**.

6. D Wang, F Li, JS Baker, P Zhang, **Z Lu**, J Yu, M Liang. (2024). The effect of simulated basketball game load on patellar tendon load during stop-jump movement. Molecular & Cellular Biomechanics, 21(2), 292-292.
7. **Z Lu**, X Li, M Rong, JS Baker, Y Gu. (2022). Effect of rearfoot valgus on biomechanics during barbell squatting: A study based on OpenSim musculoskeletal modeling. Frontiers in neurorobotics, 16, 832005. **IF: 2.8, Q2**.
8. **Z Lu**, X Li, R Xuan, Y Song, I Bíró, M Liang, Y Gu. (2022). Effect of heel lift insoles on lower extremity muscle activation and joint work during barbell squats. Bioengineering, 9(7), 301. **IF: 3.7, Q2**.
9. **Z Lu**, D Sun, D Xu, X Li, JS Baker, Y Gu. (2021). Gait characteristics and fatigue profiles when standing on surfaces with different hardness: Gait analysis and machine learning algorithms. Biology, 10(11), 1083. **IF: 3.5, Q2**.
10. X Li, **Z Lu**, X Cen, Y Zhou, R Xuan, D Sun, Y Gu. (2023). Effect of pregnancy on female gait characteristics: A pilot study based on portable gait analyzer and induced acceleration analysis. Frontiers in Physiology, 14, 1034132. **IF: 3.4, Q1**.

4th Thesis point: Systematic Validation of the Biomechanical Benefits of Lattice Footwear at the Human Scale and Demonstration of Cross-Scale Structure–Response Mapping

This dissertation systematically validates the cross-scale effects of lattice structures—from microstructural geometric modulation to human-scale movement performance—through plantar-pressure measurements (PEDAR), ground reaction forces, three-dimensional kinematics and joint-level dynamics. The experimental results show that the lattice rearfoot effectively reduces localized impact during initial contact; the midfoot region maintains a more natural subtalar posture during stance and alleviates knee extensor loading; and the forefoot structure enhances plantarflexion torque output during toe-off while avoiding excessive local pressures. Subjective evaluations further indicate clear advantages in cushioning, arch support and overall comfort when wearing the lattice-equipped footwear. Together, these findings demonstrate that localized mechanical regulation introduced through microstructural geometry can be reliably translated into meaningful biomechanical improvements at the human scale, thereby confirming both the effectiveness and the transferability of the proposed design framework.

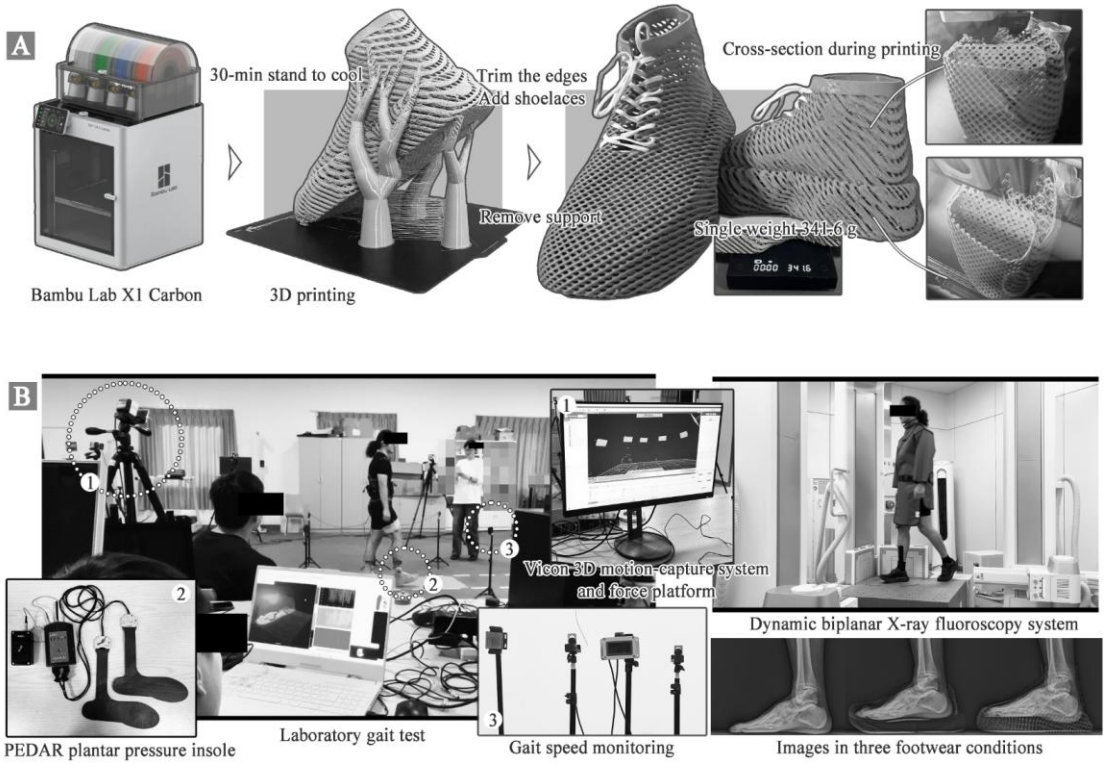

Related articles to the 4th thesis point:

1. **Z Lu**, X Li, D Sun, Y Song, G Fekete, A Kovács, Z Gao, J Zheng, L Xiang, Y Gu. (2025). Computationally tuned dual-layer lattice pads adapted to gait-induced pressure distribution. npj Advanced Manufacturing , 2(1), 43. **Nature Portfolio journal**.

2. **Z Lu**, X Li, D Sun, Y Song, G Fekete, A Kovács, K András, Y Gu. (2025). Parametric cushioning lattice insole based on finite element method and machine learning: A preliminary computational analysis. Journal of Biomechanics, 184, 112674. **IF: 2.4, Q1**.
3. **Z Lu**, D Sun, D Xu, X Li, JS Baker, Y Gu. (2021). Gait characteristics and fatigue profiles when standing on surfaces with different hardness: Gait analysis and machine learning algorithms. Biology, 10(11), 1083. **IF: 3.5, Q2**.
4. S Gao, Y Song, D Sun, X Cen, M Wang, **Z Lu**, Y Gu. (2025). Impact of Becker muscular dystrophy on gait patterns: Insights from biomechanical analysis. Gait & Posture. **IF: , Q1**.
5. Y Xu, C Zhu, Y Fang, **Z Lu**, Y Song, C Hu, D Sun, Y Gu. (2025). The effects of different carbon-fiber plate shapes in shoes on lower limb biomechanics following running-induced fatigue. Frontiers in Bioengineering and Biotechnology, 13, 1539976. **IF: 4.8, Q1**.
6. X Li, **Z Lu**, Y Song, M Liang, Y Yuan, G Fekete, A Kovács, D Sun, Y Gu. (2024). Pregnancy-induced gait alterations: meta-regression evidence of spatiotemporal adjustments. Frontiers in bioengineering and biotechnology, 12, 1506002. **IF: 4.8, Q1**.
7. X Li, **Z Lu**, X Cen, Y Zhou, R Xuan, D Sun, Y Gu. (2023). Effect of pregnancy on female gait characteristics: A pilot study based on portable gait analyzer and induced acceleration analysis. Frontiers in Physiology, 14, 1034132. **IF: 3.4, Q1**.
8. X Li, **Z Lu**, D Sun, R Xuan, Z Zheng, Y Gu. (2022). The influence of a shoe's heel-toe drop on gait parameters during the third trimester of pregnancy. Bioengineering, 9(6), 241. **IF: 3.7, Q2**.

5th Thesis point: Demonstration of the Engineering Potential of Parametric Lattice Structures for Personalized Footwear, Clinical Orthotics and Performance Enhancement, and Proposal of a Generalizable Design–Optimization–Validation Workflow

This dissertation demonstrates the strong engineering scalability of the proposed parametric lattice framework, which can generate individualized structural configurations based on foot morphology, plantar-pressure distribution and gait dynamics. The approach is applicable to a wide range of scenarios, including personalized athletic footwear, orthotic devices for populations with arch collapse or other podiatric conditions, plantar-pressure management for diabetic foot, and performance-oriented footwear for competitive sports. The study further establishes a closed-loop workflow encompassing structural modeling, mechanical simulation, gait-driven optimization, 3D-printed fabrication and experimental validation. This workflow shifts structural design from experience-based decision making to data-driven automated generation, and supports a transition in footwear manufacturing from uniform mass production toward on-demand customization. Beyond footwear, the process can be extended to diverse gait-related wearable systems. It also provides a practical engineering framework and theoretical foundation for future developments in intelligent wearable devices, adaptive footwear and systems capable of real-time gait regulation.

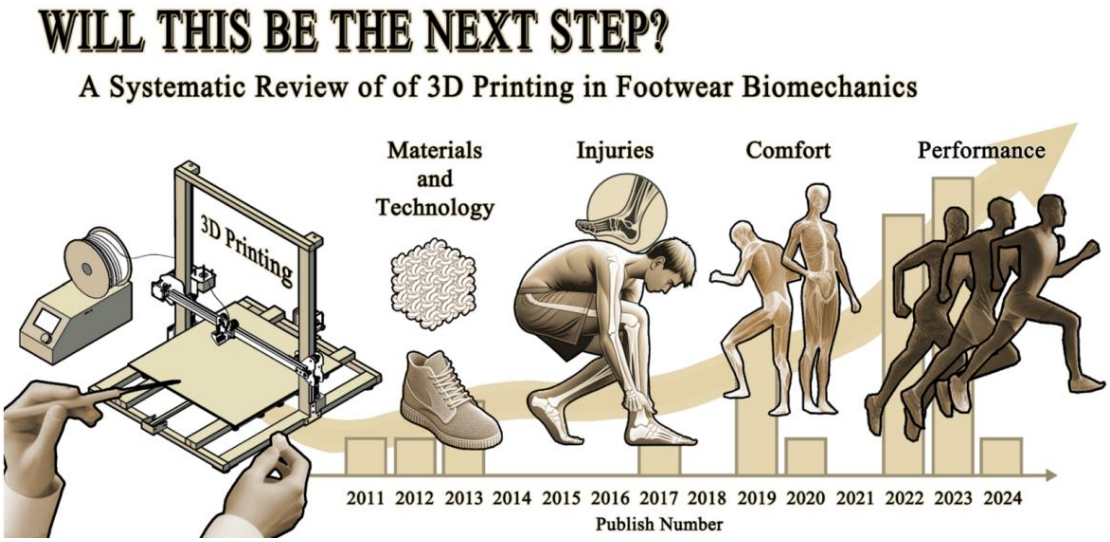

Related articles to the 5th thesis point:

1. **Z Lu**, X Li, D Sun, Y Song, G Fekete, A Kovács, Z Gao, J Zheng, L Xiang, Y Gu. (2025). Computationally tuned dual-layer lattice pads adapted to gait-induced pressure distribution. npj Advanced Manufacturing , 2(1), 43. **Nature Portfolio journal**.
2. **Z Lu**, X Li, D Sun, Y Song, G Fekete, A Kovács, K András, Y Gu. (2025). Parametric cushioning lattice insole based on finite element method and machine learning: A preliminary computational analysis. Journal of Biomechanics, 184, 112674. **IF: 2.4, Q1**.
3. **Z Lu**, X Li, D Sun, Y Song, G Fekete, A Kovács, Y Gu. (2025). Will this be the next step?

A systematic review of 3D printing in footwear biomechanics. Footwear Science, 17(2), 127-142. **IF: 3.8, Q2**.

List of publications

Referred articles related to this thesis:

1. **Z Lu**, X Li, D Sun, Y Song, G Fekete, A Kovács, Z Gao, J Zheng, L Xiang, Y Gu. (2025). Computationally tuned dual-layer lattice pads adapted to gait-induced pressure distribution. npj Advanced Manufacturing , 2(1), 43. **Nature Portfolio journal**.
2. **Z Lu**, X Li, D Sun, Y Song, G Fekete, A Kovács, K András, Y Gu. (2025). Parametric cushioning lattice insole based on finite element method and machine learning: A preliminary computational analysis. Journal of Biomechanics, 184, 112674. **IF: 2.4, Q1**.
3. **Z Lu**, X Li, D Sun, Y Song, G Fekete, A Kovács, Y Gu. (2025). Will this be the next step? A systematic review of 3D printing in footwear biomechanics. Footwear Science, 17(2), 127-142. **IF: 3.8, Q2**.
4. **Z Lu**, D Sun, B Kovács, Z Radák, Y Gu. (2023). Case study: The influence of Achilles tendon rupture on knee joint stress during counter-movement jump–Combining musculoskeletal modeling and finite element analysis. Heliyon, 9(8). **IF: 3.4, Q1**.
5. **Z Lu**, X Li, M Rong, JS Baker, Y Gu. (2022). Effect of rearfoot valgus on biomechanics during barbell squatting: A study based on OpenSim musculoskeletal modeling. Frontiers in neurorobotics, 16, 832005. **IF: 2.8, Q2**.
6. **Z Lu**, X Li, R Xuan, Y Song, I Bíró, M Liang, Y Gu. (2022). Effect of heel lift insoles on lower extremity muscle activation and joint work during barbell squats. Bioengineering, 9(7), 301. **IF: 3.7, Q2**.
7. **Z Lu**, D Sun, D Xu, X Li, JS Baker, Y Gu. (2021). Gait characteristics and fatigue profiles when standing on surfaces with different hardness: Gait analysis and machine learning algorithms. Biology, 10(11), 1083. **IF: 3.5, Q2**.
8. C Hu, Y Song, D Sun, **Z Lu**, H Chen, X Cen, D Janićijević, Z Radak, Z Gao, JS Baker, Y Gu. (2025, January). Sedentary Duration and Systemic Health Burden: Nonlinear Associations with Muscle, Fat, and Vascular Phenotypes in a US Population-Based Study. Healthcare. **IF: 2.4, Q2**.
9. C Zhu, D Sun, Y Xu, **Z Lu**, C Hu, X Cen, Y Song, Z Gao, Y Gu. (2025). Integrating footwear features into fatigue prediction models for marathon runners: A hybrid CNN-LSTM approach. Proceedings of the Institution of Mechanical Engineers, Part P: Journal of Sports Engineering and Technology, 17543371251356133. **IF: 1.1, Q2**.
10. C Hu, X Cen, D Sun, **Z Lu**, Y Xu, C Zhu, Y Xu, Y Gu. (2025). Biomechanical effects of asymmetric backpack shoulder straps on the unilateral flatfoot: a finite element analysis. Computer Methods in Biomechanics and Biomedical Engineering, 1-11. **IF: 2.4, Q2**.

11. S Gao, Y Song, D Sun, X Cen, M Wang, **Z Lu**, Y Gu. (2025). Impact of Becker muscular dystrophy on gait patterns: Insights from biomechanical analysis. Gait & Posture. **IF: , Q1**.
12. Y Xu, C Zhu, Y Fang, **Z Lu**, Y Song, C Hu, D Sun, Y Gu. (2025). The effects of different carbon-fiber plate shapes in shoes on lower limb biomechanics following running-induced fatigue. Frontiers in Bioengineering and Biotechnology, 13, 1539976. **IF: 4.8, Q1**.
13. L Shen, **Z Lu**, X Li, D Sun, Y Song, G Fekete, A Kovács, F Li, X Cen. (Forthcoming Articles). Advances and Future Directions of Foetal Finite Element Modelling in Childbirth: from Biomechanical Interactions to Clinical Implications. International Journal of Biomedical Engineering and Technology. **IF: 0.6, Q4**.
14. X Li, **Z Lu**, Y Song, M Liang, Y Yuan, G Fekete, A Kovács, D Sun, Y Gu. (2024). Pregnancy-induced gait alterations: meta-regression evidence of spatiotemporal adjustments. Frontiers in bioengineering and biotechnology, 12, 1506002. **IF: 4.8, Q1**.
15. D Wang, F Li, JS Baker, P Zhang, **Z Lu**, J Yu, M Liang. (2024). The effect of simulated basketball game load on patellar tendon load during stop-jump movement. Molecular & Cellular Biomechanics, 21(2), 292-292.
16. X Li, **Z Lu**, X Cen, Y Zhou, R Xuan, D Sun, Y Gu. (2023). Effect of pregnancy on female gait characteristics: A pilot study based on portable gait analyzer and induced acceleration analysis. Frontiers in Physiology, 14, 1034132. **IF: 3.4, Q1**.
17. X Li, **Z Lu**, D Sun, R Xuan, Z Zheng, Y Gu. (2022). The influence of a shoe's heel-toe drop on gait parameters during the third trimester of pregnancy. Bioengineering, 9(6), 241. **IF: 3.7, Q2**.

International conference abstracts related to this thesis:

1. The 17th Biennial Footwear Biomechanics Symposium. Title: Personalised footwear design method based on machine learning and finite element analysis. 2025. Norway (Oral presentation).
2. The 29th Annual Congress of the European College of Sport Science. Title: Stepping into the Future: Unveiling Biomechanical Innovations in 3D Printed Footwear Design. 2024. Scotland, UK (Oral presentation).
3. 2024 international Competitive Sports Biomechanics Forum 23rd National Sports Biomechanics Conference. Title: Customized 3D-Printed Insoles for Diabetic Foot Care: Finite Element Analysis and Machine Learning Approach. 2024. China (Oral presentation).
4. The 7th International Conference on Material Strength and Applied Mechanics (MSAM 2024). Title: Customized 3D-Printed Insoles for Diabetic Foot Care: Finite Element Analysis and Machine Learning Approach. 2024. Hungary (Oral presentation).

Other publications:

1. **Z Lu**, Y Song, H Chen, S Li, EC Teo, Y Gu. (2022). A mixed comparisons of aerobic training with different volumes and intensities of physical exercise in patients with hypertension: a systematic review and network meta-analysis. Frontiers in cardiovascular medicine, 8, 770975. **IF: 2.8, Q2**.
2. **Z Lu**, Y Xu, Y Song, I Bíró, Y Gu. (2021). A mixed comparisons of different intensities and types of physical exercise in patients with diseases related to oxidative stress: a systematic review and network meta-analysis. Frontiers in physiology, 12, 700055. **IF: 3.4, Q1**.
3. Y Li, D Sun, Y Fang, **Z Lu**, F Shi, G Liu, Y Gu. (2024). Mixed comparison of intervention with eccentric, isometric, and heavy slow resistance for Victorian Institute of Sport Assessment Patella Questionnaire in adults with patellar tendinopathy: A systematic review and network meta-analysis. Heliyon, 10(21). **IF: 3.4, Q1**.
4. F Li, Y Song, X Cen, D Sun, **Z Lu**, I Bíró, Y Gu. (2023). Comparative efficacy of vibration foam rolling and cold water immersion in amateur basketball players after a simulated load of basketball game. Healthcare. MDPI. **IF: 2.4, Q4**.
5. J Tong, **Z Lu**, X Cen, C Chen, UC Ugbolue, Y Gu. (2023). The effects of ankle dorsiflexor fatigue on lower limb biomechanics during badminton forward forehand and backhand lunge. Frontiers in Bioengineering and Biotechnology, 11, 1013100. **IF: 4.8, Q1**.
6. L Gao, **Z Lu**, M Liang, JS Baker, Y Gu. (2022). Influence of different load conditions on lower extremity biomechanics during the lunge squat in novice men. Bioengineering, 9(7), 272. **IF: 3.7, Q2**.
7. E Shao, **Z Lu**, X Cen, Z Zheng, D Sun, Y Gu. (2022). The effect of fatigue on lower limb joint stiffness at different walking speeds. Diagnostics (Q2), 12(6), 1470. **IF: 3.3, Q1**.
8. Y Lin, **Z Lu**, X Cen, A Thirupathi, D Sun, Y Gu. (2022). The influence of different rope jumping methods on adolescents' lower limb biomechanics during the ground-contact phase. Children, 9(5), 721. **IF: 2.1, Q2**.
9. D Xu, **Z Lu**, S Shen, G Fekete, UC Ugbolue, Y Gu. (2021). The differences in lower extremity joints energy dissipation strategy during landing between athletes with symptomatic patellar tendinopathy (PT) and without patellar tendinopathy (UPT).
10. X Cen, **Z Lu**, JS Baker, B István, Y Gu. (2021). A comparative biomechanical analysis during planned and unplanned gait termination in individuals with different arch stiffnesses. Applied Sciences, 11(4), 1871. **IF: 2.5, Q1**.

Reviewer for international journal articles:

1. Scientific Reports
2. European Journal of Sport Science
3. Journal of Biomechanics
4. Footwear Science
5. Journal of Functional Morphology and Kinesiology
6. Sport Sciences for Health
7. Public Health
8. Physiology International
9. Physical Activity and Health Journal
10. International Journal of Environmental Research and Public Health
11. International Journal of Biomedical Engineering and Technology

h-index: 11 (ResearchGate, December 2, 2025)

Total citations: 261 (ResearchGate, December 2, 2025)

ORCID: 0000-0002-7705-8134

ResearchGate: https://www.researchgate.net/profile/Zhenghui-Lu-2?ev=hdr_xprf

Scopus Database: https://www.scopus.com/authid/detail.uri?authorId=57222247894

ACKNOWLEDGEMENTS

As my academic journey reaches this point, the doctoral stage has come to its end, and I am about to bid farewell to this long chapter of life lived under the identity of a “student.” Looking back on the years of exploration, trial and error, and growth, I am deeply aware that arriving at this moment has been shaped by many coincidences as well as the support and help of numerous people.

Every PhD journey is unique. Now, whenever I recall those moments of naivety, exhaustion, frustration, and struggle, I cannot help but find them somewhat amusing.

When I was a child, every time I visited someone else’s home, I would make a fuss when it was time to leave, simply because they had a computer to play with. My family only had a FC game console, fun, with many games to choose from, but computer games could be played online, and to me that was something completely new and magical. One day, when I came home, I suddenly found that a computer had been installed in our house. I was overjoyed and couldn’t wait to start playing. It was only much later that I learned how poor our family was at the time, and that my parents had borrowed a considerable amount of money from relatives just to buy that computer. I am deeply grateful to them, who have always judged only right and wrong, never the cost, and have offered me unconditional support. I also remember once seeing an aircraft carrier model while out shopping. During the assembly, I grew irritable and impatient, the tiny parts were far too complicated for someone my age. As evening fell and my frustration boiled over, I lost my temper. Instead of scolding me, my mother quietly finished assembling the model after I had gone to sleep. The next morning, when I woke to find it completed, I was astonished. Since then, whenever I face difficulties, I think of that moment. I am grateful to my mother for teaching me patience.

When I was around thirteen or fourteen, I was naive and full of adolescent arrogance. I often imagined that the world existed for me alone, and that I was the sole protagonist of its story, something between solipsism and The Truman Show. In high school, I once said something childish in class, and my science teacher (who taught the combined physics–chemistry–biology course) gave me a light slap on the cheek. It barely hurt, but it helped me immensely. I often wonder: if I were a high school teacher, would I have taken such a risk of potential reprimand or complaints from parents to correct a student whose future has nothing to do with my own? There is a saying in Chinese Daoism that “Heaven shows no favoritism; each person bears their own fate.” The idea is that intervening in someone else’s destined tribulations may bring misfortune upon oneself. That teacher chose to intervene anyway, and for that reason alone, what he did was truly remarkable.

Another experience that shaped me was my very first job as a soon-to-graduate student. Although I worked there for only two full days, without that brief episode I might never have set foot on the path of scientific research. It was during my fourth undergraduate year, and at the time I had no intention of pursuing further study. I found a job in landscape design, becoming a designer had

always been a dream of mine, and in a way, designing structures and footwear today still lets me claim the title, however loosely. Back then, the salary was only 1,800 RMB, while the rent in that city cost 2,000. It was simply impossible to sustain myself. After working Thursday and Friday, I lay on the bed in my rented room, contemplating my life. I knew I didn't want to continue like that. So, with only three months left before the graduate school entrance exam, I began preparing. I was lucky enough to pass, and that eventually led me to where I am now. I was about to write "to the achievements I have today," but on second thought, I realized I haven't really achieved very much yet. Still, I am grateful for that job, despite neither receiving the two days' pay nor returning the book I took from the studio, because, in its own unexpected way, it pushed me onto the path of research.

Later, I went to Ningbo University for my master's degree. At that time, I had an almost romanticized vision of scientific research, largely shaped by movies such as Back to the Future, The Incredible Hulk, Interstellar, The Imitation Game, and A Beautiful Mind. In my mind, scientists were people who saved the world. With that belief, I threw myself into work with great enthusiasm, studying until eleven or twelve every night. Professor Gu Yaodong, my advisor, saw how hard I was trying and gave me tremendous support, helping me plan each stage of my development. I can hardly put into words how much he has helped me. When I was lost, he set goals for me; when I grew complacent, he corrected me. Despite his high position and busy schedule, he always made time to guide us. Once, I spent a long period learning OpenSim and wrote a paper based on it. I was excited to show it to him, but Professor Gu told me the work lacked novelty. Hearing that, I felt deeply frustrated—after all the time and effort, the outcome received no positive feedback. Yet from that experience I learned that while diligence and technical skill matter, it is thinking and innovation that truly drive research. After that, I stopped writing papers for nearly two years and focused on accumulating knowledge and reading the literature. Professor Gu even worried that I had lost motivation because of the setback. Eventually, I published a study in Journal of Biomechanics, one of the top journals in sports biomechanics. That result proved Professor Gu was right, and it taught me that good research requires patience, depth, and quiet persistence. Even later, when I published a paper in a Nature sub-journal, the joy I felt could not compare to the feeling of that first success. I believe Professor Gu was proud as well. During my master's program, my thesis was recognized as an excellent provincial thesis, and I received the national scholarship along with several other awards. I believe I did not disappoint him. I feel truly fortunate; it was Professor Gu's mentorship that strengthened my abilities and helped shape the researcher I am today.

During my master's studies, many teachers and classmates had a profound influence on me. Professor Sun Dong, once a student of Professor Gu and now both our senior and mentor, gave us numerous hands-on opportunities and allowed us to receive systematic research training. He always

supported us unconditionally, letting us use the laboratory freely, encouraging us to try ideas that sounded unrealistic, and even helping us secure various research funds. Professor Mei Qichang, also a former student of Professor Gu, is the reason I was able to learn OpenSim at all. I encountered countless difficulties while studying the software, and he always stepped in at just the right moments to guide me. It wasn't hand-holding; it felt more like the perfect spotter during a bench press—just enough assistance to lift the weight without taking over, leaving one feeling both relieved and empowered. His way of teaching helped me understand that on the path of research, no one can guide you forever. Eventually, you reach the edge of the map, and at that point, you must venture forward on your own. With the ability to learn independently, you can navigate the vast ocean; without it, you risk sinking into the crowd. I am also grateful to many other teachers, seniors, and peers: Liang Minjun, Liu Wei (also classmate), Song Yang, Gao Zixiang, He Yuqi, Shen Siqin,Cen Xuanzhen, Yu Peimin, Jiang Xinyan, as well as my classmates Xu Yining, Chen Hairong, and Zhang Qiaolin. My thanks also go to my junior colleagues Zhu Chengyuan, Hu Chen, Wang Dongxu, Xia Zifan, Qian Yihan, Gao Shunxiang, Xu Yufan and Liu Qian. While I was in Hungary without access to the laboratory, they carried out many gait experiments for me in the Ningbo University lab. Zhu Chengyuan and Xu Yufan, who are a couple, even bought a 3D printer and helped me fabricate the final version of the footwear. I am truly grateful to them and wish them happiness and a long, beautiful life together. I will always remember you all, thank you.

This is the part I have been most looking forward to writing, about my classmate Li Xin, who is now my fiancee. When we first met, I did not even think of her as "a girl" in the usual sense, just a straightforward, big-hearted friend who happened to be taller than me (she is 1.80 meters, and I am 1.74). With her cheerful and optimistic personality, every emotion clearly visible on her face, she was simply fun to be around. Although we often went out to eat meat together, neither of us ever considered those outings to be dates. I still remember one night when we were the last two people to leave the laboratory. Passing by a street food stall, I bought her a roasted chicken leg. She smiled so brightly and told me I looked handsome. Looking back, I suspect it was the chicken leg that made me handsome. Later, during the Chinese New Year break, when almost all our classmates went home, we stayed on campus to continue studying. To learn the software, we decided to spend the entire holiday working in the lab's duty room, and both of us gained quite a bit of weight as a result. I believed I felt nothing beyond friendship, until the holiday ended and we had to move back to the regular study hall. That change meant we could no longer stay alone in the same room, nor find natural reasons to spend extended time together. Suddenly, I felt a sense of emptiness, and she felt the same. From there, it was only natural that we became a couple. We pursued our master's degrees together, and later continued on to Europe for our PhD studies. Throughout this long journey, we have faced countless emotions and challenges side by side, supporting each other every step of the

way. This kind of happiness is something anyone studying far from home would envy. Since then, I have never felt lonely, when I was discouraged, she was there; when I succeeded, she shared my joy. I can no longer imagine life without her. Without her support and companionship, I would not have made it this far.

My doctoral years are, of course, an essential part of this dissertation, and studying abroad left a profound impact on me. I frequently attended academic conferences; in the past, I often felt pleased with my small achievements and modest technical skills. But once I stepped out into the wider world, I realized that brilliant minds are as numerous as fish in a great river; even those destined to soar often struggle against the current. How, then, could someone like me expect the waters to part so easily? It became clear to me that shutting oneself away is never the right path. Only by sharing openly, engaging in dialogue, and embracing collaboration can we learn from others and rise to a higher level. Cooperation is indispensable, closing oneself off ultimately leads only to stagnation. For this reason, I am deeply grateful to my doctoral supervisors, Dr. habil. Gusztáv Fekete and Dr. András Kovács, for their unwavering support. They connected me with materials laboratories and researchers who assisted with 3D printing and various materials tests. Without their help, I could not possibly have completed this dissertation on time. Many of the documents and materials at the university were written in Hungarian, making them extremely difficult for us to understand, yet both supervisors were always warm, patient, and willing to help us navigate every academic obstacle. Professor Gusztáv never pressured me; instead, he often recommended interesting places to visit. At the beginning of my fifth semester, I forgot to complete a required questionnaire for the Hungarian scholarship and my stipend was suspended. Worried that I might be discouraged, Professor Gusztáv came to my home with a beer to check on me. I am deeply grateful to him—for his kindness, his support, and the countless ways he ensured that my doctoral studies and daily life continued without unnecessary hardship.

I would also like to express my special gratitude to my friend Li Zijin, who is a patient with Becker muscular dystrophy. He is optimistic and resilient, dedicated to developing powered exoskeletons to assist gait and help patients with mobility impairments like himself. We first met on Bilibili, where I had posted a series of OpenSim tutorial videos. He messaged me to introduce his situation, and that was the beginning of our collaboration. We recorded and analyzed his gait data in the laboratory and held many discussions about potential research directions. The data used in my 2025 publication in npj Advanced Manufacturing were provided by him. He is now pursuing his PhD at Chiba University in Japan. I am truly grateful to him, and I wish him success in his studies and good health.

I would also like to thank The Big Bang Theory. A large part of doctoral life is monotonous and uneventful, but whenever I sat down to eat and rewatched an episode, it brought me genuine joy and

somehow strengthened my determination to complete my PhD. I am equally grateful for the wuxia novels written by Jin Yong. His writing is both delicate and bold, and I often listened to his stories while exercising. The scene of Guo Jing and Huang Rong sacrificing themselves for their nation still feels vivid before my eyes, stirring, tragic, and enough to move one to tears.

Although I am not a novelist, there is perhaps nothing more satisfying in life than writing the words "The End" with one's own hand. Today, I get to experience that satisfaction myself, finally!

After years of arduous study and a thousand nights spent working by a solitary lamp, achieving success in a single moment feels like awakening from a vast dream. Like a wandering swordsman laughing freely into the wind, I now drift away without hesitation, my lone shadow accompanying me across the horizon, riding into the distance with a long song and no thought of turning back.

The End……

References

[1] Riegger, Cheryl L.: Anatomy of the Ankle and Foot, Physical Therapy, 1.12.1988, Vol. 68, no. 12, p. 1802–1814, DOI 10.1093/ptj/68.12.1802,

[2] Golanó, Pau; Vega, Jordi; De Leeuw, Peter A. J.; Malagelada, Francesc; Manzanares, M. Cristina; Götzens, Víctor und Van Dijk, C. Niek: Anatomy of the ankle ligaments: a pictorial essay, Knee Surgery, Sports Traumatology, Arthroscopy, 1.4.2016, Vol. 24, no. 4, p. 944–956, DOI 10.1007/s00167-016-4059-4,

[3] Ker, R. F.; Bennett, M. B.; Bibby, S. R.; Kester, R. C. und Alexander, R. McN.: The spring in the arch of the human foot, Nature, 1.1987, Vol. 325, no. 6100, p. 147–149, DOI 10.1038/325147a0,

[4] Behling, Anja-Verena; Rainbow, Michael J.; Welte, Lauren und Kelly, Luke: Chasing footprints in time – reframing our understanding of human foot function in the context of current evidence and emerging insights, Biological Reviews, 2023, Vol. 98, no. 6, p. 2136–2151, DOI 10.1111/brv.12999,

[5] Procter, P. und Paul, J. P.: Ankle joint biomechanics, Journal of Biomechanics, 1.1.1982, Vol. 15, no. 9, p. 627–634, DOI 10.1016/0021-9290(82)90017-3,

[6] Gefen, A.; Megido-Ravid, M.; Itzchak, Y. und Arcan, M.: Biomechanical Analysis of the Three-Dimensional Foot Structure During Gait: A Basic Tool for Clinical Applications, Journal of Biomechanical Engineering, 9.7.2000, Vol. 122, no. 6, p. 630–639, DOI 10.1115/1.1318904,

[7] Gervis, W. H.: The Anatomy and Physiology of the Foot, Postgraduate Medical Journal, 10.1943, Vol. 19, no. 215, p. 225–230, DOI 10.1136/pgmj.19.215.225,

[8] Zhou, Huiyu; Xu, Datao; Quan, Wenjing; Ugbolue, Ukadike Chris und Gu, Yaodong: Effects of different contact angles during forefoot running on the stresses of the foot bones: a finite element simulation study, Frontiers in Bioengineering and Biotechnology [online], 8.2.2024, Vol. 12, Online im Internet: DOI 10.3389/fbioe.2024.1337540, https://www.frontiersin.org/journals/bioengineering-and-biotechnology/articles/10.3389/fbioe.2024.1337540/full (5.9.2025).

[9] Lu, Zhenghui; Li, Xin; Rong, Ming; Baker, Julien S. und Gu, Yaodong: Effect of rearfoot valgus on biomechanics during barbell squatting: A study based on OpenSim musculoskeletal modeling, Frontiers in Neurorobotics [online], 9.8.2022, Vol. 16, Online im Internet: DOI 10.3389/fnbot.2022.832005, https://www.frontiersin.org/journals/neurorobotics/articles/10.3389/fnbot.2022.832005/full (16.8.2024).

[10] Murphy, Darlene F.; Beynnon, Bruce D.; Michelson, James D. und Vacek, Pamela M.: Efficacy of Plantar Loading Parameters During Gait in Terms of Reliability, Variability, Effect of Gender and Relationship Between Contact Area and Plantar Pressure, Foot & Ankle International, 1.2.2005, Vol. 26, no. 2, p. 171–179, DOI 10.1177/107110070502600210,

[11] The effect of foot arch on plantar pressure distribution during standing: Journal of Medical Engineering & Technology: Vol 37, No 5, [online], Online im Internet: https://www.tandfonline.com/doi/abs/10.3109/03091902.2013.810788 (5.9.2025).

[12] Lu, Zhenghui; Sun, Dong; Kovács, Bálint; Radák, Zsolt und Gu, Yaodong: Case study: The influence of Achilles tendon rupture on knee joint stress during counter-movement jump–Combining musculoskeletal modeling and finite element analysis, Heliyon, 2023, Vol. 9, no. 8,

[13] Xu, Liya; Wang, Yifan und Wen, Xu: The role of footwear in improving running economy: a systematic review with meta-analysis of controlled trials, Scientific Reports, 1.2.2025, Vol. 15, no. 1, p. 3963, DOI 10.1038/s41598-025-88271-2,

[14] Salian, Shivani Chowdhury und Tiwari, Arushi: Intra- and Inter-reliability of Cervical Goniometer Used to Measure Cervical Range of Motion in Young Adults, In: Ray, Gaur G., Iqbal, Rauf, Ganguli,

Anindya K. und Khanzode, Vivek (Hrsg.), Ergonomics in Caring for People. Springer, Singapore, 2018, ISBN 978-981-10-4980-4, p. 223–232,
[15] Malisoux, Laurent; Chambon, Nicolas; Delattre, Nicolas; Gueguen, Nils; Urhausen, Axel und Theisen, Daniel: Injury risk in runners using standard or motion control shoes: a randomised controlled trial with participant and assessor blinding, British Journal of Sports Medicine, 1.4.2016, Vol. 50, no. 8, p. 481–487, DOI 10.1136/bjsports-2015-095031,
[16] Motion Control Shoes: Controlling Motion or Just a Notion? - ProQuest, [online], Online im Internet: https://www.proquest.com/openview/ff451929215969613e97c640774497ac/1?pq-origsite=gscholar&cbl=18750&diss=y (5.9.2025).
[17] Jannink, Michiel J.; IJzerman, Maarten J.; Groothuis-Oudshoorn, Karin; Stewart, Roy E.; Groothoff, Johan W. und Lankhorst, Gustaaf J.: Use of orthopedic shoes in patients with degenerative disorders of the foot, Archives of Physical Medicine and Rehabilitation, 1.4.2005, Vol. 86, no. 4, p. 687–692, DOI 10.1016/j.apmr.2004.06.069,
[18] Su, Shonglun; Mo, Zhongjun; Guo, Junchao und Fan, Yubo: The Effect of Arch Height and Material Hardness of Personalized Insole on Correction and Tissues of Flatfoot, Journal of Healthcare Engineering, 2017, Vol. 2017, no. 1, p. 8614341, DOI 10.1155/2017/8614341,
[19] Jurca, Ales; Žabkar, Jure und Džeroski, Sašo: Analysis of 1.2 million foot scans from North America, Europe and Asia, Scientific Reports, 16.12.2019, Vol. 9, no. 1, p. 19155, DOI 10.1038/s41598-019-55432-z,
[20] Lee, Jiwon und Chun, Jaehoon: Development of personalized cast shoes using 3D printing technology, Fashion and Textiles, 17.3.2025, Vol. 12, no. 1, p. 7, DOI 10.1186/s40691-024-00409-4,
[21] Digitization of the work environment for sustainable production, [online], Online im Internet: https://publica.fraunhofer.de/handle/publica/473915 (5.9.2025).
[22] Lu, Zhenghui; Li ,Xin; Sun ,Dong; Song ,Yang; Fekete ,Gusztáv; Kovács ,András und And Gu, Yaodong: Will this be the next step? A systematic review of 3D printing in footwear biomechanics, Footwear Science, P. 1–16, DOI 10.1080/19424280.2025.2472251,
[23] Hu, Che-Wei; Nguyen, Canh Toan; Hölbling, Dominik; Pang, Toh Yen; Baca, Arnold und Dabnichki, Peter: A novel 3D printed personalised insole for improvement of flat foot arch compression and recoil – preliminary study, Proceedings of the Institution of Mechanical Engineers, Part L: Journal of Materials: Design and Applications, 2.2023, Vol. 237, no. 2, p. 329–342, DOI 10.1177/14644207221112362,
[24] Jandova, Sona und Mendricky, Radomir: Benefits of 3D Printed and Customized Anatomical Footwear Insoles for Plantar Pressure Distribution, 3D Printing and Additive Manufacturing, 1.12.2022, Vol. 9, no. 6, p. 547–556, DOI 10.1089/3dp.2021.0002,
[25] Trapp, Markus; Kreutz, Markus; Lütjen, Michael und Freitag, Michael: Improving Sustainability of Footwear Production through 3D Printing of Shoes, In: , 2022, p. 1–15, ISBN 978-3-95545-407-4.
[26] Introducing adidas 4DFWD, The Future of Running Shoes, Carbon [online], Online im Internet: https://www.carbon3d.com/resources/case-study/introducing-adidas-4dfwd-the-worlds-first-3d-printed-anisotropic-lattice-midsole-designed-to-move-you-forward (6.9.2025).
[27] 4DFWD: DATA-DRIVEN 3D PRINTED PERFORMANCE TECHNOLOGY DESIGNED TO MOVE YOU FORWARD, adidas News [online], Online im Internet: https://news.adidas.com/running/4dfwd--data-driven-3d-printed-performance-technology-designed-to-move-you-forward/s/514baddb-1029-4686-abd5-5ee3985a304a (6.9.2025).
[28] Kumar, Ravi und Sarangi, Saroj Kumar: 3D Printed customized diabetic foot insoles with

architecture designed lattice structures - a case study, Biomedical Physics & Engineering Express, 29.12.2023, Vol. 10, no. 1, DOI 10.1088/2057-1976/ad1732,
[29] Wojciechowski, Elizabeth; Chang, Angela Y.; Balassone, Daniel; Ford, Jacqueline; Cheng, Tegan L.; Little, David; Menezes, Manoj P.; Hogan, Sean und Burns, Joshua: Feasibility of designing, manufacturing and delivering 3D printed ankle-foot orthoses: a systematic review, Journal of Foot and Ankle Research, 2019, Vol. 12, no. 1, p. 11, DOI 10.1186/s13047-019-0321-6,
[30] NEW BALANCE LAUNCHES A PREMIUM 3D PRINTING PLATFORM, The NewsMarket [online], Online im Internet: https://newbalance.newsmarket.com/latest-news/new-balance-launches-a-premium-3d-printing-platform/s/5c2b466a-13b7-4218-a18a-61d2889e6adc (6.9.2025).
[31] Maconachie, Tobias; Leary, Martin; Lozanovski, Bill; Zhang, Xuezhe; Qian, Ma; Faruque, Omar und Brandt, Milan: SLM lattice structures: Properties, performance, applications and challenges, Materials & Design, 5.12.2019, Vol. 183, p. 108137, DOI 10.1016/j.matdes.2019.108137,
[32] Design and Optimization of Lattice Structures: A Review, [online], Online im Internet: https://www.mdpi.com/2076-3417/10/18/6374 (6.9.2025).
[33] Helou, Mark und Kara, Sami: Design, analysis and manufacturing of lattice structures: an overview, International Journal of Computer Integrated Manufacturing, 4.3.2018, Vol. 31, no. 3, p. 243–261, DOI 10.1080/0951192X.2017.1407456,
[34] Challapalli, Adithya und Li, Guoqiang: Machine learning assisted design of new lattice core for sandwich structures with superior load carrying capacity, Scientific Reports, 17.9.2021, Vol. 11, no. 1, p. 18552, DOI 10.1038/s41598-021-98015-7,
[35] Wallat, Leonie; Altschuh, Patrick; Reder, Martin; Nestler, Britta und Poehler, Frank: Computational Design and Characterisation of Gyroid Structures with Different Gradient Functions for Porosity Adjustment, Materials, 1.2022, Vol. 15, no. 10, p. 3730, DOI 10.3390/ma15103730,
[36] Maurizi, Marco; Gao, Chao und Berto, Filippo: Inverse design of truss lattice materials with superior buckling resistance, npj Computational Materials, 29.11.2022, Vol. 8, no. 1, p. 1–12, DOI 10.1038/s41524-022-00938-w,
[37] Li, Tiantian; Chen, Yanyu; Hu, Xiaoyi; Li, Yangbo und Wang, Lifeng: Exploiting negative Poisson's ratio to design 3D-printed composites with enhanced mechanical properties, Materials & design, 2018, Vol. 142, p. 247–258,
[38] Geiger, Franziska; Kebbach, Maeruan; Vogel, Danny; Weissmann, Volker und Bader, Rainer: Efficient Computer-Based Method for Adjusting the Stiffness of Subject-Specific 3D-Printed Insoles during Walking, Applied Sciences, 17.3.2023, Vol. 13, no. 6, p. 3854, DOI 10.3390/app13063854,
[39] Leung, Matthew Sin-hang; Yick, Kit-lun; Sun, Yue; Chow, Lung und Ng, Sun-pui: 3D printed auxetic heel pads for patients with diabetic mellitus, Computers in Biology and Medicine, 7.2022, Vol. 146, p. 105582, DOI 10.1016/j.compbiomed.2022.105582,
[40] Leung, Matthew Sin-hang; Yick, Kit-lun; Sun, Yue; Chow, Lung und Ng, Sun-pui: 3D printed auxetic heel pads for patients with diabetic mellitus, Computers in Biology and Medicine, 2022, Vol. 146, p. 105582,
[41] Daryabor, Aliyeh; Kobayashi, Toshiki; Saeedi, Hassan; Lyons, Samuel M.; Maeda, Noriaki und Naimi, Sedigheh Sadat: Effect of 3D printed insoles for people with flatfeet: A systematic review, Assistive Technology, 4.3.2023, Vol. 35, no. 2, p. 169–179, DOI 10.1080/10400435.2022.2105438,
[42] Song, Yang; Shao, Enze; Bíró, István; Baker, Julien Steven und Gu, Yaodong: Finite element modelling for footwear design and evaluation: A systematic scoping review, Heliyon, 1.10.2022, Vol. 8, no. 10, p. e10940, DOI 10.1016/j.heliyon.2022.e10940,

[43] Cho, Jin-Rae; Park, Seung-Bum; Ryu, Sung-Hyun; Kim, Sung-Ho und Lee, Shi-Bok: Landing impact analysis of sports shoes using 3-D coupled foot-shoe finite element model, Journal of Mechanical Science and Technology, 1.10.2009, Vol. 23, no. 10, p. 2583–2591, DOI 10.1007/s12206-009-0801-x,
[44] Lu, Zhenghui; Li, Xin; Gao, Zixiang; Chen, Hairong; Zhang, Qiaolin; Xu, Yining; Fekete, Gusztá V und Gu, Yaodong: Customized 3D-Printed Insoles for Diabetic Foot Care: Finite Element Analysis and Machine Learning Approach, In: Material Strength and Applied Mechanics [online], IOS Press, 2024, p. 515–522, Online im Internet: https://ebooks.iospress.nl/doi/10.3233/ATDE240588 (7.9.2025).
[45] Mun, Frederick und Choi, Ahnryul: Deep learning approach to estimate foot pressure distribution in walking with application for a cost-effective insole system, Journal of NeuroEngineering and Rehabilitation, 16.1.2022, Vol. 19, no. 1, p. 4, DOI 10.1186/s12984-022-00987-8,
[46] Dindorf, Carlo; Dully, Jonas; Simon, Steven; Perchthaler, Dennis; Becker, Stephan; Ehmann, Hannah; Diers, Christian; Garth, Christoph und Fröhlich, Michael: Toward automated plantar pressure analysis: machine learning-based segmentation and key point detection across multicenter data, Frontiers in Bioengineering and Biotechnology [online], 19.6.2025, Vol. 13, Online im Internet: DOI 10.3389/fbioe.2025.1579072, https://www.frontiersin.org/journals/bioengineering-and-biotechnology/articles/10.3389/fbioe.2025.1579072/full (7.9.2025).
[47] Fay, Sarah C. und Hosoi, A. E.: Modeling Running via Optimal Control for Shoe Design, Journal of Biomechanical Engineering [online], 9.2.2024, Vol. 146, no. 041004, Online im Internet: DOI 10.1115/1.4064405, https://doi.org/10.1115/1.4064405 (7.9.2025).
[48] Foot pressure distribution during walking in young and old adults | BMC Geriatrics, [online], Online im Internet: https://link.springer.com/article/10.1186/1471-2318-5-8 (7.9.2025).
[49] Lu, Zhenghui; Sun, Dong; Xu, Datao; Li, Xin; Baker, Julien S. und Gu, Yaodong: Gait characteristics and fatigue profiles when standing on surfaces with different hardness: Gait analysis and machine learning algorithms, Biology, 2021, Vol. 10, no. 11, p. 1083,
[50] Zhao, Yangyang; Zhou, Jiali; Qiu, Fei; Liao, Xuying; Jiang, Jianhua; Chen, Heqing; Lin, Xiaomei; Hu, Yiqun; He, Jianquan und Chen, Jian: A deep learning method for foot-type classification using plantar pressure images, Frontiers in Bioengineering and Biotechnology [online], 11.9.2023, Vol. 11, Online im Internet: DOI 10.3389/fbioe.2023.1239246, https://www.frontiersin.org/journals/bioengineering-and-biotechnology/articles/10.3389/fbioe.2023.1239246/full (7.9.2025).
[51] Lu, Zhenghui; Li, Xin; Sun, Dong; Fekete, Gusztáv; Kovácsb, András und Gu, Yaodong: Personalised footwear design method based on machine learning and finite element analysis, Footwear Science, 23.7.2025, Vol. 17, no. sup1, p. S160–S161, DOI 10.1080/19424280.2025.2493755,
[52] Lu, Zhenghui; Li, Xin; Sun, Dong; Song, Yang; Fekete, Gusztáv; Kovács, András; András, Kámán und Gu, Yaodong: Parametric cushioning lattice insole based on finite element method and machine learning: A preliminary computational analysis, Journal of Biomechanics, 1.5.2025, Vol. 184, p. 112674, DOI 10.1016/j.jbiomech.2025.112674,
[53] Lu, Zhenghui; Li, Xin; Sun, Dong; Song, Yang; Fekete, Gusztáv; Kovács, András; Gao, Zixiang; Zheng, Jianjun; Xiang, Liangliang und Gu, Yaodong: Computationally tuned dual-layer lattice pads adapted to gait-induced pressure distribution, npj Advanced Manufacturing, 2025, Vol. 2, no. 1, p. 43,
[54] Kim, Jungmi; Choi, Juyoung; Kang, Young-Jin und Noh, Yoojeong: Development of Customized Insole Design Framework Based on Digital Twin, International Journal of Precision Engineering and Manufacturing, 1.4.2024, Vol. 25, no. 4, p. 785–798, DOI 10.1007/s12541-023-00952-y,

[55] Petch, Jeremy; Di, Shuang und Nelson, Walter: Opening the black box: the promise and limitations of explainable machine learning in cardiology, Canadian Journal of Cardiology, 2022, Vol. 38, no. 2, p. 204–213,
[56] Chatzistergos, Panagiotis E.; Gatt, Alfred; Formosa, Cynthia; Farrugia, Kurt und Chockalingam, Nachiappan: Optimised cushioning in diabetic footwear can significantly enhance their capacity to reduce plantar pressure, Gait & Posture, 6.2020, Vol. 79, p. 244–250, DOI 10.1016/j.gaitpost.2020.05.009,
[57] Hsu, Chia-Yi; Wang, Chien-Shun; Lin, Kuang-Wei; Chien, Mu-Jung; Wei, Shun-Hwa und Chen, Chen-Sheng: Biomechanical Analysis of the FlatFoot with Different 3D-Printed Insoles on the Lower Extremities, Bioengineering, 17.10.2022, Vol. 9, no. 10, p. 563, DOI 10.3390/bioengineering9100563,
[58] Clermont, Christian; Barrons, Zachary B.; Esposito, Michael; Dominguez, Eugene; Culo, Marina; Wannop, John W. und Stefanyshyn, Darren: The influence of midsole shear on running economy and smoothness with a 3D-printed midsole, Sports Biomechanics, 4.3.2023, Vol. 22, no. 3, p. 410–421, DOI 10.1080/14763141.2022.2029936,
[59] Bjelopetrovich, Anastasia und Barrios, Joaquin A.: Effects of incremental ambulatory-range loading on arch height index parameters, Journal of Biomechanics, 3.10.2016, Vol. 49, no. 14, p. 3555–3558, DOI 10.1016/j.jbiomech.2016.08.017,
[60] Peng, Yinghu; Wong, Duo Wai-Chi; Chen, Tony Lin-Wei; Wang, Yan; Zhang, Guoxin; Yan, Fei und Zhang, Ming: Influence of arch support heights on the internal foot mechanics of flatfoot during walking: A muscle-driven finite element analysis, Computers in Biology and Medicine, 1.5.2021, Vol. 132, p. 104355, DOI 10.1016/j.compbiomed.2021.104355,
[61] Lu, Zhenghui; Li, Xin; Xuan, Rongrong; Song, Yang; Bíró, István; Liang, Minjun und Gu, Yaodong: Effect of Heel Lift Insoles on Lower Extremity Muscle Activation and Joint Work during Barbell Squats, Bioengineering, 7.2022, Vol. 9, no. 7, p. 301, DOI 10.3390/bioengineering9070301,
[62] Paquette, Max R.; Melaro, Jake A.; Smith, Ross und Moore, Isabel S.: Time to stability of treadmill running kinematics in novel footwear with different midsole thickness, Journal of Biomechanics, 2024, P. 111984,
[63] Peng, Xing; Huang, Qiyuan; Zhang, Yali; Zhang, Xiaogang; Shen, Tongtong; Shu, Haoyu und Jin, Zhongmin: Elastic response of anisotropic Gyroid cellular structures under compression: Parametric analysis, Materials & Design, 1.7.2021, Vol. 205, p. 109706, DOI 10.1016/j.matdes.2021.109706,
[64] Ramlee, Muhammad Hanif; Abdul Kadir, Mohammed Rafiq; Murali, Malliga Raman und Kamarul, Tunku: Biomechanical evaluation of two commonly used external fixators in the treatment of open subtalar dislocation—A finite element analysis, Medical Engineering & Physics, 1.10.2014, Vol. 36, no. 10, p. 1358–1366, DOI 10.1016/j.medengphy.2014.07.001,
[65] Abul, Kadir; Ozer, Devrim; Sakizlioglu, Secil Sezgin; Buyuk, Abdul Fettah und Kaygusuz, Mehmet Akif: Detection of Normal Plantar Fascia Thickness in Adults via the Ultrasonographic Method, Journal of the American Podiatric Medical Association, 1.2015, Vol. 105, no. 1, p. 8–13, DOI 10.7547/8750-7315-105.1.8,
[66] Koivunen-Niemelä, T. und Parkkola, K.: Anatomy of the Achilles tendon (tendo calcaneus) with respect to tendon thickness measurements, Surgical and Radiologic Anatomy, 1.9.1995, Vol. 17, no. 3, p. 263–268, DOI 10.1007/BF01795061,
[67] Chen, Tony Lin-Wei; Wong, Duo Wai-Chi; Peng, Yinghu und Zhang, Ming: Prediction on the plantar fascia strain offload upon Fascia taping and Low-Dye taping during running, Journal of Orthopaedic Translation, 1.1.2020, Vol. 20, p. 113–121, DOI 10.1016/j.jot.2019.06.006,

[68] Chen, Tony Lin-Wei; Wang, Yan; Peng, Yinghu; Zhang, Guoxin; Hong, Tommy Tung-Ho und Zhang, Ming: Dynamic finite element analyses to compare the influences of customised total talar replacement and total ankle arthroplasty on foot biomechanics during gait, Journal of Orthopaedic Translation, 1.1.2023, Vol. 38, p. 32–43, DOI 10.1016/j.jot.2022.07.013,
[69] Nie, Bingbing; Panzer, Matthew B.; Mane, Adwait; Mait, Alexander R.; Donlon, John-Paul; Forman, Jason L. und Kent, Richard W.: Determination of the in situ mechanical behavior of ankle ligaments, Journal of the Mechanical Behavior of Biomedical Materials, 1.1.2017, Vol. 65, p. 502–512, DOI 10.1016/j.jmbbm.2016.09.010,
[70] Siegler, Sorin; Block, John und Schneck, Carson D.: The Mechanical Characteristics of the Collateral Ligaments of the Human Ankle Joint, Foot & Ankle, 4.1988, Vol. 8, no. 5, p. 234–242, DOI 10.1177/107110078800800502,
[71] Bok, Soo-Kyung; Kim, Bong-Ok; Lim, Jun-Ho und Ahn, So-Young: Effects of custom-made rigid foot orthosis on pes planus in children over 6 years old, Annals of rehabilitation medicine, 2014, Vol. 38, no. 3, p. 369–375,
[72] Lee, Eui Chang; Kim, Myeong Ok; Kim, Hyo Sang und Hong, Sang Eun: Changes in resting calcaneal stance position angle following insole fitting in children with flexible flatfoot, Annals of rehabilitation medicine, 2017, Vol. 41, no. 2, p. 257,
[73] Ohuchi, Hiroshi; Chavez, Joverienne S. und Alvarez, Carlo Antonio D.: Changes in calcaneal pitch and heel fat pad thickness in static weight bearing radiographs while wearing shoes with arch support and heel cup orthotics, Asia-Pacific Journal of Sports Medicine, Arthroscopy, Rehabilitation and Technology, 1.7.2019, Vol. 17, p. 21–24, DOI 10.1016/j.asmart.2019.07.001,
[74] Delgado, Domenica A.; Lambert, Bradley S.; Boutris, Nickolas; McCulloch, Patrick C.; Robbins, Andrew B.; Moreno, Michael R. und Harris, Joshua D.: Validation of digital visual analog scale pain scoring with a traditional paper-based visual analog scale in adults, JAAOS Global Research & Reviews, 2018, Vol. 2, no. 3, p. e088,
[75] Babaee, Sahab; Jahromi, Babak Haghpanah; Ajdari, Amin; Nayeb-Hashemi, Hamid und Vaziri, Ashkan: Mechanical properties of open-cell rhombic dodecahedron cellular structures, Acta Materialia, 2012, Vol. 60, no. 6–7, p. 2873–2885,
[76] Ahmadi, S. M.; Campoli, G.; Yavari, S. Amin; Sajadi, B.; Wauthlé, Ruben; Schrooten, Jan; Weinans, H. und Zadpoor, A. A.: Mechanical behavior of regular open-cell porous biomaterials made of diamond lattice unit cells, Journal of the mechanical behavior of biomedical materials, 2014, Vol. 34, p. 106–115,
[77] Lu, Zi-Xing; Li, Xiang; Yang, Zhen-Yu und Xie, Fan: Novel structure with negative Poisson's ratio and enhanced Young's modulus, Composite Structures, 2016, Vol. 138, p. 243–252,
[78] Healy, Aoife; Dunning, David N. und Chockalingam, Nachiappan: Materials used for footwear orthoses: a review, Footwear Science, 2010, Vol. 2, no. 2, p. 93–110,
[79] Iftekar, Syed Fouzan; Aabid, Abdul; Amir, Adibah und Baig, Muneer: Advancements and limitations in 3D printing materials and technologies: a critical review, Polymers, 2023, Vol. 15, no. 11, p. 2519,
[80] Hajare, Dipak M. und Gajbhiye, Trupti S.: Additive manufacturing (3D printing): Recent progress on advancement of materials and challenges, Materials Today: Proceedings, 2022, Vol. 58, p. 736–743,
[81] Law, Mark HC; Choi, Eric MF; Law, Stephanie HY; Chan, Subrina SC; Wong, Sonia MS; Ching, Eric CK; Chan, Zoe YS; Zhang, Janet H.; Lam, Gilbert WK und Lau, Fannie OY: Effects of footwear midsole thickness on running biomechanics, Journal of sports sciences, 2019, Vol. 37, no. 9, p. 1004–1010,

[82] Perry, Stephen D.; Radtke, Alison und Goodwin, Chris R.: Influence of footwear midsole material hardness on dynamic balance control during unexpected gait termination, Gait & posture, 2007, Vol. 25, no. 1, p. 94–98,
[83] De Lateur, Barbara J.; Giaconi, Ruth M.; Questad, Kent; Ko, Mike und Lehmann, Justus F.: Footwear and posture: compensatory strategies for heel height, American journal of physical medicine & rehabilitation, 1991, Vol. 70, no. 5, p. 246–254,
[84] Stefanyshyn, Darren J. und Wannop, John W.: The influence of forefoot bending stiffness of footwear on athletic injury and performance, Footwear Science, 2016, Vol. 8, no. 2, p. 51–63,
[85] Huang, Meizhen; Yick, Kit-lun; Ng, Sun-pui; Yip, Joanne und Cheung, Roy Tsz-hei: The effect of support surface and footwear condition on postural sway and lower limb muscle action of the older women, PLoS One, 2020, Vol. 15, no. 6, p. e0234140,
[86] Perhamre, S.; Lundin, F.; Klässbo, M. und Norlin, Rolf: A heel cup improves the function of the heel pad in Sever's injury: effects on heel pad thickness, peak pressure and pain, Scandinavian journal of medicine & science in sports, 2012, Vol. 22, no. 4, p. 516–522,
[87] Mohammadi, Mohammad Mahdi und Nourani, Amir: Testing the effects of footwear on biomechanics of human body: A review, Heliyon, 2025,
[88] Hennig, Ewald M.; Valiant, Gordon A. und Liu, Q. I.: Biomechanical variables and the perception of cushioning for running in various types of footwear, Journal of Applied Biomechanics, 1996, Vol. 12, no. 2, p. 143–150,
[89] Hoitz, Fabian; Mohr, Maurice; Asmussen, Michael; Lam, Wing-Kai; Nigg, Sandro und Nigg, Benno: The effects of systematically altered footwear features on biomechanics, injury, performance, and preference in runners of different skill level: a systematic review, Footwear Science, 2020, Vol. 12, no. 3, p. 193–215,
[90] Liu, Hongyuan; Hou, Feng; Li, Ang; Lei, Yongpeng und Wang, Hui: High-efficient and reversible intelligent design for perforated auxetic metamaterials with peanut-shaped pores, International Journal of Mechanics and Materials in Design, 1.9.2023, Vol. 19, no. 3, p. 553–566, DOI 10.1007/s10999-023-09648-7,
[91] Chen, Yu-Chi; Lou, Shu-Zon; Huang, Chen-Yu und Su, Fong-Chin: Effects of foot orthoses on gait patterns of flat feet patients, Clinical biomechanics, 2010, Vol. 25, no. 3, p. 265–270,
[92] Korada, Hrishikesh; Maiya, Arun; Rao, Sharath Kumar und Hande, Manjunath: Effectiveness of customized insoles on maximum plantar pressure in diabetic foot syndrome: A systematic review, Diabetes & Metabolic Syndrome: Clinical Research & Reviews, 2020, Vol. 14, no. 5, p. 1093–1099,
[93] Ma, Zheng; Lin, Jiacheng; Xu, Xiaoyue; Ma, Ziwei; Tang, Lei; Sun, Changning; Li, Dichen; Liu, Chaozong; Zhong, Yongming und Wang, Ling: Design and 3D printing of adjustable modulus porous structures for customized diabetic foot insoles, International Journal of Lightweight Materials and Manufacture, 2019, Vol. 2, no. 1, p. 57–63,
[94] Zuñiga, Juan; Moscoso, Miguel; Padilla-Huamantinco, Pierre G.; Lazo-Porras, Maria; Tenorio-Mucha, Janeth; Padilla-Huamantinco, Wendy und Tincopa, Jean Pierre: Development of 3D-printed orthopedic insoles for patients with diabetes and evaluation with electronic pressure sensors, Designs, 2022, Vol. 6, no. 5, p. 95,
[95] Ntagios, M. und Dahiya, Ravinder: 3D printed soft and flexible insole with intrinsic pressure sensing capability, IEEE Sensors Journal, 2022, Vol. 23, no. 20, p. 23995–24003,
[96] Akkawutvanich, Chaicharn und Manoonpong, Poramate: Personalized symmetrical and asymmetrical gait generation of a lower limb exoskeleton, IEEE Transactions on Industrial Informatics,

2023, Vol. 19, no. 9, p. 9798–9808,
[97] Slade, Patrick; Kochenderfer, Mykel J.; Delp, Scott L. und Collins, Steven H.: Personalizing exoskeleton assistance while walking in the real world, Nature, 2022, Vol. 610, no. 7931, p. 277–282,
[98] Cheung, Jason Tak-Man und Zhang, Ming: Finite element modeling of the human foot and footwear, In: ABAQUS users' conference. 2006, p. 145–58,
[99] Telfer, Scott; Erdemir, Ahmet; Woodburn, James und Cavanagh, Peter R.: Simplified versus geometrically accurate models of forefoot anatomy to predict plantar pressures: A finite element study, Journal of biomechanics, 2016, Vol. 49, no. 2, p. 289–294,
[100] Cui, Tong Zhan; Raji, Rafiu King; Han, Jian Lin und Chen, Yuan: Application of 3D printing technology in footwear design and manufacture–A review of developing trends, Textile & Leather Review, 2024, Vol. 7, p. 1304–1321,
[101] Kumar, Ranvijay; Kumar, Mohit; Ramniwas, Seema; Rangappa, Sanjay Mavinkere und Siengchin, Suchart: Advancement in three-dimensional printing material and printed footwear accessories, In: Footwear Innovation, Elsevier, 2026, p. 157–170,
[102] Mohamed, Toaa Salama; Nassef, Ehssan; Morsy, Ashraf; Ewais, Hassan A.; Abdel-Salam, Ahmed H.; Morsy, Ahmed und Abd El-Moneim, Nabil Mahmoud: Enhancing 3D printing sustainability: Reinforcing thermoplastic polyurethane with recycled polyurethane foam for durable applications in orthopedic footwear, Journal of Vinyl and Additive Technology, 2024, Vol. 30, no. 5, p. 1153–1163,